





# Reappraisal of the hyperdiverse *Platynereis dumerilii* (Annelida: Nereididae) species complex in the Northern Atlantic, with the description of two new species

Marcos A. L. Teixeira<sup>A,B,\*</sup> , Joachim Langeneck<sup>C</sup> , Pedro E. Vieira<sup>A,B</sup> , José Carlos Hernández<sup>D</sup> ,  
Bruno R. Sampieri<sup>E</sup> , Panagiotis Kasapidis<sup>F</sup> , Serena Mucciolo<sup>G</sup> , Torkild Bakken<sup>H</sup> ,  
Ascensão Ravara<sup>I</sup> , Arne Nygren<sup>J</sup>  and Filipe O. Costa<sup>A,B</sup> 

For full list of author affiliations and declarations see end of paper

**\*Correspondence to:**

Marcos A. L. Teixeira  
Department of Biology, Centre of  
Molecular and Environmental Biology  
(CBMA), University of Minho, Campus de  
Gualtar, PT-4710-057 Braga, Portugal  
Email: [mark-us\\_teixeira@hotmail.com](mailto:mark-us_teixeira@hotmail.com)

**Handling Editor:**

Greg Rouse

**Received:** 24 December 2021

**Accepted:** 28 August 2022

**Published:** 17 November 2022

**Cite this:**

Teixeira MAL *et al.* (2022)  
*Invertebrate Systematics*  
**36**(11), 1017–1061. doi:[10.1071/IS21084](https://doi.org/10.1071/IS21084)

© 2022 The Author(s) (or their  
employer(s)). Published by  
CSIRO Publishing.

## ABSTRACT

Morphologically similar species are often overlooked but molecular techniques have been effective in signalling potential hidden diversity, boosting the documentation of unique evolutionary lineages and ecological diversity. *Platynereis dumerilii* and *Platynereis massiliensis* are part of a recognised species complex, where differences in the reproductive biology have mainly been highlighted to date. Analyses of DNA sequence data (*COI*, *16S* rDNA and D2 region of the *28S* rDNA) of populations of the apparent morphotype of *P. dumerilii* obtained from a broader sampling area along European marine waters, including the Azores and Webbnesia islands (Madeira and Canaries), provided compelling evidence for the existence of at least 10 divergent evolutionary lineages. Complementing the genetic data, morphological observations of the better represented lineages revealed two major groups with distinctive paragnath patterns. Two new *Platynereis* species were erected: *P. nunezi* sp. nov., widespread in the Azores and Webbnesia islands, and *P. jourdei* sp. nov., restricted to the western Mediterranean. The new combination *P. agilis* is also proposed for *Nereis agilis*, previously unaccepted for one of the lineages present both in the Northeast Atlantic and western Mediterranean. *Platynereis dumerilii* is redescribed based on topotypic material. However, uncertainty in the identity of *P. massiliensis* due to the original brief description and the absence of type and topotypic material prevents the unequivocal assignment to the lineage assumed in this and previous studies. The remaining five lineages are represented by only a few small specimens with morphological features poorly preserved and were therefore not described in this study.

ZooBank: urn:lsid:zoobank.org:pub:50079615-85E5-447E-BDD7-21E81C2A6F4D

**Keywords:** Annelida, Azores, cryptic species, Europe, integrative taxonomy, mitochondrial DNA, nuclear DNA, systematics, Webbnesia.

## Introduction

An increasing number of studies have been challenging the broadly distributed or cosmopolitan status of multiple marine benthic invertebrates (e.g. Nygren *et al.* 2018; Hupalo *et al.* 2019; Sampieri *et al.* 2021), unveiling instead the occurrence of complexes of cryptic or pseudo cryptic species with more restricted geographic distributions (Hutchings and Kupriyanova 2018; Struck *et al.* 2018; Cerca *et al.* 2020). Morphologically similar species are often overlooked but molecular techniques have been extremely effective in signalling potential hidden species. Detection of these, associated with detailed morphological descriptions, has the ability to boost the documentation of unique evolutionary lineages and associated diversity of ecological attributes (Nygren 2014; Langeneck *et al.* 2020; Martin *et al.* 2020).

Species with no clear and stable morphological differences, but with two or more molecular lineages involved, i.e. cryptic species, can sometimes be distinguished by life

history traits. Evidence of this apparent morphological stasis can be exemplified by the annelids *Platynereis dumerilii* (Audouin & Milne Edwards, 1833) and *P. massiliensis* (Moquin-Tandon, 1869). Based on previous studies, these sibling species can mainly be distinguished by reproductive and developmental traits (Hauenschild 1951; Schneider *et al.* 1992; Valvassori *et al.* 2015) despite the reported morphological variability between the two and even from specimens within the same species (Moquin-Tandon 1869; Claparède 1870). *Platynereis dumerilii* is gonochoric and semelparous (with a single reproductive event in life), with males and females being attracted to each other by pheromones (Zeeck *et al.* 1988, 1998), transforming into a pelagic epitokous form called *heteronereis* (Zantke *et al.* 2014). The larval stage has planktotrophic development (Zeeck *et al.* 1988; Fischer and Dorresteijn 2004), whereas *P. massiliensis* shows no epitokous transformation and is a protandrous hermaphrodite, characterised by egg brooding and lecithotrophic larval stages with semi-direct development (Schneider *et al.* 1992).

*Platynereis dumerilii* is a meso-herbivorous species (Ricevuto *et al.* 2015) first described from the French Atlantic coast (type locality: La Rochelle by Audouin and Milne-Edwards 1833). This species is also reported throughout the Mediterranean inhabiting shallow hard bottoms covered by seaweeds (Giangrande 1988; Gambi *et al.* 2000), often misidentified and sympatrically distributed with *P. massiliensis* (type locality: Marseille, France by Moquin-Tandon 1869). Beyond the Mediterranean, *P. dumerilii* has been reported from other parts of the world such as the Gulf of Mexico (Hartman 1951), Cuba (Ibarzábal 2006), North Africa to the Irish Sea and the Isefjord in Denmark (Hartmann-Schroeder 1996), the Black Sea (Popa *et al.* 2014) and South Africa (Day 1967). This species is considered a bioindicator of organic pollution (Bellan 1980), a model species for basic biology and Evo-Devo studies (Fischer and Dorresteijn 2004; Helm *et al.* 2014; Özpolat *et al.* 2021) can also be used as a model to address various aspects of acclimatisation and adaptation to ocean acidification (Wäge *et al.* 2017), being one of the dominant species present in volcanic CO<sub>2</sub> vents (Ricevuto *et al.* 2015). Although reported in several Mediterranean locations, e.g. Naples (Hauenschild 1951), Banyuls (Schneider *et al.* 1992), Villefranche-sur-Mer as a host of gregarines *Lecudina platynereidis* (Theodorides 1969) and Mediterranean Spain (Coll *et al.* 2010), *P. massiliensis* is often overlooked and not included in Mediterranean polychaete check-lists and revisions (e.g. Arvanitidis 2000; Mikac 2015; Faulwetter *et al.* 2017). Based on reproductive biology studies, Valvassori *et al.* (2015) also found evidence of the occurrence of *P. massiliensis* in the CO<sub>2</sub> vents system of the Italian island of Ischia.

Studies suggesting *P. dumerilii* as a complex of cryptic species where particular lineages could be linked to different ecological adaptations are already available (e.g. Calosi *et al.* 2013). Evidence of additional lineages belonging to the

*P. dumerilii* complex were also found by Wäge *et al.* (2017) after integrating cytochrome *c* oxidase subunit I (COI) sequence data with reproductive biology and life history observations of some selected populations thriving in the vent areas from the Italian islands of Ischia and Vulcano. This analysis highlighted the presence of four distinct *Platynereis* lineages, two of these primarily present in CO<sub>2</sub> vents and presumably all brooders, and the other two clades dominating the non-acidified sites, appearing to be epitokous free spawners. Based on these genetic data and the fact that there is no evidence of accidental human translocation of *P. dumerilii* to other regions (Read 2007), at least some of the 28 species (Read and Fauchald 2022) previously synonymised with *P. dumerilii* are highly likely valid distinct species. These synonyms belong to 13 different type localities, ranging from the Atlantic to the Pacific Ocean, 10 of which were reported for European coasts and might correspond to morphotype variants within the *P. dumerilii* cryptic complex that were inadequately synonymised. Recently, a South African taxon formerly thought to be *P. dumerilii* was also ascribed to a new species (*P. entshonae* Kara, Santos, Macdonald & Simon, 2020) mainly based on molecular data, with principal component analysis scores revealing no separation based on morphological characters (Kara *et al.* 2020).

To investigate the possible existence of additional hidden *Platynereis* species within *P. dumerilii* and in an attempt to resolve the current existing European complex in this group, we used a multi-locus approach and morphological data to examine populations from Scandinavia, the north-eastern Atlantic, the West and East Mediterranean Sea, and the Azores and Webbnesia (Canary and Madeira islands) archipelagos.

## Methods

### Taxon sampling

Nereidid specimens were collected at several localities along the Atlantic and Mediterranean coasts of Europe, including the Azores and Webbnesia islands, and at Mazagan (Morocco). The Atlantic localities include Norway (Stavanger, Bergen and Trondheim), Sweden (Tjärnö), Great Britain (Plymouth), France (Morlaix Bay, La Rochelle and Arcachon Bay), Portugal (northern beach of Canto Marinho, Azorean islands of Santa Maria, São Miguel and Terceira, Madeira and Porto Santo islands) and Spain (Canary islands of Tenerife, Gran Canaria, El Hierro, La Palma, Lanzarote and Fuerteventura). The Mediterranean localities include France (Banyuls), Spain (Calpe), Italy (Tuscany area (Calafuria, Antignano, Ardenza, Vada, Livorno and the islands of Montecristo, Pianosa and Elba), Trieste and Taranto) and Greece (Mazoma and Crete island (Paralia Skinaria)). Detailed numbers of *Platynereis* (all atokous and mainly intertidal samples) specimens per locality, region codes and respective coordinates are

listed in Table 1. *Nereis* specimens are listed in Table 2. The specimens were picked from among algae on rocky beaches, at low tide or by scuba diving down to 10-m depths and fixed in 96% ethanol. Additionally, some specimens from the Arrabida Natural Park (Lisbon, Portugal) were provided by the National Museum of Science and Natural History (MUHNAC, Portugal).

Sample collection was performed under approved ethics guidelines and no special permits were needed for the sampling campaigns at the time.

## Molecular procedures and data mining

DNA sequences of the 5' end of the mitochondrial cytochrome oxidase subunit I (mtCOI-5P, ~658 bp) were obtained for 193 of the 201 *Platynereis* specimens. The remaining 8 from Lisbon (PTA, Table 1) were only used for morphological purposes. Sequences of 16S rDNA (~368 bp) and the D2 region of 28S rDNA (~420 bp) were also obtained for a representative number of specimens (total number of 100 sequences for each marker) per location (at least 1 sequence per marker). For purposes of comparison, molecular data

**Table 1.** Numbers of *Platynereis* specimens acquired for this study (*n*), respective sampling areas, code abbreviations for the sampling location and institution responsible for storing the samples.

| Code | Region  | Location                        | <i>n</i> | Coordinates  |              | Storing institution         |
|------|---|---------------------------------|----------|--------------|--------------|-----------------------------|
|      |   |                                 |          | Latitude     | Longitude    |                             |
| PTA  | Southern European Atlantic Shelf, Atlantic Ocean    | Portugal, Arrabida Natural Park | 24       | 38°26.22'N   | 9°3.78'W     | MUHNAC (16) + CoBI-DBUA (8) |
| PTC  |   | Portugal, Canto Marinho         | 15       | 41°44.22'N   | 8°52.56'W    | CoBI-DBUA                   |
| FRA  |   | France, Arcachon Bay            | 1        | 44°39.72'N   | 1°9.18'W     |                             |
| FRR  |   | France, La Rochelle             | 17       | 46°8.79'N    | 1°12.6'W     |                             |
| FRM  | North-eastern Atlantic                              | France, Morlaix Bay             | 2        | 48°43.8'N    | 3°59.16'W    |                             |
| GBP  | North-eastern Atlantic                              | Great Britain, Plymouth         | 1        | 50°21.59'N   | 4°9.03'W     |                             |
| SWT  | Scandinavia, Kattegat Sea                           | Sweden, Tjörnö-Saltö canal      | 11       | 58°52'26.4"N | 11°08'42.0"E |                             |
| NOT  | Scandinavia, Norway Sea                             | Norway, Trondheim               | 1        | 63°26'09.6"N | 10°29'56.4"E | NTNU                        |
| NOB  | Scandinavia, Northern European Sea                  | Norway, Bergen                  | 2        | 60°23.76'N   | 5°19.5'E     |                             |
| SPC  | Balearic Sea, Western Mediterranean                 | Spain, Calpe                    | 16       | 38°38.3966'N | 0°3.5'E      | CoBI-DBUA                   |
| FRB  | Gulf of Lion, Western Mediterranean                 | France, Banyuls-sur-Mer         | 3        | 42°28.8983'N | 3°8.005'E    |                             |
| ITT  | Ligurian and Tyrrhenian Seas, Western Mediterranean | Italy, Tuscany Area             | 48       | 43°32.765'N  | 10°18.1433'E |                             |
| ITR  | Adriatic Sea, Eastern Mediterranean                 | Italy, Trieste                  | 1        | 45°38.86'N   | 13°45.5483'E | CoBI-DBUA                   |
| ITTA | Ionian Sea, Eastern Mediterranean                   | Italy, Taranto                  | 1        | 40°27.9833'N | 17°14.3333'E |                             |
| GRA  | Ionian Sea, Eastern Mediterranean                   | Greece, Amvrakikos Lagoon       | 8        | 39°02'45.6"N | 20°46'15.6"E | DNA only                    |
| GRC  | Sea of Crete, Eastern Mediterranean                 | Greece, Crete, Skinaria Beach   | 1        | 35°9.96'N    | 24°25.2833'E | CoBI-DBUA                   |
| TER  | Azorean ecoregion, Atlantic Ocean                   | Portugal, Azores, Terceira      | 3        | 38°41'N      | 27°3.4517'W  | CoBI-DBUA                   |
| SMA  |   | Portugal, Azores, Santa Maria   | 3        | 36°56.995'N  | 25°5.7'W     |                             |
| MA   | Webbnesia, Atlantic Ocean                           | Portugal, Madeira, Funchal      | 4        | 32°38.7667'N | 16°49.45'W   |                             |
| PS   |   | Portugal, Madeira, Porto Santo  | 1        | 33°4.38'N    | 16°17.76'W   |                             |
| LP   |   | Spain, Canaries, La Palma       | 5        | 28°48.3296'N | 17°45.6932'W |                             |
| EH   |   | Spain, Canaries, El Hierro      | 1        | 27°47.085'N  | 18°0.695'W   |                             |
| TE   |   | Spain, Canaries, Tenerife       | 3        | 28°25.1142'N | 16°32.9752'W |                             |
|      |   |                                 | 3        | 28°34.2854'N | 16°20.0175'W |                             |
| GC   |   | Spain, Canaries, Gran Canaria   | 12       | 27°59.108'N  | 15°22.5493'W |                             |
| FV   |   | Spain, Canaries, Fuerteventura  | 5        | 28°3.995'N   | 14°30.415'W  |                             |
| LA   |   | Spain, Canaries, Lanzarote      | 6        | 29°13.0883'N | 13°26.5067'W |                             |
| MOR  | Saharan Upwelling, Atlantic Ocean                   | Morocco, Mazagan                | 3        | 33°15.8417'N | 8°30.6433'W  |                             |

from *Pseudonereis* sp. (Treadwell, 1923) specimens collected at Crete island, and 33 small *Nereis* specimens from the Mediterranean, Azores and Canary islands for all the analysed loci, and *COI* sequences from *Perinereis marionii* (Audouin & Milne Edwards, 1833) collected in north-western Portugal (Canto Marinho) and Great Britain (Plymouth) were used as outgroups (Table 2). Additionally, *COI* sequences from the four *Platynereis* lineages obtained by Wäge *et al.* (2017) and *Platynereis* sequences from Calosi *et al.* (2013) and Kara *et al.* (2020) were mined from GenBank. Furthermore, for a better phylogenetic representation, *COI* sequences belonging to the outgroups *Neanthes fucata* (Savigny, 1822), *Nereis zonata* (Malmgren, 1867), *Nereis pelagica* Linnaeus, 1758, *Nereis heterocirrata* Treadwell, 1931 and *Ceratonereis tentaculata* Kinberg, 1865 were mined from GenBank and completed the final dataset used for the phylogenetic analysis (Table 2).

DNA was extracted, amplified, sequenced and assembled as described in Lobo *et al.* (2016) and Nygren *et al.* (2018). PCR conditions and primers used are listed in Supplementary Table S1. GenBank sequences batch for the original material were: *COI*, OP347321–OP347546; *16S*, OP347547–OP347664; and *28SD2*, OP347666–OP347782. Sampling locations, GenBank accession numbers and voucher data for each specimen are also listed in Supplementary Table S2. As only a few parapodia or a small portion of the posterior end were used for the DNA extraction, DNA voucher specimens are deposited at the Research Collection of Marine Invertebrates of the Department of Biology of the University of Aveiro (CoBI-DBUA), Portugal and available for further morphological or molecular study. Specimens that were exhausted in the DNA analysis were assigned only with the Process ID from the BOLD systems (<http://v4.boldsystems.org/>), corresponding to the ones from northern Greece (MTPD194-20–MTPD201-20), and the specimens MTPD191-20 (France, Morlaix) and MTPD144-20 (Spain, Gran Canaria). The specimens from Norway are deposited at NTNU University Museum (Bakken *et al.* 2021). The full dataset (excluding the sequences from Calosi *et al.* (2013) that cannot be found in BOLD) and associated meta-data can be accessed at BOLD Systems under the project title ‘*Platynereis* Species Complex (DS-MTPD)’ and in the following link: doi:10.5883/DS-MTPD.

## Phylogenetic analysis

The phylogenetic analyses of the different loci were performed through maximum likelihood (ML) and Bayesian inference (BI). MrBayes (ver. 3.1.2, see <https://nbisweden.github.io/MrBayes/index.html>; Ronquist and Huelsenbeck 2003) was used to conduct the Bayesian analysis and MEGA (ver. 10.0.5, see <https://www.megasoftware.net/>; Kumar *et al.* 2018) to perform Maximum Likelihood phylogenies. Sequences from the mtDNA *COI-5P*, rDNA *16S* and the D2 region of the rDNA *28S* were aligned and concatenated in MEGA software (ver. 10.0.5) with Clustal W (ver. 1.6, see <http://www.clustal.org/clustal2/>; Thompson *et al.* 1994).

Best-fit models were selected using the Akaike Information Criterion in the jModeltest software (Guindon and Gascuel 2003; Darriba *et al.* 2012). For *COI* we applied the Hasegawa–Kishino–Yano gamma distributed rates across sites (HKY + G) for the first two positions and the General Time Reversible model with gamma distributed rates across sites (GTR + G) for the third position. The latter model was also applied to the remaining loci (*16S* and *28SD2*). Number of generations was set to 10 000 000 and sample frequency to 500. In total, 25% of the samples were discarded as burn-in (burninfrac = 0.25). The resulting tree files were checked for convergence in the effective sampling sizes (ESSs > 200) with Tracer software (ver. 1.7, see <https://beast.community/tracer>; Rambaut *et al.* 2018) and subsequently analysed in Figtree (ver. 1.4.3, see <http://tree.bio.ed.ac.uk/software/figtree/>). The final version of the tree was edited with the software Inkscape (ver. 0.92.3, see <https://www.inkscape.org>). Maximum Likelihood phylogenies were built with 1000 bootstrap runs with the GTR model with gamma distributed rates across sites (GTR + G) for the concatenated dataset. A maximum likelihood amino acid radiation tree was also performed in MEGA 10.0.5 using the Jones–Taylor–Thornton model with equal rates across sites (JTT) for all the *COI Platynereis* lineages to visualise amino acid differences between lineages. The BI tree was displayed in the results with the addition of the ML support values if a similar topology was found.

The alignments (fasta and nexus format) for each individual marker and the concatenated markers are all publicly available online at Figshare: doi:10.6084/m9.figshare.21429000.

## MOTU clustering

To depict Molecular Operational Taxonomic Units (MOTUs), three delineation methods were applied to the concatenated dataset, except for *COI* where the Barcode Index Number (BIN), which makes use of the Refined Single Linkage (RESL) algorithm implemented in BOLD (Ratnasingham and Hebert 2013). The Automatic Barcode Gap Discovery (ABGD, Puillandre *et al.* 2012) was implemented on a web interface (see <https://bioinfo.mnhn.fr/abi/public/abgd/abgdweb.html>) with default settings using the K2P distance matrix. The Generalised Mixed Yule Coalescent (GYMC) single threshold model (Fujisawa and Barraclough 2013) and Poisson Tree Processes (bPTP) (Zhang *et al.* 2013) were applied, with both analyses performed on a web interface (see <https://species.h-its.org/>). BEAST (ver. 2.4.6, see <https://beast.community/beast>; Bouckaert *et al.* 2014) was used to generate the Bayesian ultrametric tree for the GYMC with the appropriate best model (based on AIC criteria; GTR equal rates) and four independent runs for 50 000 000 MCMC generations, sampled every 5000 generations. Tracer (ver. 1.7) software was used to estimate convergence ESSs > 200 for all parameters. The consensus tree was obtained using TreeAnnotator (ver. 2.4.6, see <https://beast.community/treeannotator>; Bouckaert *et al.* 2014) and loaded

**Table 2.** Species, number of sequences and respective Genbank accession numbers for the outgroups used in this study.

| Species  | GenBank COI  | Location                       | n  | Reference   |
|--|--|--------------------------------|----|---|
| <i>Perinereis marionii</i> (Audouin & Milne Edwards, 1833) | OP347386   | Portugal, Canto Marinho        | 1  | This study  |
|  | OP347380   | Great Britain, Plymouth        | 1  |   |
| <i>Nereis</i> spp.   | OP347355; OP347432; OP347521   | Spain, Calpe                   | 3  |   |
|  | OP347334; OP347345; OP347381;<br>OP347389; OP347400; OP347423;<br>OP347430; OP347433; OP347452;<br>OP347455; OP347532; OP347541;<br>OP347543 | Greece, Crete, Skinaria Beach  | 13 |   |
|  | OP347326; OP347504; OP347539   | Portugal, Azores, São Miguel   | 3  |   |
|  | OP347408; OP347422; OP347434;<br>OP347522  | Spain, Canaries, La Palma      | 4  |   |
|  | OP347369   | Spain, Canaries, El Hierro     | 1  |   |
|  | OP347321; OP347425   | Spain, Canaries, Gran Canaria  | 2  |   |
|  | OP347457; OP347471; OP347478   | Spain, Canaries, Fuerteventura | 3  |   |
|  | OP347391; OP347537   | Greece, Crete, Skinaria Beach  | 2  |   |
| <i>Platynereis</i> sp.                                     | KT124712   | Italy, Vulcano Island          | 2  | Wäge <i>et al.</i> (2017)   |
|  | KT124716   |                                |    |   |
| ' <i>P. dumerilii</i> '                                    | KC591811   | Italy                          | 1  | Calosi <i>et al.</i> (2013)   |
| <i>P. dumerilii</i> (Audouin & Milne-Edwards, 1833)        | KF737174   | India                          | 1  | R. Singh, S. K. Sahu, M. Thangaraj and R. Rajasekaran, unpubl. data |
|  | MH114981   | Germany                        | 1  | E. Tilic, T. Herkenrath and T. Bartolomaeus, unpubl. data           |
|  | KC591825   | Italy, S. Pietro               | 1  | Calosi <i>et al.</i> (2013)   |
|  | KT124685   | Italy, Ischia Island           | 1  | Wäge <i>et al.</i> (2017)   |
| <i>Platynereis</i> sp.                                     | KC591880   | Italy, Ischia Island           | 2  | Calosi <i>et al.</i> (2013)   |
|  | KT124684   |                                |    | Wäge <i>et al.</i> (2017)   |
| <i>Platynereis</i> sp.                                     | MT196851   | South Africa, Kidd's Beach     | 1  | Kara <i>et al.</i> (2020)   |
|  | MT196856   | South Africa, Plettenberg Bay  | 2  |   |
|  | MT196857   |                                |    |   |
|  | KT124674   | South of Spain, Blanes         | 1  |   |
|  | KC591870   | Italy, Ischia Island           | 3  |   |
|  | KC591872   |                                |    |   |
|  | KC591875   |                                |    |   |
| <i>P. cf. massiliensis</i>                                 | KC591833   | Italy, Ischia Island           | 2  | Calosi <i>et al.</i> (2013)   |
|  | KT124681   |                                |    | Wäge <i>et al.</i> (2017)   |
| <i>P. entshonae</i> Kara, Santos, Macdonald & Simon, 2020  | MT196859   | South Africa, Cannon Rocks     | 1  | Kara <i>et al.</i> (2020)   |
|  | MT196867   | South Africa, Cape Agulhas     | 1  |   |
|  | MT196888   | South Africa, Plettenberg Bay  | 1  |   |
| <i>Nereis heterocirrata</i> Treadwell, 1931                | MN256589–MN256591  | South-eastern Asia             | 3  | B. P. Xing and Z. L. Zhang, unpubl. data                            |
|  | GU362684   |                                | 1  | Zhou <i>et al.</i> (2010)   |

(Continued on next page)

**Table 2.** (Continued)

| Species  | GenBank COI | Location                | n | Reference  |
|--|-------------|-------------------------|---|--|
| <i>Nereis pelagica</i><br>Linnaeus, 1758         | JN852947    | Sweden                  | 1 | Norlinder et al. (2012)  |
|  | KR916894    | Portugal, Canto Marinho | 2 | Lobo et al. (2016)   |
|  | KR916895    |                         |   |  |
| ' <i>Neanthes fucata</i> '<br>(Savigny, 1822)    | KR916876    | Portugal, Canto Marinho | 3 | Lobo et al. (2016)   |
|  | KR916879    |                         |   |  |
|  | KR916880    |                         |   |  |
|  | KU714730    | Northern Spain          | 2 | Miralles et al. (2016)   |
|  | KU714731    |                         |   |  |
| <i>Nereis zonata</i><br>(Malmgren, 1867)         | HQ024401    | Arctic Canada           | 3 | Carr et al. (2011)   |
|  | HQ024403    |                         |   |  |
|  | HQ024404    |                         |   |  |
| <i>Ceratonereis tentaculata</i><br>Kinberg, 1865 | MW277910    | USA, Hawaii             | 2 | G. Paulay, C. Pittman, A. Bemis,<br>A. Marques, J. Slapcinsky, D. Uyeno,<br>J. Vicente, W. Magalhaes and<br>C. Craig, unpubl. data |
|  | MW277876    |                         |   |  |

into the Figtree software. ML phylogenies obtained (phylogenetic analysis section above) contributed to the bPTP results. A final consensus MOTU was chosen using the majority rule (i.e. most common number of MOTUs across different delimitation methods and in case of draw, MOTUs were separated if more than 3.5% COI genetic divergence was present).

### Genetic distances, diversity and structure

The mean genetic distances (Kimura-2-parameters, K2P) within and between MOTUs were calculated in MEGA (ver. 10.0.5). Haplotype networks were made for the original sequences through the PopART software (ver. 1.0, see <https://popart.maths.otago.ac.nz/>; Leigh and Bryant 2015) using the method of Templeton, Crandall and Sing (TCS, Clement et al. 2002) to evaluate the relationship between the haplotypes and geographical distribution. Indices of genetic diversity, namely number of haplotypes ( $h$ ), haplotype diversity ( $hd$ ), polymorphic sites ( $S$ ), nucleotide diversity ( $\pi$ ), Fu & Li D and Tajima D statistical tests, were estimated based on COI for each MOTU using DNASP (ver. 5.10.1, see [http://www.ub.edu/dnasp/index\\_v5.html](http://www.ub.edu/dnasp/index_v5.html); Librado and Rozas 2009).

### Morphological analysis

Morphological observations were carried out with an Olympus stereo microscope (model SZX9) equipped with a camera lucida for line drawings and Leica M80 for photographs. Stereo microscope images were taken with a Canon EOS1100D camera. Compound microscope images of parapodia and chaetae were obtained with a Zeiss Axioplan 2 imaging light microscope (Carl Zeiss, Oberkochen, Germany), equipped with a DP70 Olympus camera (Olympus Corp., Tokyo, Japan), after mounting the parapodia on a slide

preparation using Aquamount (Gurr) liquid. The software Inkscape (ver. 0.92.3, see <https://www.inkscape.org>) was used to create the final images for the drawings of the parapodia, pharynx and anterior region of the specimens. For measuring length of dorsal and ventral ligules, not only the lengths of the tips were taken into account (e.g. Conde-Vela and Salazar-Vallejo 2015; Villalobos-Guerrero and Carrera-Parra 2015) as exemplified in Fig. 1c. Also, the length:width ratio for notopodial dorsal ligules in posteriormost chaetigers was included, defined as the ratio between the length of notopodial dorsal ligules and the width at the base of such ligules. Measurements between the tentacular cirri, antennae, palps, head, apodous segment and first chaetiger were also taken.

For analysis of variation, both complete and incomplete specimens were taken into account, with incomplete specimens lacking a very small part of the tissue in the posterior end that was used for molecular purposes; total length (TL), length up to chaetiger 15 (L15) and width at chaetiger 15 (W15) were measured with a millimetre rule under the stereomicroscope and number of chaetigers (NC) was included. TL was measured from the anterior margin of the prostomium to the end of the pygidium or the posterior end and W15 were measured excluding parapodia.

Representative specimens from each *Platynereis* lineage (usually one or two specimens per lineage) were used for paragnath (Fig. 1b) and jaw observations and scanning electron microscopy (SEM) was used to observe the nuchal organs. When not everted, longitudinal dissections in the mid-ventral oral region were carried out to observe features on invaginated pharynxes and number of teeth of the jaws were counted. Specimens used for SEM were transferred to 100% ethanol, dehydrated for 2 h with hexamethyldisilazane (HMDS  $\geq 99\%$ ) and left to dry overnight. No coating

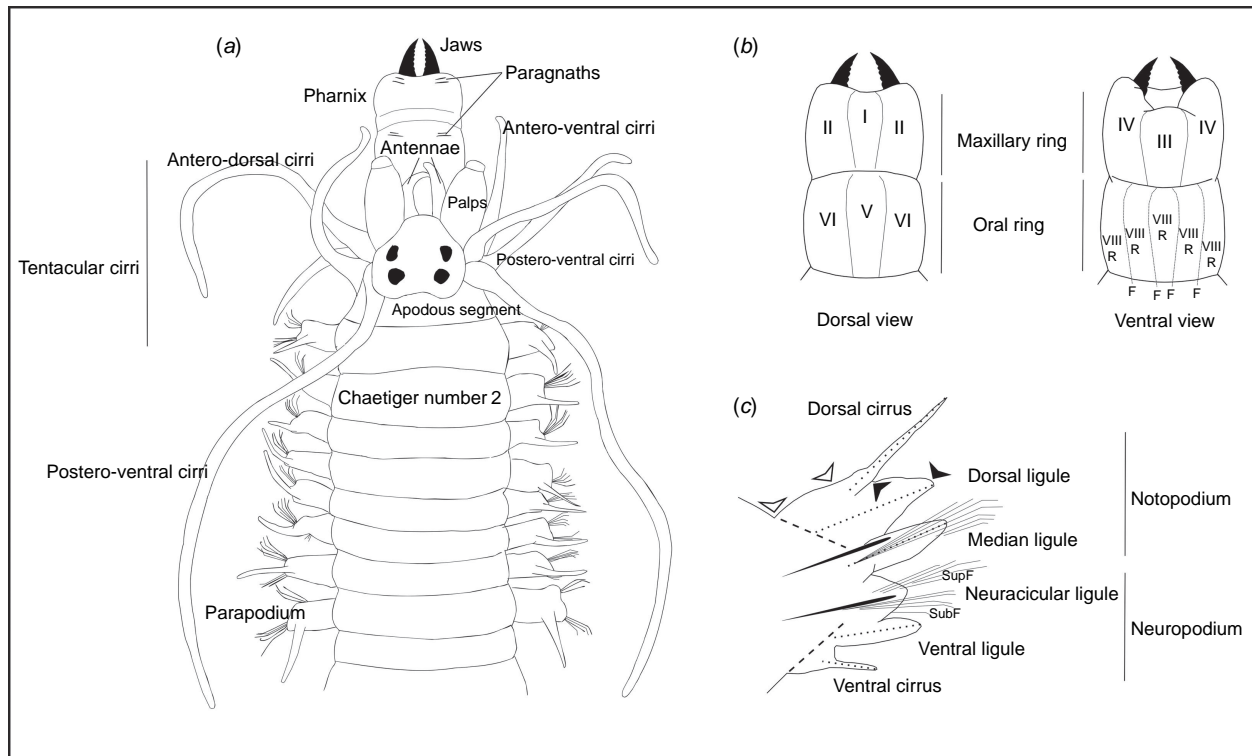


**Fig. 1.** Terminology based on the references cited in the Methods. Dashed lines and dots mark the delimitation used for the measurements of the ligules. (a) *Platynereis dumerillii* morphotype for the prostomium and anterior dorsal body. (b) Different areas in the pharynx used for the description of paragnaths. (c) Terminology used for the parapodium. Black arrowheads show points used for measuring entire length of distal part of dorsal ligule; white arrowheads show points used for measuring entire length of proximal part of dorsal ligule. Abbreviations: SupF, Neurochaetae supracicular fascicle; SubF, Neurochaetae subacicular fascicle; R, Ridge regions; F, Furrow regions.

was applied. Images were obtained using a TM3030Plus tabletop microscope (Hitachi).

Parapodial and chaetal terminology in the taxonomic section follows (Bakken and Wilson 2005) with the modifications made by Villalobos-Guerrero and Bakken (2018) (Fig. 1a). Pharynx paragnath terminology follows (Bakken *et al.* 2009) and paragnath description of areas VII and VIII follow Conde-Vela (2018). *Platynereis* lineages (MOTUs) with very low number of specimens, very small specimens lacking or degraded key morphological features, such as appendices in the prostomium or parapodia, were not described, following King *et al.* (2022). Terminology for molecular vouchers follows Pleijel *et al.* (2008) and Astrin *et al.* (2013). Overall description from the taxonomic section follows a similar structure from Villalobos-Guerrero (2019) in line with other recent descriptions of nereidid species.

## Results

### Phylogenetic reconstruction

The BI tree (Fig. 2a) is split into two major clades. The first clade (Clade A, including MOTUs 1–10) generally complies

with the description of the *Platynereis dumerillii* pseudo cryptic complex. The second clade includes *P. entshonae*, a sibling species of *P. dumerillii* distinguished mainly at the molecular level (Kara *et al.* 2020), a group of *Nereis* spp. that share the same habitat and some morphological similarities with juveniles of *Platynereis* species if observing the pharynx is not possible (Clade B, including MOTUs 11–15) and all the remaining outgroup species included in the analysis. Clade A is further divided into three sub-clades (A1, MOTU 1; A2, MOTUs 2–6; A3, MOTUs 7–10) based on close genetic distances, topology, information regarding the reproductive biology and paragnath variations.

A total of 15 unique consensus MOTUs was obtained, four of which are singletons with only one sequence available (MOTUs 8, 13, 14 and 15). The remaining MOTUs correspond to monophyletic clades with low divergence ( $COI < 3\%$  K2P) and are collapsed in Fig. 2a. Apart from the outgroups, additional *Platynereis* MOTUs from other studies are also represented in the tree (GB1–4). GB2 and GB3 (included in Clade A3) present low support values ( $< 0.85$ ) and lack well-defined bifurcated clades, and might belong to MOTU 9. However, morphological analysis would need to be undertaken to confirm this. MOTU GB1 seems to be a new

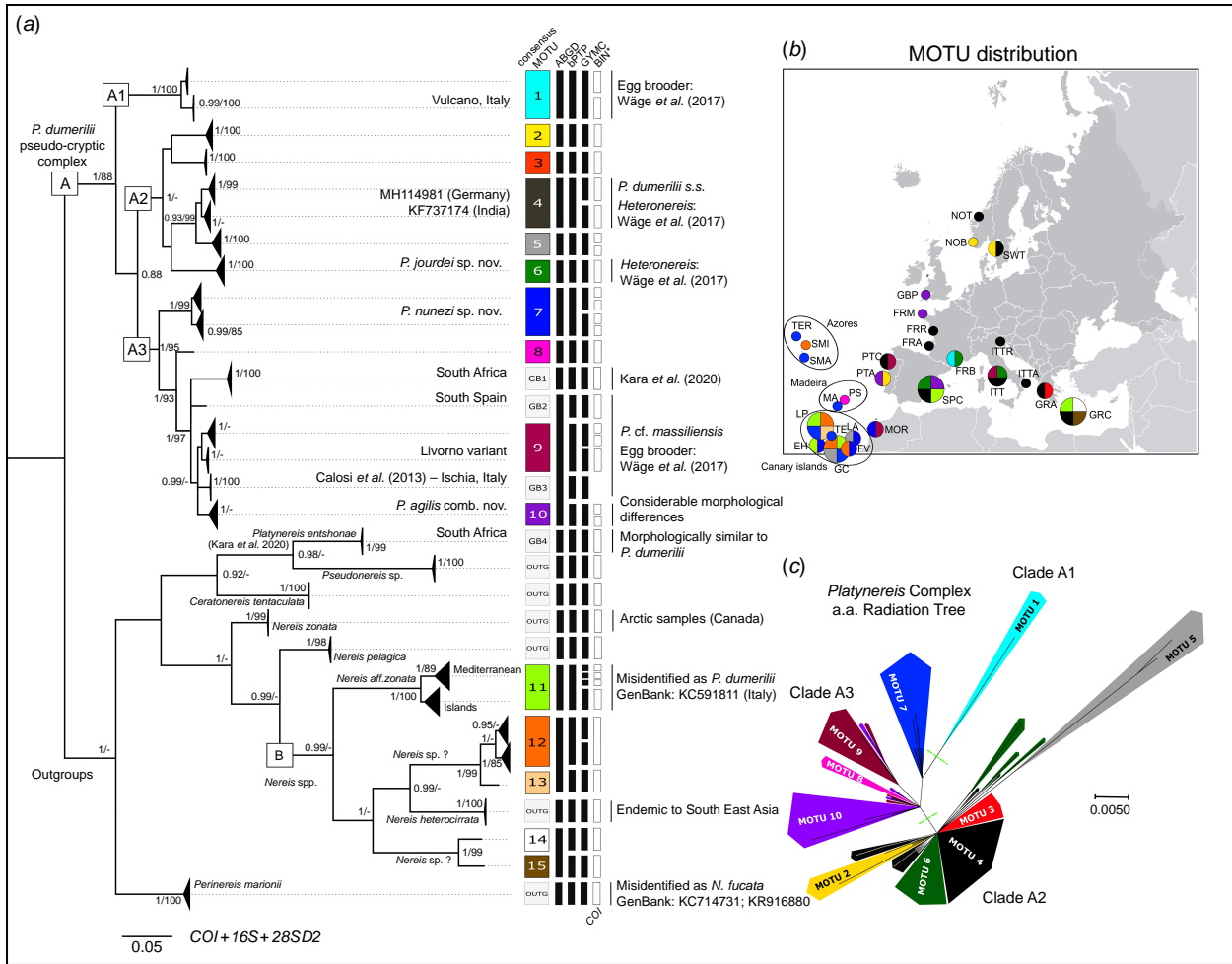


**Fig. 2.** (a) Phylogenetic tree reconstructed using Bayesian inference based on concatenated *COI*, *16S* and *28SD2* sequences, with information regarding the different MOTU delineation methods. BINs were used only for *COI*. Outgroups ('OUTG' and 'GB'), with the exception of *Pseudonereis* sp., only have *COI* sequences. Collapsed clades have less than 3.5% genetic divergence. Only the bootstrap values over 0.85 BI and 85 ML support are shown. Each different consensus MOTU is represented by the respective number, with the different colours corresponding to the respective geographic distribution. (b) Geographical distribution of the 15 retrieved MOTUs in Europe. (c) Maximum likelihood amino acid (a.a.) radiation tree based on *COI* sequences belonging to MOTUs 1–10 (clade A). Region abbreviations as in Table 1.

lineage from South Africa and MOTU GB4 is the recently described species *P. entshonae*.

Focusing only on Clade A (*P. dumerilii* complex), three MOTUs are unique to the Azores and Webbnesia (MOTUs 5, 7 and 8), one of which occurs exclusively in Porto Santo island (MOTU 8) and two sympatric ones occur in the Gran Canaria and Lanzarote islands alone (MOTUs 5 and 7). Additionally, three lineages are present exclusively in the Mediterranean (MOTU 1 and MOTU 6 in the western part, and MOTU 3 in the Eastern part of the Sea) of which MOTU 1 was only found at Banyuls. Three sympatric MOTUs were identified in the south-eastern part of Spain (MOTUs 4, 6 and 10) and in the Northern Tyrrhenian Sea (MOTUs 4, 6 and 9). Four different MOTUs were found in the Northeast Atlantic: three shared with the Mediterranean

(MOTUs 4, 9 and 10) and one exclusive to this part of the European coastline (MOTU 2). The specimens from the type locality of *P. dumerilii* species (La Rochelle) all grouped within MOTU 4. This particular lineage is the most widespread and easy to find among all the mainland samples, being present both in the Northeast Atlantic and the whole Mediterranean Sea, whereas MOTU 7 was the most widespread and abundant among the Azores and Webbnesia islands. A radiation amino acid tree based on *COI* sequences from the 10 retrieved *Platynereis* MOTUs was also able to separate the three main sub-clades (A1, A2 and A3) found in the BI tree, with MOTUs 1, 2, 5 and 7 not sharing the same amino acids with any of the remaining lineages.

A non-collapsed ML tree with 1000 bootstrap support is in the supplementary material (Supplementary Fig. S1).



## Genetic distances

The global mean genetic distances (K2P) for the clades A and B are listed in Table 3. Regarding only the *Platynereis* complex (clade A), the mean intra-MOTU distance was 0.2% (0–3.5%) for *COI* and 0.3% (0–1.4%) for *16S*, whereas the average inter-MOTU distances were 19.4% (4.4–26.6%) and 6.2% (1.5–9.9%) respectively. For the *28SD2* region, this ranged between 0.2% (0–1.4%) and 1.1% (0.1–3.9%) for intra- and inter-MOTU divergence respectively. Detailed mean genetic distances for the three genetic markers between each MOTU are listed in Supplementary Table S3. When comparing between major clades A and B, the maximum interspecific genetic distances are significantly higher in all loci, especially for *16S* and *28SD2*. In this scenario, maximum divergences of 32.6% *COI*, 35.7% *16S* and 36.9% *28SD2* were recorded, as opposed to the 26.9, 9.9 and 3.9% found only within clade A, based on the same respective loci. Furthermore, minimum *COI* distances with less than 10% divergence and no apparent morphological differences between MOTUs 12 v. 13, and MOTUs 14 v. 15 might also indicate possible cryptic diversity.

## Haplotype networks and diversity

All *COI* (Fig. 3a) and *16S* (Fig. 3c) haplotypes were completely sorted among MOTUs, i.e. no haplotypes were shared among more than one MOTU. However, some MOTUs (4, 5 and 6; 12 and 13; 14 and 15) shared the same haplotype in the *28SD2* loci (Fig. 3b). The *28SD2* network provided two major groups segregating clade B as seen in the BI, with more than 90 mutations separating this from clade A.

**Table 3.** Mean intra and inter-MOTU genetic distances (K2P) for the three analysed markers (*COI*, *16S*, *28SD2*), either only for the 10 MOTUs corresponding to the *Platynereis dumerillii* pseudo-cryptic complex (Clade A, Fig. 1a) or using the additional 5 MOTUs from the undetermined Nereidids (Clade B, Fig. 1a).

|                    | Marker       | Minimum distance (%) | Mean distance (%) | Maximum distance (%) |
|--------------------|--------------|----------------------|-------------------|----------------------|
| Within All MOTUs   | <i>COI</i>   | 0                    | 1.4               | 5.3                  |
|                    | <i>16S</i>   | 0                    | 0.4               | 2.0                  |
|                    | <i>28SD2</i> | 0                    | 0.4               | 3.1                  |
| Between All MOTUs  | <i>COI</i>   | 4.4                  | 22.6              | 32.6                 |
|                    | <i>16S</i>   | 0.9                  | 19.1              | 35.7                 |
|                    | <i>28SD2</i> | 0                    | 16.6              | 36.9                 |
| Within MOTUs 1–10  | <i>COI</i>   | 0                    | 0.2               | 3.5                  |
|                    | <i>16S</i>   | 0                    | 0.3               | 1.4                  |
|                    | <i>28SD2</i> | 0                    | 0.2               | 1.4                  |
| Between MOTUs 1–10 | <i>COI</i>   | 4.4                  | 19.4              | 26.6                 |
|                    | <i>16S</i>   | 1.5                  | 6.2               | 9.9                  |
|                    | <i>28SD2</i> | 0.1                  | 1.1               | 3.9                  |

The *COI* network also revealed geographically structured populations within MOTUs 9 and 10, corresponding to the five distinct BINs shown in the BI (Fig. 2a), except the populations from the north of France and south of Great Britain that did not split into separate BINs in MOTU 10. By contrast, not all populations from different Atlantic islands were completely sorted in MOTU 7, with the presence of shared haplotypes between all islands, except Gran Canaria and La Palma. Further geographic sorting in the *COI* network can also be identified within MOTU 4 regarding populations from the West and East Mediterranean Sea.

For the most sampled MOTUs (4, 6, 7, 9, 10) *COI* haplotype diversity is relatively high ( $H_d > 0.89$ – $0.99$ , Table 4), except for MOTU 6 ( $H_d$ , 0.65). The latter, together with MOTU 4, are the only cases with a significant Tajima *D* and *Fu* and *Li's D* tests, where the negative values indicate possible population expansion after a recent bottleneck or the occurrence of selective sweeps, with the neutral model of nucleotide substitutions accepted for the remaining MOTUs.

## *Platynereis dumerillii* pseudo-cryptic complex (clade A): morphological findings

A compilation of European species currently considered as synonyms of *P. dumerillii* either close to places from the type locality or same regions of the *Platynereis* specimens sampled in this study, with the main available morphological traits based on the original descriptions is given in Table 5. *Nereis massiliensis* was also included in this table, as was *Platynereis nadiae* Abbiati & Castelli, 1992, despite being currently accepted by WoRMS, given the similarity of this species' description with juveniles from *Platynereis dumerillii*. Descriptions based on epitoke forms (*Heteronereis fucicola* Örsted, 1843, *Nereilepas variabilis* Örsted, 1843, *Heteronereis malmgreni* Claparède and *Nereis taurica* Grube, 1850) and *Heteronereis maculata* Bobretzky, 1868, the latter due the difficulty in translating the original Russian texts, were not included in the Table. A similar summary was made for the ten different *Platynereis* MOTUs analysed in this study (Table 6). The previously synonymised name *Nereis agilis* Keferstein, 1862 is reinstated as *Platynereis agilis* comb. nov. for MOTU 10 and redescribed (Fig. 4, 5). Amended descriptions of *P. dumerillii* corresponding to MOTU 4 (Fig. 6, 7) and descriptions of two new species are also provided in the taxonomic section below, corresponding to MOTUs 6 (Fig. 8, 9) and MOTU 7 (Fig. 10, 11). Additionally, a description for *P. cf. massiliensis* (MOTU 9) is also provided, using the specimens studied herein (Fig. 12, 13). The remaining MOTUs are represented by a smaller number of specimens in suboptimal conditions and are therefore not fully described here. However, these seem to share the same morphological features from the respective phylogenetically nearest neighbours (see Fig. 2a), except for a few different characteristics shown by MOTUs 2 and 5. In MOTU 2 the morphology of parapodia and tentacular cirri appears to be

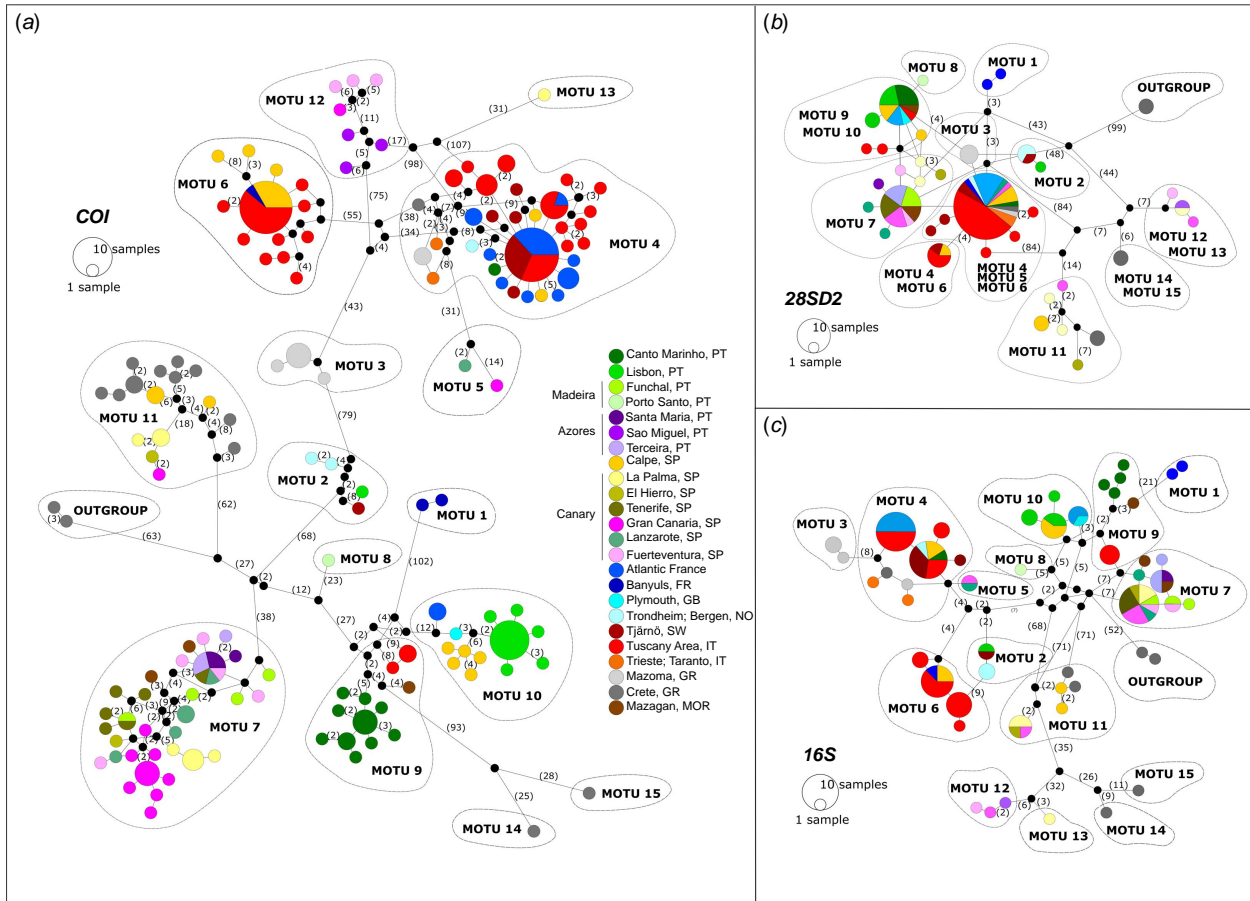


**Fig. 3.** Haplotype networks based on *COI* (a), *28SD2* (b) and *16S* (c) for the 15 MOTUs based on the original *Platynereis* and *Nereis* data, and *Pseudonereis* sp. as outgroup. Each haplotype is represented by a circle and number of haplotypes are indicated according to the displayed scale. Colours indicate the geographic location of the haplotype. Numbers correspond to the number of mutational steps between haplotypes. Lines without numbers represent only one mutation between haplotypes. Country abbreviations: PT, Portugal; SP, Spain; FR, France; GB, Great Britain; NO, Norway; SW, Sweden; IT, Italy; GR, Greece; MOR, Morocco.

closer to MOTU 10 instead of the remaining MOTUs from clade A2, whereas in MOTU 5 the tentacular cirri are similar to those in MOTU 9 (Table 6). Specimens from MOTU 3 were very small with the entire worm being used for DNA extraction, therefore only a preliminary morphological analysis was undertaken. MOTU 1 seems to be morphologically similar to MOTU 4 (Table 6) and seems to share a similar pigmentation to the Livorno population from MOTU 9.

Differences in the sizes of the tentacular cirri, paragnath patterns, numbers of chaetigers, serration types in the spiniger chaetae, jaw canals and variations in the number and location of the homogomph falcigers contributed to the main differences between lineages. In our observations, pigmentation in preserved specimens does not seem to be a reliable character since this can sometimes be absent in very small specimens or partially lost upon fixation in ethanol. However, a designated MOTU based on the pigmentation patterns as seen in the respective figures is generally identifiable, except between MOTUs 4 and 6 where some specimens might share similar pigmentation density and pattern.

**Non *Platynereis* nereidids (clade B): morphological findings**

Five additional MOTUs, belonging to small nereidid specimens collected in the same algae samples as the *Platynereis* specimens, were retrieved and may be confused with small juvenile specimens of other *Platynereis* species when performing rapid identifications in general ecological studies, or if observing the pharynx is not possible as often occurs in very small specimens. Apart from the genetic evidence (Fig. 2, Table 3) and considering morphological features alone (particularly the chaetae types, the tentacular cirri and pharynx paragnaths), MOTUs 11, 12 and 13 clearly belong to a different genus, most probably *Nereis* Linnaeus, 1758. Compared to descriptions and figures in Fauna Iberica (Núñez 2004), MOTU 11 (Supplementary Fig. S2), present in the Mediterranean and Canary islands, is morphologically close to *Nereis zonata* Malmgren, 1867, with similar proportions between the antennae in relation to the palps and very short tentacular cirri. However, there are some differences in

**Table 4.** Indices of genetic diversity estimated for each MOTU, based on *COI*.

|         | Region  | <i>n</i> | <i>h</i> | Hd   | <i>S</i> | $\pi$   | Fu and Li's D                             | Tajima's D                                |
|---------|---|----------|----------|------|----------|---------|---|---|
| MOTU 1  | FRB   | 2        | 2        | 1.00 | 1        | 0.00152 | –   | –   |
| MOTU 2  | SWT, NOB, PTA   | 4        | 4        | 1.00 | 19       | 0.0165  | 0.46, $P > 0.10$                          | 0.46, $P > 0.10$                          |
| MOTU 3  | GRA   | 6        | 3        | 0.60 | 3        | 0.00152 | -1.26013, $P > 0.10$                      | -1.23311, $P > 0.10$                      |
| MOTU 4  | PTC, SPC, GC, LA, FRR, FRA, NOT, SWT, ITT, ITTR, ITTA, GRA, GRC | 62       | 32       | 0.89 | 66       | 0.00826 | <b>-2.99788, <math>P &lt; 0.05</math></b> | <b>-2.11036, <math>P &lt; 0.05</math></b> |
| MOTU 5  | LP, GC  | 2        | 2        | 1.00 | 16       | 0.02432 | –   | –   |
| MOTU 6  | FRB, SPC, ITT   | 30       | 13       | 0.65 | 27       | 0.00364 | <b>-3.91387, <math>P &lt; 0.02</math></b> | <b>-2.37595, <math>P &lt; 0.01</math></b> |
| MOTU 7  | TER, SMA, LP, EH, TE, GC, FV, LA, MA, MOR                       | 45       | 32       | 0.97 | 53       | 0.01949 | -1.43196, $P > 0.10$                      | -0.05629, $P > 0.10$                      |
| MOTU 8  | PS  | 1        | 1        | –    | –        | –       | –   | –   |
| MOTU 9  | PTC, MOR, ITT   | 18       | 13       | 0.95 | 39       | 0.00154 | -0.77408, $P > 0.10$                      | -0.91319, $P > 0.10$                      |
| MOTU 10 | GBP, PTA, SPC, FRM  | 23       | 13       | 0.81 | 26       | 0.00673 | -1.26506, $P > 0.10$                      | -0.91717, $P > 0.10$                      |
| MOTU 11 | LP, EH, GC, SPC, GRC  | 19       | 16       | 0.98 | 59       | 0.02870 | 0.06698, $P > 0.10$                       | 0.26444, $P > 0.10$                       |
| MOTU 12 | LP, GC, FV, SMI   | 7        | 7        | 1.00 | 39       | 0.02345 | -0.63865, $P > 0.10$                      | -0.44925, $P > 0.10$                      |
| MOTU 13 | LP  | 1        | 1        | –    | –        | –       | –   | –   |
| MOTU 14 | GRC   | 1        | 1        | –    | –        | –       | –   | –   |
| MOTU 15 | GRC   | 1        | 1        | –    | –        | –       | –   | –   |

Number of sequences (*n*), nucleotide diversity ( $\pi$ ), number of haplotypes (*h*), haplotype diversity (Hd) and number of variable sites (*S*). Region abbreviations as in Table 1. Values in bold are statistically significant.

paragnath patterns (Núñez 2004). The latter species may also display a high degree of variation in paragnath arrangements, some of which may be similar to the ones described for *Neanthes fucata* (Núñez 2004; Gravina *et al.* 2015). This was also observed in our specimens from MOTU 11 (Supplementary Fig. S2a, b) that shared a similar pattern to *N. fucata*. However, parapodia from the posterior part do not have the characteristic broad leaf-like dorsal ligules found in *N. fucata* or in some other species belonging to *Neanthes*. Furthermore, the presence of homogomph falcigers (Supplementary Fig. S2g) that are lacking in *Neanthes*, resemble *Nereis* species instead.

The outgroups from GenBank identified as *N. fucata* grouped with our samples identified as *Perinereis marionii* (Audouin & Milne Edwards, 1833). The latter species possess a characteristic paragnath pattern in the oral ring with a continuous dorso-ventral band composed of multiple small paragnaths and an irregular line of larger paragnaths in the anterior margin, especially in Area V with a large conical triangular paragnath and Area VI with a small transverse bar. Parapodia are also characterised by the presence of a very long dorsal ligule in the posterior parapodia (Núñez 2004; see photo of our specimen of *P. marionii* with focus on the dorsal view of the pharynx, in Supplementary Fig. S3). This result strongly suggests misidentifications in the genetic databases for this group.

Based on photos deposited in BOLD (Zhou *et al.* 2010), MOTUs 12–13 (Supplementary Fig. S4), unique to the Azores and Canary islands, showed some resemblance with specimens identified as *Nereis heterocirrata* Treadwell, 1931, also

grouping very closely in the phylogenetic tree (Fig. 2a). The most noticeable feature of the latter species, however, relates to the antero-ventral cirri, that is much more swollen than the remaining tentacular cirri (Treadwell 1931) that is not observed in our specimens (Supplementary Fig. S4a). This species appears to be reported only from Eastern Asia (Zhou *et al.* 2010), with no reports from the Mediterranean to date (Coll *et al.* 2010; Read and Fauchald 2021).

MOTUs 14 and 15 appear to share similar morphological features with MOTU 12, especially regarding the tentacular cirri, being very small and all similar in size. However, since the respective single specimens lacked proper structural integrity, no further conclusions could be made.

## Taxonomic section

### *Platynereis* Kinberg, 1865

*Platynereis* Kinberg, 1865, p. 177. – Glasby 2015, p. 230.

*Iphinereis* Malmgren, 1865.

*Leontis* Malmgren, 1867.

*Nectonereis* Verrill, 1873.

*Nereis* (*Platynereis*) (Kinberg, 1865).

*Pisenoe* Kinberg, 1865.

*Uncinereis* Chamberlin, 1919.

*Type species: Platynereis magalhaensis* Kinberg, 1865 (designated by Hartman 1948).

**Table 5.** List of current European synonyms of *P. dumerilii* based on the WoRMS database, with the main distinctive morphological traits based on the original descriptions.

| Species (original comb.)                                 | Type locality                  | Live colour  | Length (mm)/ NC | Number of jaw teeth | Paragnaths (dorsal view)   | Tentacular cirri                                       | Parapodia (mid-body)   | Reproduction  | Available chaetae data                                    | Sources                          |
|--|--------------------------------|--|-----------------|---------------------|--|--|--|---|---|----------------------------------|
| <i>Nereis dumerilii</i><br>Audouin & Milne Edwards, 1833 | La Rochelle, northern France   | Yellowish with brown spots at the basis of parapodia (probably from preserved samples) | 80/80           | 11?                 | Present in the maxillary ring. Present in double rows in the oral ring | 1 long ( $\frac{1}{2}$ of the body length) and 3 short | Dorsal cirri twice the length of dorsal ligule; Ventral cirri much shorter than ventral ligule   | Gonochoristic + heteronereis  | Homogomph falcigers in posterior segments                 | Audouin and Milne Edwards (1833) |
| <i>Nereis zostericola</i><br>Örsted, 1843                | Hellebæk, Denmark              | Yellowish with many brownish spots   | 50/70           | ?                   | ?  | 1 long, reaching chaetiger 9, and 3 short              | Notopodia with 2 ligules, $\frac{1}{2}$ the length of neuropodia. Neuropodia with 3 ligules  | ?   | Presence of homogomph spinigers and heterogomph falcigers | Örsted (1843)                    |
| <i>Nereis agilis</i><br>Keferstein, 1862                 | St Vaast, northern France      | Pale with scattered brown and red spots  | 10–15/<br>40–42 | 8                   | ?  | 1 long and 3 short                                     | Four ligules are noticeable, although the third is very short  | Simultaneous hermaphrodite with different gonads in different parts of the body | ?   | Keferstein (1862)                |
| <i>Nereis megodon</i><br>Quatrefages, 1866               | Bretagne, northern-France      | ?  | 15–20/<br>60–80 | 11                  | ?  | Not clear, but most likely 1 long and 3 short          | Dorsal cirri $\frac{1}{3}$ longer than dorsal ligule; Ventral cirri shorter than ventral ligule  | Gonochoristic + no heteronereis?  | Two chaetae-bearing humps                                 | Quatrefages (1866, p. 514)       |
| <i>Nereis peritonealis</i><br>Claparède, 1868            | Gulf of Naples, Italy          | More or less colourless, with pigmented violet cells in the peritoneum                 | 45/65           | 8–9 (curved jaws)   | Absent in the maxillary ring. No further data                          | 1 long and 3 short                                     | Dorsal most ligule slightly inflated. Dorsal cirri longer than dorsal ligule   | Gonochoristic? Heteronereis?  | ?   | Claparède (1868)                 |
| <i>Nereis massiliensis</i><br>Moquin-Tandon, 1869        | Marseille, southern France     | Greenish-brown, mottled with wine-purple   | 40–50/<br>60–70 | 12                  | Absent   | 2 long (dorsal), 2 short (ventral)                     | Parapodia 'similar to those of <i>Nereis bilineata</i> '   | Simultaneous hermaphrodite with commingled sexual products                      | ?   | Moquin-Tandon (1869)             |
| <i>Platynereis nadiae</i><br>Abbiati & Castelli, 1992    | Capraia Island, Tyrrhenian Sea | Pale with large, scattered purple spots (A. Castelli, pers. comm.)                     | 5–10/43         | 7–8                 | Absent in the maxillary ring. Single rows in the oral ring             | 4 short, irregularly annulate                          | With variable morphology along the body. Dorsal cirri long and tapered in posterior segments, with indistinct annulation (similar to tentacular cirri) | ?   | Heterogomph and homogomph falcigers and spinigers         | Abbiati and Castelli (1992)      |

*Platynereis nadiae* is not considered a synonym but was included based on the similarity with the juveniles of *P. dumerilii*. Descriptions based on epitoke forms were not included. NC, number of chaetigers.

**Table 6.** Summary of the main morphological features for the 10 different *Platynereis* MOTUs obtained in this study.

| Species                                    | Distribution   | Pigmentation  | Length (mm)/ NC | Number of jaw teeth | Jaw canals                                       | Paragnaths  | Postero-dorsal tentacular cirri and palps                                | Homogomph falciger  | Spiniger chaetae           | Ligules   |
|--|--|---|-----------------|---------------------|--|---|--|---|----------------------------|---|
| MOTU 1 – <i>Platynereis</i> sp.            | Mediterranean Sea (Banyuls, France)  | Small dots covering most of the anterior region               | Jun-40          | ?                   | ?  | ?   | Reaching chaetigers 9–12   | ?   | ?                          | ?   |
| MOTU 2 – <i>Platynereis</i> sp.            | North-eastern Atlantic (Scandinavia, Portugal)   | Absent  | 12–15/ 35–45    | ?                   | ?  | ?   | Reaching chaetiger 15  | ?   | ?                          | ?   |
| MOTU 3 – <i>Platynereis</i> sp.            | Ionian Sea (Greece)  | ?   | Very small      | ?                   | ?  | ?   | ?  | ?   | ?                          | ?   |
| <b>MOTU 4 – <i>P. dumerilii</i> s.s.</b>   | European Atlantic and Mediterranean coast<br><br><b>Type locality:</b> La Rochelle, France | Small dots covering most of the anterior region (Fig. 6a, 7a) | 7.4–34.9/ 30–76 | 7–9                 | 2 canals. Both close to the inner edge (Fig. 7g) | Area II – double rows; VI – double rows; VII–VIII – continuous band of double rows (Fig. 6b, c) | Reaching chaetigers 9–12 (Fig. 6a). Palpophore twice as long as wide     | One present in notochaetae from the last 5–10 posterior chaetigers (Fig. 7b)  | Lightly serrated (Fig. 7c) | Less globular from chaetiger 11–13. Dorsal cirri much longer in anterior body. Posterior body: dorsal ligule 1.8–2× width of median one; Neuracicular ligule long (Fig. 6d–f) |
| MOTU 5 – <i>Platynereis</i> sp.            | Atlantic (Canary Islands)  | Small dots covering most of the anterior region.              | 10–20/45        | ?                   | ?  | ?   | Reaching chaetigers 5–7  | ?   | ?                          | ?   |
| <b>MOTU 6 – <i>P. jourdei</i> sp. nov.</b> | West Mediterranean Sea (eastern Spain, Italy)<br><br><b>Type locality:</b> Calpe, Spain    | Similar to MOTU 4 but with lower dot density (Fig. 8a, 9a, b) | 6–26/ 25–71     | 8–9                 | 2 canals. One close to the outer edge (Fig. 9g)  | Area II – double rows; VI – double rows; VII–VIII – continuous band of double rows (Fig. 8b, c) | Reaching chaetigers 9–12 (Fig. 8a). Palpophore slightly longer than wide | Two present in notochaetae from the last 5–10 posterior chaetigers (Fig. 9d). | Lightly serrated (Fig. 9e) | Less globular from chaetiger 11–13. Dorsal cirri much longer in anterior body. Posterior body: dorsal ligule 1.8–2× width of median one; Neuracicular ligule long (Fig. 8e–g) |

(Continued on next page)

**Table 6.** (Continued)

| Species   | Distribution  | Pigmentation  | Length (mm)/ NC | Number of jaw teeth | Jaw canals                                       | Paragnaths  | Postero-dorsal tentacular cirri and palps                                 | Homogomph falciger  | Spiniger chaetae             | Ligules   |
|---|---|---|-----------------|---------------------|--|---|---|---|------------------------------|---|
| <b>MOTU 7 –<br/><i>P. nunezi</i><br/>sp. nov.</b> | Northern Atlantic (Macaronesia Islands, Morocco)<br><br><b>Type locality:</b> Tenerife, Spain                   | Usually ring-like in segment I; semi ring-like pattern may appear in the anterior region (Fig. 10a, 11a, g) | 7.4–15/33–49    | 7–9                 | 2 canals. One close to the outer edge (Fig. 11i) | Area II – absent; VI – group of 3 rows; VII–VIII – continuous band of single rows (Fig. 10b, c) | Reaching chaetigers 5–7 (Fig. 10a). Palpophore slightly longer than wide  | One present in notochaetae from the last 5–10 posterior chaetigers (Fig. 11d, e)                | Lightly serrated (Fig. 11f)  | Less globular from chaetiger 8–9. Dorsal cirri uniformly longer throughout the body. Posterior body: dorsal ligule 2.6–2.8× width of median one; Neuracicular ligule very short (Fig. 10d–f)  |
| MOTU 8 –<br><i>Platynereis</i> sp.                | North-eastern Atlantic (Porto Santo island, Madeira)  | Ring-like in segment I; semi ring-like pattern may appear in the anterior region                            | 11–15/40        | ?                   | ?  | ?   | Reaching chaetigers 5–7   | ?   | ?                            | ?   |
| <b>MOTU 9 –<br/><i>P. cf. massiliensis</i></b>    | Southern European Atlantic and West Mediterranean coast, Morocco<br><br><b>Type locality:</b> Marseille, France | Ring-like in most of the anterior segments or as scattered dots throughout the body (Fig. 12a, d, e, 13a)   | 4.6–26.4/23–55  | 8–9                 | 2 canals. One close to the outer edge (Fig. 13g) | Area II – absent; VI – group of 3 rows; VII–VIII – continuous band of single rows (Fig. 12b, c) | Reaching chaetigers 5–7 (Fig. 12a). Palpophore slightly longer than wide  | One present neurochaetal supracular fascicle from the last 5–10 posterior chaetigers (Fig. 13b) | Coarsely serrated (Fig. 13e) | Less globular from chaetiger 10–12. Dorsal cirri uniformly longer throughout the body. Posterior body: dorsal ligule 1.9–2.1× width of median one; Neuracicular ligule very short (Fig. 6f–h) |
| <b>MOTU 10<br/><i>P. agilis</i></b>               | European Atlantic and Western Mediterranean Spanish coast<br><br><b>Type locality:</b> St Vaast, France         | Absent (Fig. 4a, 5a)  | 6.29–12/25–50   | 7–8                 | 2 canals. One close to the outer edge (Fig. 5g)  | Area II – absent; VI – group of 3 rows; VII–VIII – continuous band of single rows (Fig. 4b, c)  | Reaching chaetigers 10–15 (Fig. 4a). Palpophore slightly longer than wide | One present in notochaetae from the last 5–10 posterior chaetigers (Fig. 5b)                    | Coarsely serrated (Fig. 5d)  | Less globular from chaetiger 8–9. Dorsal cirri much longer in median body. Posterior body: dorsal ligule 3.6× width of median one; Neuracicular ligule very short (Fig. 4d–f)                 |

Species in bold correspond to those described in the taxonomic section. Pigmentation as seen in preserved samples. Serration type in spiniger chaetae at the base of blade. NC, number of chaetigers.

## Diagnosis (emended from Glasby 2015, p. 230)

Frontal antennae present, 1 pair. Palpophore with transverse groove present, palpostyles conical. Prostomium with entire anterior margin. Eyes present, 2 pairs. One apodous anterior segment, longer than chaetiger 1. Tentacular cirri with distinct cirrophores. Jaws with dentate cutting edge. Maxillary ring of pharynx with paragnaths; pectinate rows (**may be absent**). Oral ring paragnaths present; pectinate rows. Dorsal notopodial ligule present. Prechaetal notopodial lobe present. Ventral notopodial ligule present. Dorsal cirrus simple, lacking basal cirrophore. Neuropodial postchaetal lobe absent. Ventral neuropodial ligule of anterior chaetigers present. Ventral cirri single. Notoaciculae absent from segments 1 and 2. Notochaetae with homogomph spinigers, homogomph falcigers (may be absent); terminal tendon present with articulation fused on some segments. Neurochaetae supracular fascicle with homogomph spinigers, heterogomph falcigers; blades having teeth only slightly longer proximally than distally. Neurochaetae subacicular fascicle with heterogomph spinigers, heterogomph falcigers; blades either lacking **or with a** distinct tendon on terminal tooth. Anal cirri cirriform or conical.

## Remarks

The presence of a prechaetal notopodial lobe as stated by Glasby 2015, was either not observed or the lobe was not well developed in the *Platynereis* species from this work, but this result could be related to the slide preparation and contraction of the parapodia. Additionally, absence of paragnaths in Area II from the maxillary ring and heterogomph falcigers with a distinct terminal tendon seem to be a key feature in some species from the *P. dumerilii* complex analysed in our study and the diagnosis of the genus is therefore emended accordingly.

## *Platynereis dumerilii* species complex

### Diagnosis

Prostomium cordiform. Antennae present, shorter than or subequal to palp length. Palps consist of a palpophore and oval palpostyles. Two pairs of eyes, anterior pair more widely spaced than posterior pair. Four pairs of tentacular cirri with distinct cirrophores and considerably long postero-dorsal cirri reaching chaetigers 5–15. Apodous anterior segment longer than chaetiger 1. Eversible pharynx with one pair of jaws, each with two longitudinal canals emerging from the pulp cavity. Maxillary and oral ring of pharynx with rod-like paragnaths, arranged in tight rows. Maxillary ring: Area I, absent; Area II, absent or with two slightly oblique or parallel rows in rectangular patch; Area III, three main transverse lines of short rows (distal, 4–5 rows; medial, 3–5 rows; proximal, 1–6 rows) in triangular patch; Area IV, five rows varying in length (distal, long rows; medial, intermediate length rows;

proximal, short rows) in pyramidal arrangement. Oral ring: Area V, absent; Area VI, forming a group of three transverse rows or double parallel rows; Areas VII–VIII, one or two ridge rows composed of paragnaths grouped in 5 small rows, in a single band (furrow regions without paragnaths). Dorsal cirri cirriform, longer than dorsal ligule. Dorsal ligule digitiform, uneven throughout body, becoming barely expanded and less globular usually from the first 10 parapodia. Homogomph spinigers with blades lightly or coarsely serrated, evenly spaced; absent in subacicular neurochaetae. Heterogomph spinigers with blades lightly or coarsely serrated, evenly spaced; absent in notochaetae and supracular neurochaetae. Heterogomph falcigers with short blades present in neurochaetae. Homogomph falcigers with long blade present in the posteriormost chaetigers.

## Remarks

*Platynereis dumerilii* has been part of a known cryptic complex where previous studies have reported this species as being apparently morphological identical to *P. massiliensis* but distinguishable based on the different reproductive features and life histories (Hauenschild 1951; Schneider *et al.* 1992; Valvassori *et al.* 2015; Wäge *et al.* 2017). However, remarkable morphological variation in the pharynx paragnath patterns and number of teeth per half jaw has been reported in the analysis of large numbers of individuals of the different forms of *P. dumerilii* by several authors (Malmgren 1867; Ehlers 1868; Claparède 1870). For example, and as pointed out by Claparède (1870), the oral ring of the pharynx is indicated by Malmgren (1867) as carrying seven small combs of denticles (paragnaths) on the ventral side (Areas VII–VIII) and two on the dorsal side (Area VI). This is in contrast to Claparède's (1870) observations who only encountered five on the ventral side. Ehlers (1868) also gives a description of paragnath distribution that differs from that of Malmgren (1867), where he assigns six groups of denticles to the ventral side of the oral ring (Areas VII–VIII). Moreover, Claparède (1870) often noted the absence of combs of denticles in the middle of the ventral side of the maxillary ring (Area III), especially in small individuals and that, when present, these are extremely variable in dimensions. Sometimes these are double, sometimes simple or represented by 2 or 3 isolated denticles. Furthermore, Claparède (1870) also observed complete paragnath absence at the dorsal side of the oral ring (Areas V, VI). Claparède (1870) also mentioned that sometimes the paragnaths are equally long and wide, and at other times four or five times as long as wide. Indeed, even in *P. massiliensis*, as originally described by Moquin-Tandon (1869), complete absence of paragnaths was reported. These differences could be related to phenotypic variability, pseudo-cryptic diversity, specimen age or even due to sampling techniques. Jaw morphology also seems to present striking variation among specimens as pointed out by Claparède (1870).

The size of the anterior toothed region relative to the posterior muscular one varies greatly regardless of specimen size and age, e.g. the jaws of fig. 1a and 2b of Claparède (1870, p. IV) are taken from two individuals of the same size at the time of the transformation into a *heteronereis*, and in the first, the muscular region is longer than the toothed one, whereas in the second figure the muscular region is practically null. Claparède (1870) also observed remarkable variation in the number of teeth, with these fluctuating between five and twenty per half jaw. Claparède (1870) advised restraint in associating old specimens with higher numbers of teeth, e.g. in large heteronereidids, there were rarely more than seven to eight teeth with a maximum of ten. On the contrary, the jaw with nineteen teeth presented in Claparède (1870, pl. IV, fig. 3) is taken from an individual only 2 cm long. Additionally, the jaws in fig. 1a and 2b of Claparède (1870, p. IV), taken from individuals of the same size at the time of the metamorphosis into *heteronereis*, have six and ten teeth respectively. Malmgren (1867) attributes twelve or thirteen teeth to the jaws of *P. dumerilii*, and Ehlers (1868) only five or six teeth, again showing remarkable variation that does not seem to be associated with specimen age but could reflect either phenotypic variability or evidence of possible cryptic lineages.

Increasing availability of relatively cheap molecular tools enabled morphological observations to be complemented with DNA data to clarify these taxonomic ambiguities and screening for potential cryptic diversity. Molecular data already revealed two additional Italian lineages with the same apparent morphotype as *P. dumerilii* and *P. massiliensis* (Wäge et al. 2017). Given that the study mixed genetic methodologies with reproductive features of four different *Platynereis* lineages, this allowed us to match our own COI data with Wäge et al. (2017) to better understand the dynamics and differences found in the complex. This enabled the association of two molecular lineages sharing the same reproductive features as *P. massiliensis* (egg brooders; our MOTUs 1 and 9, Fig. 2) and two other clades matching *P. dumerilii* (*heteronereis* stage; our MOTUs 4 and 6, Fig. 2). The reproductive history is therefore still unknown for six other European MOTUs. Two main morphotypes based on paragnath pattern variation seem to match the differences found in the reproductive features, dividing this complex into two main groups: the *dumerilii*-type (Clade A2, Fig. 2) and the *massiliensis*-type (Clade A3, Fig. 2), with paragnath variations found mainly in Areas II and III. The *massiliensis*-type, corresponding to the egg brooders, lacks paragnaths in Area II and the triangular arrangement on Area III points distally (to maxillae) opposed to the *dumerilii*-type that points basally (to the apodous segment) and have paragnaths in Area II. Unfortunately, observing paragnath patterns in the very small specimens from MOTU 1 (Clade A1, Fig. 2) that also grouped with the egg brooders from Wäge et al. (2017) was not possible; and no reproductive information is yet known for *P. agilis* comb. nov. (MOTU 10) that is genetically very close and sister to MOTU 9 (*P. cf. massiliensis*), therefore a 100% match

between paragnath patterns and reproduction type was not possible to confirm currently.

The detailed descriptions of five of the ten European lineages (mainly obtained from intertidal samples) belonging to the *P. dumerilii* species complex are provided below, namely for: *P. agilis* comb. nov., *P. dumerilii* s.s., *P. jourdei* sp. nov., *P. nunezi* sp. nov. and *P. cf. massiliensis*. The five remaining lineages remain unnamed due to the lack of sufficient specimens to attempt an adequate description, but both molecular and geographic distributions associated with these MOTUs provide a great starting point for future research (Table 6, Fig. 2). All of these lineages from the *Platynereis dumerilii* pseudo-cryptic complex are phylogenetically very close to each other, both in topology and genetic distances (19.4% (4.4–26.6%) COI K2P, Fig. 2), contrasting to what is observed between the other non-cryptic species used as outgroups (26% (18.1–33.6%) COI K2P, Fig. 2). Recently, a South African taxon formerly thought to be *P. dumerilii* was ascribed to a new species: *P. entshonae* Kara, Santos, Macdonald & Simon, 2020. This was achieved based mainly on molecular data, with principal component analysis scores revealing no separation based on morphological characters (Kara et al. 2020). However, the study also reported shorter postero-dorsal tentacular cirri (up to chaetigers 6–8, opposed to 9–12 found in topotypic specimens from *P. dumerilii* in our study) and a unique bidentate notopodial homogomph falciger, that could distinguish this new species from the original *P. dumerilii* that lacks the bidentate feature. Based on tentacular cirrus size, paragnath patterns and presence of homogomph falcigers in the notopodium, the new South African species appear to be similar to our *P. nunezi* sp. nov. However, *P. entshonae* is phylogenetically very divergent from the remaining lineages of the complex, instead grouping close to the outgroup *Pseudonereis* sp. Unlike *P. entshonae*, an additional unnamed South African lineage (MOTU GB1, Fig. 2, with high bootstrap support) from Kara et al. (2020) grouped within the *P. dumerilii* complex and is phylogenetically very close to *P. cf. massiliensis* and *P. agilis* comb. nov. (10 and 10.2% COI mean K2P respectively), opening the possibility for additional non-European lineages that could be added to the *P. dumerilii* complex in future research.

## Key to the five European *Platynereis* species described in this study

1. Homogomph falcigers present in the supracicular fascicle of posterior neuropodia. Notopodial homogomph falcigers absent.....  
.....*P. cf. massiliensis*
- Homogomph falcigers absent in posterior neuropodia; homogomph falciger present in posterior notopodia.....2
- 2(1) With 2 notopodial homogomph falcigers.....*P. jourdei* sp. nov.
- With 1 notopodial homogomph falciger.....3
- 3(2) Double row of rod-like paragnaths present in Area II of the pharynx; 2 jaw canals, both close to the inner edge.....*P. dumerilii* s.s.
- Paragnaths absent in Area II of the pharynx; 2 jaw canals, one of which is closer to the outer edge.....4



- 4(3) Spiniger chaetae with coarsely serrated blades; postero-dorsal cirri very long, reaching chaetigers 10–15.....*P. agilis* comb. nov.  
 Spiniger chaetae with lightly serrated blades; postero-dorsal cirri short, reaching chaetigers 5–7.....*P. nunezi* sp. nov.

***Platynereis agilis* (Keferstein, 1862), comb. nov., reinstated**

(Fig. 4, 5)

ZooBank: urn:lsid:zoobank.org:act:9A71F6CB-2626-4865-A6D7-2CA9975DC667

*Nereis agilis* Keferstein, 1862, pp. 97–99, taf. VIII, fig. 8–11.

**Material examined**

Spain (Balearic Sea), Calpe: 5 spms, DBUA0002421.01.v01-v05, 38°38'23.8"N, 0°03'30.0"E, low tide, among algae, collected by Pedro E Vieira, 05/08/2019. Portugal, Arrabida Natural Park (Lisbon): 23 spms, MB29-000369–MB29-000375, MB29-000377–MB29-000383, DBUA0002519.01.v01-v03, DBUA0002519.01, 38°26'13.1"N, 9°03'47.3"W, 9-m depth, among algae, kindly provided by the National Museum of Science and Natural History (MUHNAC, Portugal), 22/09/2014. France, Morlaix Bay: 2 spms, DBUA0002422.01.v01, MTPD191-20, 48°43'48.0"N, 3°59'09.6"W, low tide, among algae, collected by Celine Houbin, 17/09/2020. Great Britain, Plymouth: 1 spm, DBUA0002423.01.v01, 50°21'35.4"N, 4°09'01.8"W, low tide, among algae, collected by Felicia Ulltin, 27/03/2017.

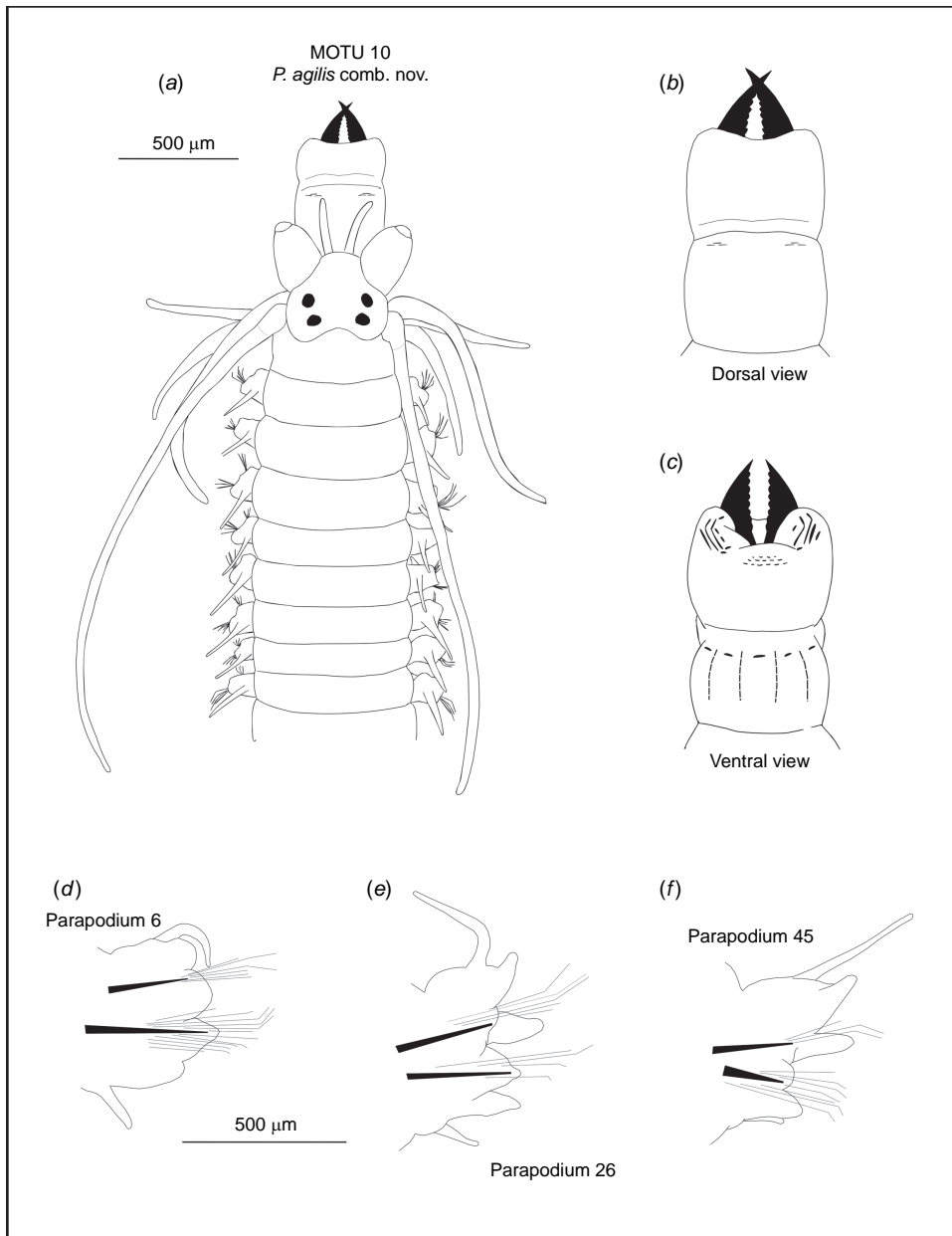


**Fig. 4.** *Platynereis agilis* comb. nov. (MOTU 10). (a) Dorsal view of the anterior region with absence of pigmentation; prostomium and pharynx based on Portuguese samples (MB29-000373; MB29-000377; DBUA0002519.01.v02; DBUA0002519.01.v03). (b) Dorsal view of the pharynx. (c) Ventral view of the pharynx. (d) 10th parapodium, posterior view (DBUA0002519.01.v03). (e) 28th parapodium, posterior view (DBUA0002519.01.v03). (f) 45th parapodium, posterior view (DBUA0002519.01.v03).

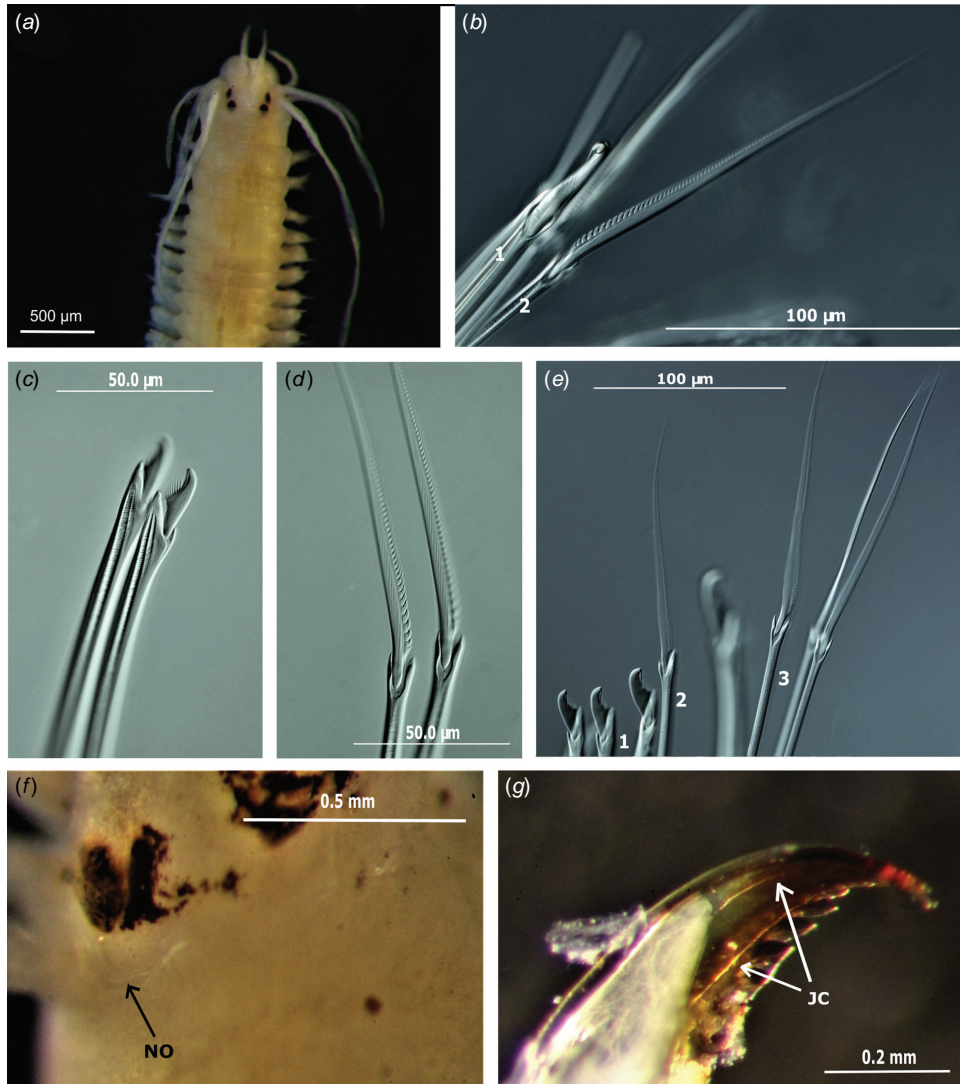


**Fig. 5.** *Platynereis agilis* comb. nov. (MOTU 10). (a) Absence of pigmentation as seen in a preserved specimen (MB29-000373). (b) Notochaetae: homomorph falciger (1), homomorph spiniger with coarsely serrated blades (2), chaetiger 50 (DBUA0002519.01.v01). (c) Neurochaeta, subacicular fascicle: heteromorph falcigers, chaetiger 10 (MB29-000373). (d) Notochaetae: homomorph spinigers with coarsely serrated blades, chaetiger 10 (MB29-000373). (e) Neurochaetae, subacicular fascicle: heteromorph falcigers (1), heteromorph spiniger (2); supracicular fascicular: homomorph spinigers (3), chaetiger 30 (DBUA0002519.01.v01). (f) Microscope image with the presence of nuchal organs (NO) in specimen DBUA0002421.01.v04. (g) Jaw image with two canals (JC), one of which is closer to the outer edge (DBUA0002519.01.v01).

## Diagnosis

Specimens with no pigmentation, well separated antennae; palpophores almost as long as wide; nuchal organs deeply embedded, slightly oblique, shorter than or subequal in width to posterior eyes; postero-dorsal tentacular cirri almost twice as long as antero-dorsal ones, reaching chaetigers 10–15. Jaws with 2 canals, one of which is closer to the outer edge. Approximately 25–55 chaetigers. Maxillary ring: Area I, absent; Area II, absent; Area III, three main transverse lines of short rows (distal, 4 rows; medial, 5 rows;

proximal, 6 rows) in triangular patch; Area IV, five rows varying in length (distal, medium rows; medial, long rows; proximal, short rows) in pyramidal arrangement. Oral ring: Area V, absent; Area VI, forming a group of three short transverse rows (distal, 1 row; proximal, 2 rows); Areas VII–VIII, one ridge row composed of rod-like paragnaths grouped in 5 small rows (1 paragnath rows per ridge), furrow regions without paragnaths. Dorsal ligule digitiform, uneven throughout body, becoming barely expanded and less globular from chaetigers 8–9; 3.6 times width of median

ligule in posterior parapodia. Neuroacicular ligule large, triangular, longer than globular ventral ligule in anterior parapodia; shorter than triangular ventral ligule from mid-body parapodia; much shorter and narrower than the ventral ligule in posterior parapodia. Dorsal cirrus cirriform, longer than dorsal ligule throughout the body; much longer in median body. Ventral cirrus cirriform, shorter than ventral ligule. Homogomph spinigers with blades coarsely serrated, evenly spaced; present in notopodia and neuropodial supracular fascicles. Heterogomph spinigers as homogomph ones; present in neuropodial subacicular fascicle. Heterogomph falcigers with short, incurved blades with a terminal tendon, present in both neuropodial fascicles. One homogomph falciger with long, incurved blades with a terminal tendon present in the notopodia of posteriormost chaetigers.

### Molecular data

*COI*, *16S* and *28SD2* sequences as in specimens MB29-000369–MB29-000375, MB29-000377–MB29-000383, DBUA0002421.01.v01–v05, DBUA0002422.01.v01, MTPD191-20 and DBUA0002423.01.v01 (Supplementary Table S2). Phylogenetic relationship within the *Platynereis dumerilii* pseudo cryptic complex as in Fig. 2, belonging to MOTU 10, with high support values and low intraspecific (<3%) genetic divergence for both the mitochondrial and nuclear markers. Interspecific *COI* mean distances to the closest and most distant neighbour are 5% (K2P, *P. cf. massiliensis*) and 24.2% (K2P, MOTU 5) respectively. DOI for the species' BIN for the Northeast Atlantic clade: doi:10.5883/BOLD:AEE0899.

### Distribution and habitat

Northeast Atlantic to the West Mediterranean Sea, from Great Britain to Mediterranean Spain. Found in rocky beaches among algae in intertidal or subtidal habitats.

### Reproduction

The claim by Keferstein (1862) of hermaphroditism has not been confirmed by recent studies, but given the genetic proximity for this species to the nearest neighbour (MOTU 9, *P. cf. massiliensis*), this possibly shares the same hermaphrodite features, egg brooding and lecithotrophic larval stages (Wäge *et al.* 2017).

### Description

Specimens used: DBUA0002519.01.v02; DBUA0002421.01.v01, DBUA0002421.01.v04; DBUA0002519.01.v01 and DBUA0002519.01.v03.

### Body measurements

Non-type, DBUA0002519.01.v02, atoke, complete, total length = 12 mm, L15 = 3.875 mm, W15 = 0.9375 mm, and

55 chaetigers. Non-types, DBUA0002421.01.v01, DBUA0002421.01.v04; DBUA0002519.01.v01 and DBUA0002519.01.v03, smaller, posteriorly incomplete, TL = 6.29–11 mm, L15 = 3.51–3.775 mm, W15 = 0.5–0.90 mm, with 25–55 chaetigers.

### Pigmentation

Preserved specimens pale yellowish without pigmentation (Fig. 4a, 5a). The apodous anterior segment lacks a ring-like dot pattern (Fig. 5a). No pigmentation appears to be present in the middle and posterior part of the dorsal body adjacent to the parapodia.

### Head

Prostomium cordiform (Fig. 4a); approximately as long as wide. Palps with an oval palpostyle; palpophore slightly longer than wide, shorter than the entire length of prostomium. Antennae separated, gap between two antennae subequal of antennal diameter (Fig. 4a); digitiform, slender, subequal to the length of the palpophore. Eyes black, anterior and posterior pairs well separated (Fig. 4a, 5a). Anterior pair of eyes round to oval, wider than antennal diameter; posterior pair of eyes round to oval, subequal to anterior pair. Nuchal organs deeply embedded, slightly oblique, shorter than or subequal to posterior eyes (Fig. 5f).

### Apodous anterior segment and tentacular cirri

Apodous anterior segment 3 times wider than long, slightly longer but narrower than chaetiger 1. Tentacular cirri pattern: postero-dorsal cirri twice as long as the antero-dorsal ones; antero-ventral cirri slightly shorter than postero-ventral one. Antero-dorsal cirri reaching chaetigers 4–5; antero-ventral twice as longer as palpophore. Postero-dorsal reaching chaetigers 10–15. Dorsal cirrophores wrinkled, cylindrical; postero-dorsal cirrophores slightly longer, 1.4 times the length of postero-ventral wrinkled ones.

### Pharynx

Jaws dark brown to yellow-amber and finely toothed until a short distance as wide as 2 teeth from the tip, with 7–8 denticles; 2 longitudinal canals emerging from pulp cavity, one of these closer to the outer edge (Fig. 5g). Pharynx consisting of maxillary and oral ring with rod-like paragnaths (Fig. 4b, c) arranged in tight rows: Areas I, II and V, absent; Area III, three main transverse lines of short rows (distal, 4 rows; medial, 5 rows; proximal, 6 rows) in triangular patch; Area IV, forming five rows varying in length (distal, medium rows; medial, large rows; proximal, short rows) in pyramidal arrangement; Area VI, forming a group of three short transverse rows (distal, 1 row; proximal, 2 rows); Areas VII–VIII, one ridge row composed of rod-like paragnaths grouped in five small rows (1 paragnath row per ridge), furrow regions without paragnaths.

## Notopodia

Dorsal cirrus cirriform, longer than dorsal ligule throughout body; much longer than ligule in median body (Fig. 4d–f), 1.1–1.3 times longer in anterior parapodia (Fig. 4d), 1.5–1.6 times longer in median (Fig. 4e), 1.3–1.4 times longer in posterior ones (Fig. 4f); cirrus longer than length of proximal part of dorsal ligule from median body, subequal to slightly longer in anterior parapodia (Fig. 4e); cirri inserted subdistally in anterior parapodia (Fig. 4d), one-half in median and posterior ones (Fig. 4e, f). Dorsal ligule digitiform, uneven throughout body, becoming barely expanded and less globular from chaetigers 8–9; 3.6 times width of median ligule in posterior parapodia (Fig. 4f). Distal part of dorsal ligule bluntly conical in anterior parapodia, conical from median parapodia; much shorter than proximal one in anterior parapodia (Fig. 4d), subequal to proximal in median and posterior ones (Fig. 4e, f). Dorsal ligule barely longer than median ligule in anterior parapodia (Fig. 4d), 1.3 times to this from median ones (Fig. 4e, f). Dorsal and median ligules round from chaetigers 3–4 to 8–9. Median ligule triangular from median parapodia. Notopodial prechaetal lobe not observed.

## Neuropodia

Neuracicular ligule triangular, shorter, twice as wide as ventral ligule until median parapodia; subequal to ventral ligule in posterior parapodia (Fig. 4f). Neuracicular ligule much shorter in posterior parapodia. Ventral ligule subequal in length to median ligule in anterior and median parapodia (Fig. 4d, e), 1.5 times smaller from median in posterior ones (Fig. 4f). Ventral cirri cirriform, smaller than ventral ligule throughout body. Neuropodial postchaetal lobe absent.

## Chaetae

Notochaetae with homogomph spinigers and heterogomph falcigers; spinigers with  $\frac{3}{4}$  length of the blade coarsely serrated, evenly spaced (Fig. 5b, d), numerous and present throughout the whole body; falcigers similar to neuropodial ones (Fig. 5c), replaced by a single homogomph falciger with long incurved blades and a distinct terminal tendon in posteriormost chaetigers, usually in the last 5–10 chaetigers (Fig. 5b). Neurochaetal supraticular fascicle with homogomph spinigers and heterogomph falcigers, both present throughout the whole body; spinigers similar to notopodial ones (Fig. 5d), more numerous than falcigers in same fascicle; falcigers with short incurved blades with a terminal tendon, serrated in  $\frac{1}{3}$  the length of blade (Fig. 5c). Neurochaetal subacicular fascicle with heterogomph spinigers and heterogomph falcigers, both present throughout the whole body; spinigers similar to notopodial ones, less numerous than falcigers; falcigers similar to supraticular ones.

## Pygidium

With pair of slender anal cirri, as long as last 9–10 parapodia.

## Remarks

*Platynereis agilis*, originally described as *Nereis agilis* (Keferstein, 1862) from St Vaast (Northern France) and until the present considered as a junior synonym of *P. dumerilii* is here reinstated. Like *N. agilis*, the current synonym *N. megodon* (Quatrefages, 1866) also seems to fit the morphological description for this species, which is apparently synonymous with *N. agilis*. The latter name was chosen based on priority.

*Platynereis agilis* comb. nov. is clearly part of the *P. dumerilii* species complex, given the similar morphology and genetic proximity to the other species of this group (Fig. 2, Table 6). However, visible differences can easily be found from *P. dumerilii* s.s.: slightly surpassing half the number of chaetigers in worms of similar length, distinct paragnath arrangement (of *massiliensis*-type), no pigmentation (although this may not always be a reliable character due to fixation in ethanol), disposition of the two jaw canals (one of which closer to the outer edge), anterior parapodia with longer triangular-like ligules, and spinigerous chaetae with coarsely serrated blades. All these differences, along with the genetic distances (mean 21.8% COI K2P), justify the removal from synonymy and re-establishment of the species. *Platynereis agilis* also shares a similar paragnath arrangement and the coarsely serrated chaetae with the species *P. cf. massiliensis*, but greatly differs from the latter due to lack of pigmentation, the longer size of the postero-dorsal cirri, reaching up to chaetiger 15, instead of chaetiger 7, even in specimens with equal or smaller size, absence of neuropodial homogomph falciger and presence of notopodial homogomph falciger in the posteriormost chaetigers. Despite the low genetic COI distance (mean 5% K2P) compared to *P. cf. massiliensis*, the distinct morphological differences justify the resurrection of this species.

*Platynereis agilis* comb. nov. is sympatrically distributed with *P. dumerilii* s.s. and *P. jourdei* sp. nov. in the Western Mediterranean region. On the Northeast Atlantic coast it is probably also sympatric with *P. dumerilii* s.s. although not found during our study, and with MOTU 2 (Fig. 2a, b). This species might be confused with the latter based on preliminary morphological data applied to the unnamed lineage (Table 6), where both lack pigmentation in the dorsal body, share similar postero-dorsal cirrus length (reaching up to chaetiger 15) and a similar number of chaetigers (25–50). However, if paragnath patterns indeed correspond to the respective independent phylogenetic clade, then MOTU 2 might be associated with the *dumerilii*-type in future research (Clade A2, Fig. 2), unlike the *massiliensis*-type as observed in the reinstated species (Clade A3, Fig. 2).

***Platynereis dumerilii* (Audouin & Milne-Edwards, 1833), s.s.**

(Fig. 6, 7)

*Nereis dumerilii* Audouin & Milne Edwards, 1833, pp. 218–219, p. XIII, fig. 10–12.

– Ehlers 1868, pp. 535–542, taf. XX, fig. 21–37.

– McIntosh 1910, p. 302, p. LII fig. 5, LX fig. 10, LXXII fig. 4, LXXXI fig. 4.

*Eunereis africana* Treadwell, 1943.

*Heteronereis fucicola* Örsted, 1843.

*Heteronereis maculata* Bobretzky, 1868.

*Heteronereis malmgreni* Claparède, 1868.

*Iphinereis fucicola* (Örsted, 1843).

*Leontis dumerilii* (Audouin & Milne Edwards, 1833).

*Leptonereis maculata* Treadwell, 1928.

*Mastigonereis quadridentata* Schmarida, 1861.

*Mastigonereis striata* Schmarida, 1861.

*Nereilepas variabilis* Örsted, 1843.

*Nereis (Platynereis) dumerilii* Audouin & Milne Edwards, 1833.

*Nereis (Platynereis) dumerilii striata* (Schmarida, 1861).

*Nereis (Platynereis) striata* (Schmarida, 1861).

*Nereis alacris* Verrill, 1879.

*Nereis antillensis* McIntosh, 1885.

*Nereis dumerilii* Audouin & Milne Edwards, 1833.

*Nereis glasiovi* Hansen, 1882.

*Nereis gracilis* Hansen, 1882.

*Nereis megodon* Quatrefages, 1866.

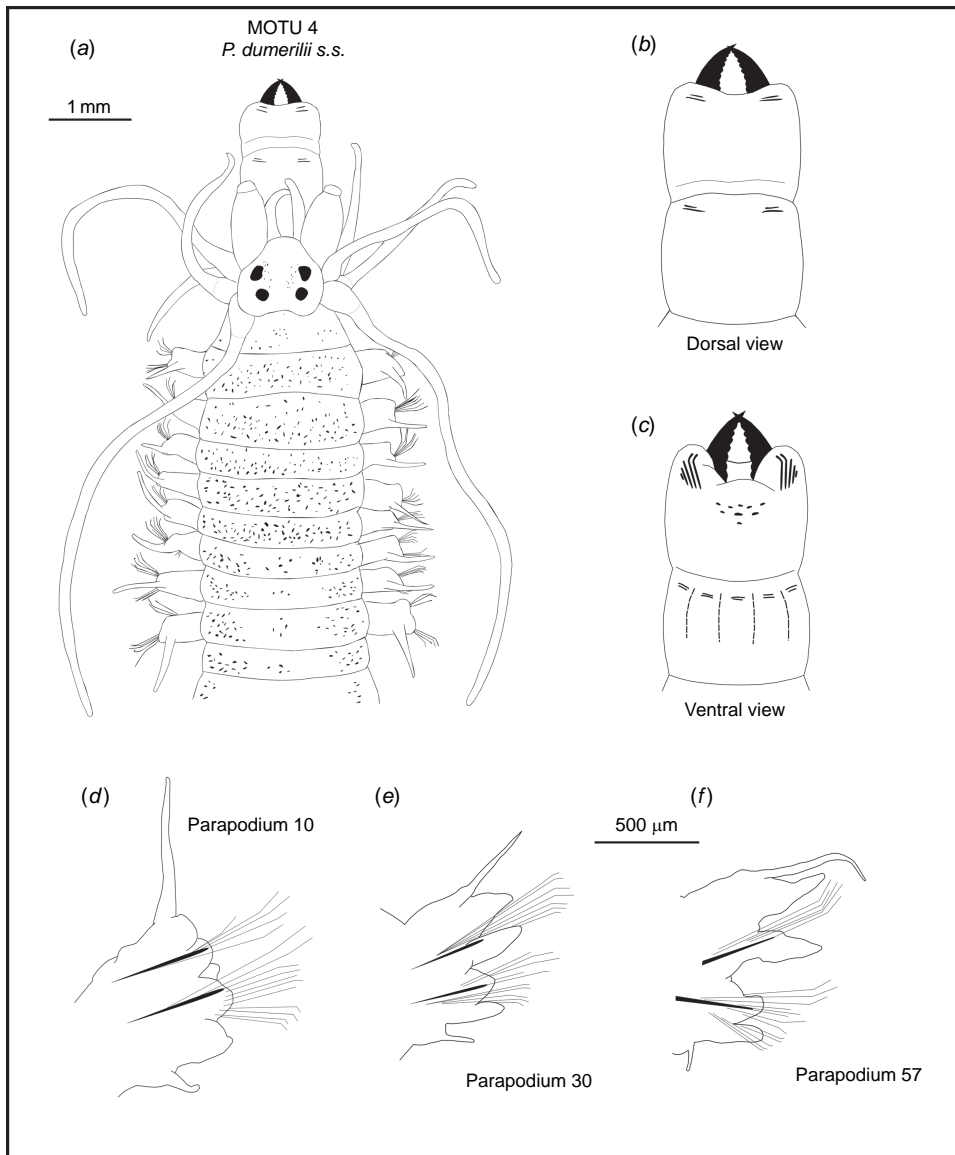


**Fig. 6.** *Platynereis dumerilii* s.s. (MOTU 4). (a) Dorsal view of the anterior region with dot-like pigmentation; prostomium and pharynx based on topotypic material (DBUA0002438.01.v01; DBUA0002438.01.v04; DBUA0002438.01.v07 and DBUA0002438.01.v14). (b) Dorsal view of the pharynx. (c) Ventral view of the pharynx. (d) 10th parapodium, posterior view. (e) 30th parapodium, posterior view. (f) 57th parapodium, posterior view.

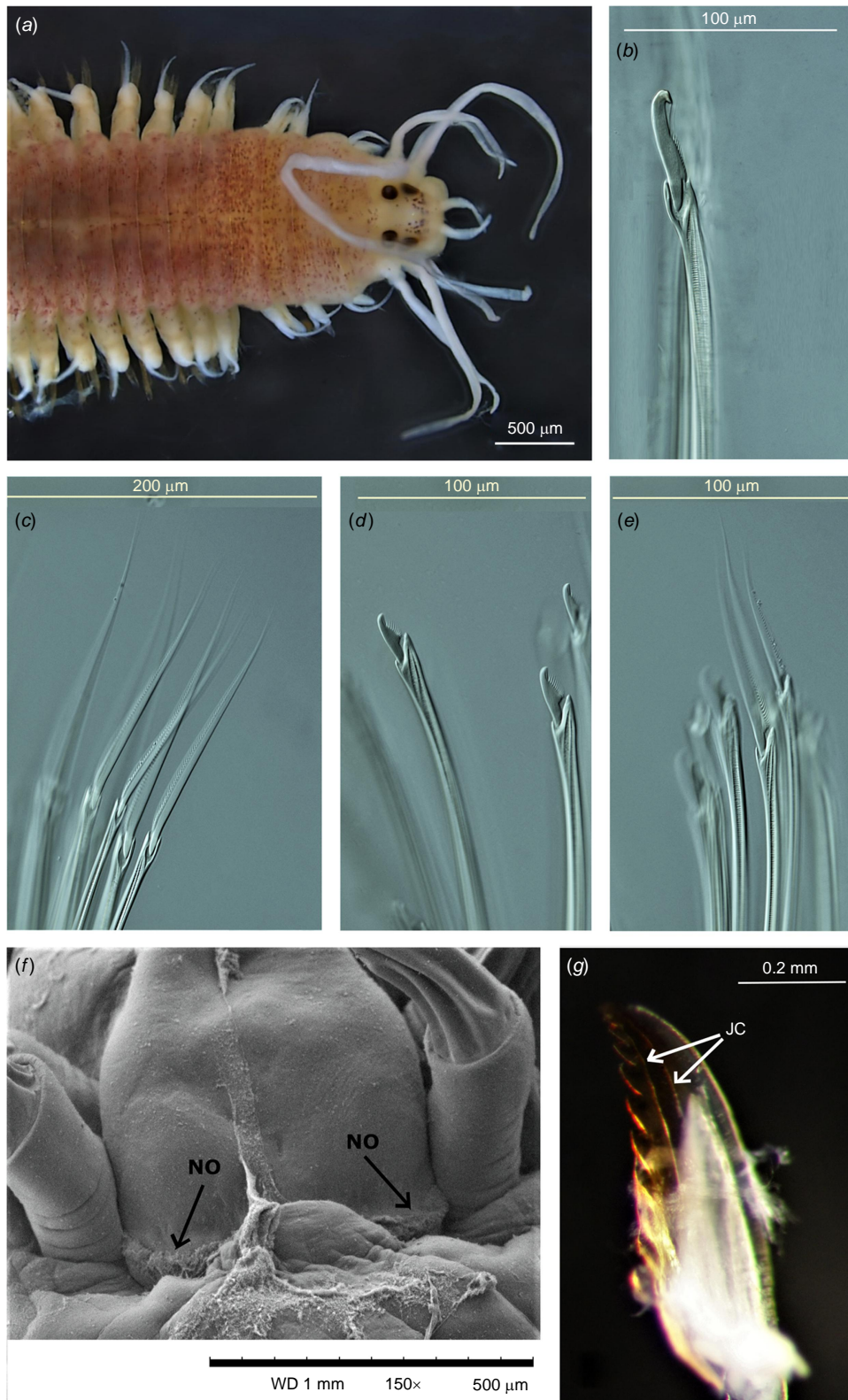


**Fig. 7.** (Caption on next page)

**Fig. 7.** *Platynereis dumerili* s.s. (MOTU 4). (a) Dorsal view, anterior region, pigmentation as seen in a preserved specimen from La Rochelle, France (DBUA0002438.01.v10), with high dot density scattered around the anterior region. (b) Notochaetae: homogomph falciger, chaetiger 57 (DBUA0002438.01.v04). (c) Neurochaeta, supracular fascicle: homogomph spinigers with lightly serrated blades, chaetiger 30 (DBUA0002438.01.v14). (d) Neurochaeta, subacicular fascicle: heterogomph falcigers, chaetiger 30 (DBUA0002438.01.v14). (e) Neurochaeta, subacicular fascicle: heterogomph spinigers, chaetiger 30 (DBUA0002438.01.v14). (f) SEM scan (DBUA0002438.01.v08) of the nuchal organs (NO). (g) Jaw image with two canals (JC) close to the inner edge (DBUA0002438.01.v07). WD, working distance between the sample and the lens.

*Nereis peritonealis* Claparède, 1868.

*Nereis taurica* Grube, 1850.

*Nereis zostericola* Örsted, 1843.

*Platynereis dumerili* [auctt. misspelling].

*Platynereis jucunda* Kinberg, 1865.

*Platynereis striata* (Schmarda, 1861).

*Uncinereis lutea* Treadwell, 1928.

*Uncinereis trimaculosa* Treadwell, 1940.

## Material examined

Sweden, Tjärnö: 10 spms, DBUA0002435.01.v01-v10, 58°52'27.6"N, 11°08'43.4"E, 3–5 m, among algae, collected by Felicia Ulltin and Marcos AL Teixeira, 20/12/2018. Norway, Trondheim: 1 spm, NTNU-VM-76216, 63°26'24.0"N, 10°30'14.4"E, 2-m depth, among algae, collected by Torkild Bakken, 04/09/2018. France, La Rochelle: 17 spms, DBUA0002438.01.v01-v17, 46°08'47.4"N, 1°12'36.0"W, low tide, among red algae, collected by Jérôme Jourde, 18/09/2020. France, Arcachon Bay: 1 spm, DBUA0002439.01.v01, 44°39'44.2"N, 1°09'10.0"W, low tide, among algae, collected by Nicolas Lavesque, 18/09/2020. Portugal, Canto Marinho: 1 spm, DBUA0002436.01.v01, 41°44'13.2"N, 8°52'33.6"W, low tide, among algae, collected by Marcos AL Teixeira, 20/05/2019. Spain (Balearic Sea), Calpe: 2 spms, DBUA0002434.01.v01-v02, 38°38'23.8"N, 0°03'30.0"E, low tide, among algae, collected by Pedro E Vieira, 05/08/2019. Italy (Ligurian Sea), Antignano: 2 spms, DBUA0002437.01.v01-v02, 43°29'32.0"N, 10°19'01.2"E, 3 m, among algae, collected by Joachim Langeneck, 10/09/2019; 3 spms, DBUA0002437.01.v04-v06, 43°29'32.0"N, 10°19'01.2"E, 6 m, among *Posidonia oceanica* rhizomes, collected by Joachim Langeneck, 20/09/2019; 1 spm, DBUA0002437.01.v03, 43°29'32.0"N, 10°19'01.2"E, 3 m, among algae, collected by Joachim Langeneck, 27/06/2019. Italy (Ligurian Sea), Ardenza: 5 spms, DBUA0002437.02.v01-v05, 43°30'43.3"N, 10°18'52.3"E, 2 m, gravel with *Posidonia oceanica* debris, collected by Joachim Langeneck, 18/09/2019. Italy (Ligurian Sea), Vada: 4 spms, DBUA0002437.03.v01-v04, 43°18'39.8"N, 10°25'54.6"E, 10 m, among algae, collected by Joachim Langeneck, 26/10/2019. Italy (Ligurian Sea), Elba Island: 3 spms, DBUA0002437.04.v01-v03, 42°48'41.1"N, 10°19'23.7"E, 3 m, among algae, collected by Joachim Langeneck, 15/01/2020. Italy (Tyrrhenian Sea), Montecristo Island: 7 spms, DBUA0002437.05.v01-v07, 42°20'05.9"N, 10°17'22.3"E, low tide, among algae, collected by Joachim Langeneck, 05/09/2020. Italy (Ionian Sea), Taranto: 1 spm, DBUA0002437.06.v01, 40°27'59.0"N, 17°14'20.0"E, 12-m depth, on mud with shell fragments, collected by Joachim Langeneck, 20/03/2019. Italy (Adriatic Sea), Trieste: 1 spm, DBUA0002437.07.v02, 45°38'51.6"N, 13°45'32.9"E, low tide, among algae, collected by Joachim Langeneck, 19/02/2020. Greece (Ionian Sea), Mazoma: 2 spms, MTPD200-20, MTPD201-20, 39°03'21.3"N, 20°50'00.5"E, low tide, among algae, collected by Katerina Vasileidou, 01/01/2017. Greece (Sea of Crete), Crete: 1 spm, DBUA0002440.01.v01, 35°09'57.6"N, 24°25'17.0"E, 5–10 m, among algae, collected by Giorgos Chatzigeorgiou, 14/03/2020.

## Diagnosis

Specimens with well separated antennae; palpophores much longer than wide; nuchal organs deeply embedded, slightly convex, wider than posterior eyes; postero-dorsal tentacular cirri 2 times longer than antero-dorsal ones, reaching chaetigers 9–12, very rarely to chaetiger 15. High concentration of pigmentation dots may be present throughout the dorsal body. Jaws with 2 canals both close to the inner edge. Approximately 30–75 chaetigers. Maxillary ring: Area I, absent; Area II, with two slightly oblique and parallel rows in rectangular patch; Area III, three main transverse lines of short rows (distal, 5 rows; medial, 3 rows; proximal, 1 row) in triangular patch; Area IV, five rows varying in length (distal, long rows; medial, medium rows; proximal, short rows) in pyramidal arrangement. Oral ring: Area V, absent; Area VI, double parallel rows; Areas VII–VIII, two ridge rows, each composed of rod-like paragnaths grouped in 5 small rows (2 paragnath rows per ridge), in a single band, furrow regions without paragnaths. Dorsal ligule digitiform, uneven throughout body, becoming barely expanded and less globular from chaetigers 11–13; 1.8–2 times width of median ligule in posterior parapodia. Neuroacicular ligule short, rounded in anterior chaetigers, triangular and slightly shorter than ventral ligule from mid-body chaetigers. Dorsal cirri cirriform, longer than the parapodial dorsal ligule throughout the body; much longer in anterior parapodia. Ventral cirri cirriform, much shorter than ventral ligule. Homogomph spinigers with blades lightly serrated, evenly spaced; present in notopodia and neuropodial supracular fascicles. Heterogomph spinigers as homogomph ones; present in neuropodial subacicular fascicle. Heterogomph falcigers with short, incurved blades with a terminal tendon, present in both neuropodial fascicles. One homogomph falciger with long, incurved blades with a terminal tendon present in the notopodia of posteriormost chaetigers.

## Molecular data

*COI*, *16S* and *28SD2* sequences as in specimens DBUA0002434.01.v01–v02, DBUA0002435.01.v01–v10, NTNU-VM-76216, DBUA0002436.01.v01, DBUA0002437.01.v01–v06, DBUA0002437.02.v01–v05, DBUA0002437.03.v01–v04, DBUA0002437.04.v01–v03, DBUA0002437.05.v01–07, DBUA0002437.06.v01, DBUA0002437.07.v02, DBUA0002438.01.v01–v17, DBUA0002439.01.v01, DBUA0002440.01.v01, MTPD200-20 and MTPD201-20 (Supplementary Table S2). Phylogenetic relationship within the *Platynereis*

*dumerilii* pseudo cryptic complex as in Fig. 2, belonging to MOTU 4, with high support values and low intraspecific (<3%) genetic divergence for both the mitochondrial and nuclear markers. Interspecific *COI* mean distances to the closest and distant neighbour are 8.2% (K2P, MOTU 5) and 21.8% (K2P, MOTU 10) respectively. DOI for the species' BIN for the type locality clade: doi:10.5883/BOLD:AAH9446.

### Distribution and habitat

Northeast Atlantic, from Scandinavia to Mediterranean Sea, among green or red algae and gravel with *Posidonia oceanica* rhizomes, in subtidal or intertidal areas.

### Reproduction

A gonochoric species, with a single reproductive event in life (semelparous) transforming into a pelagic epitokous form (*heteronereis*) and a larval stage with planktotrophic development (Wäge et al. 2017). Regarding epitokes, there is little reliable data available from wild populations but long-running laboratory culture of *P. dumerilii* of unstated, probably mixed provenance there are typically 15 pre-natatory segments in males and 21 in females (Fischer and Dorresteijn 2004).

### Description

Specimens used: DBUA0002434.01.v01 and topotypic material DBUA0002438.01.v01, DBUA0002438.01.v04, DBUA0002438.01.v07, DBUA0002438.01.v08 and DBUA0002438.01.v14.

### Body measurements

Non-type, DBUA0002438.01.v01, atoke, complete, total length = 34.9 mm, L15 = 5.65 mm, W15 = 1.20 mm, and 76 chaetigers. Non-types, DBUA0002438.01.v04, DBUA0002438.01.v07, DBUA0002438.01.v08 and DBUA0002438.01.v14, DBUA0002434.01.v01, smaller, posteriorly incomplete, TL = 7.4–26 mm, L15 = 3.2–4.55 mm, W15 = 0.5–0.92 mm, with 30–75 chaetigers.

### Pigmentation

Preserved specimens yellowish-brown or yellowish-red, with small pigmentation dots covering most of the anterior dorsal region and the prostomium area adjacent to the eyes (Fig. 6a, 7a). The apodous anterior segment lacks a ring-like dot pattern, instead with presence of irregular scattered pigmentation dots (Fig. 7a). Pigmentation may be present in the middle and posterior part of the dorsal body adjacent to the parapodia.

### Head

Prostomium cordiform (Fig. 6a); approximately as long as wide. Palps with an oval, pronounced palpostyle (Fig. 6a);

palpophore long, twice as long as wide, slightly surpassing the entire length of prostomium. Antennae separated, gap subequal of antennal diameter (Fig. 6a); digitiform, slender, extending backward to equal the size of prostomium. Eyes black, anterior and posterior pairs well separated (Fig. 6a, 7a). Anterior pair of eyes circular to oval, wider than antennal diameter; posterior pair of eyes round to oval, slightly smaller than anterior pair. Nuchal organs deeply embedded, slightly convex, wider than posterior eyes (Fig. 7f).

### Apodous anterior segment and tentacular cirri

Apodous anterior segment 3.5 times wider than long, slightly longer but narrower than chaetiger 1. Tentacular cirri pattern: postero-dorsal cirri twice as long as antero-dorsal ones; antero-ventral cirri slightly shorter than postero-ventral one. Antero-dorsal cirri reaching chaetigers 3–5; antero-ventral two times longer than palpophore. Postero-dorsal reaching chaetigers 9–12. Dorsal cirrophores wrinkled, cylindrical; postero-dorsal cirrophores longest, twice as long as the postero-ventral wrinkled ones.

### Pharynx

Jaws dark brown to yellow-amber and finely toothed until a short distance as wide as 2 teeth from the tip, with 7–9 denticles; 2 longitudinal canals emerging from pulp cavity, both close to the inner edge (Fig. 7g). Pharynx consisting of maxillary and oral rings (Fig. 6b, c) with rod-like paragnaths arranged in tight rows: Areas I and V, absent; Area II, two slightly oblique and parallel rows in rectangular patch; Area III, three main transverse lines of short rows (distal, 5 rows; medial, 3 rows; proximal: 1 row) in triangular patch; Area IV, forming five rows varying in length (distal, long rows; medial, medium rows; proximal, short rows) in pyramidal arrangement; Area VI, forming double parallel rows; Areas VII–VIII, two ridge rows, each composed of rod-like paragnaths grouped in 5 small rows (2 paragnath rows per ridge) in a single band, furrow regions without paragnaths.

### Notopodia

Dorsal cirrus cirriform, longer than dorsal ligule throughout body; much longer than ligule in first 11–13 parapodia (Fig. 6d), 1.5–1.7 times longer in anterior parapodia (Fig. 6d), 1.4–1.5 times longer in median (Fig. 6e), 1.3–1.4 times longer in posterior ones (Fig. 6f); cirrus longer than length of proximal part of dorsal ligule throughout body (Fig. 6d–f); cirri inserted subdistally in anterior parapodia (Fig. 6d), one-half in median and posterior ones (Fig. 6e, f). Dorsal ligule digitiform, uneven throughout body, becoming barely expanded and less globular from chaetigers 11–13; 1.8–2 times width of median ligule in posterior parapodia (Fig. 6f). Distal part of dorsal ligule bluntly conical in anterior parapodia, conical from median parapodia; much shorter than proximal in anterior parapodia (Fig. 6d), subequal to proximal



in median and posterior ones (Fig. 6e, f). Dorsal ligule barely longer than median ligule in anterior parapodia (Fig. 6d), subequal to this from median ones (Fig. 6e). Dorsal and median ligules round from chaetigers 4–5 to 11–13. Median ligule triangular-shaped starting from median parapodia. Notopodial prechaetal lobe not observed.

### Neuropodia

Neuracicular ligule triangular, shorter, twice as wide as ventral ligule from median parapodia (Fig. 6e); subequal to ventral ligule in anterior parapodia (Fig. 6d). Ventral ligule subequal in length to median ligule in anterior parapodia (Fig. 6d), 1.6 times smaller than median (Fig. 6e) and 1.8 times than posterior ones (Fig. 6f). Ventral cirri cirri-form, smaller than ventral ligule throughout body. Neuropodial postchaetal lobe absent.

### Chaetae

Notochaetae with homogomph spinigers and heterogomph falcigers; spinigers similar to neuropodial ones (Fig. 7c), numerous and present throughout the whole body; falcigers similar to neuropodial ones (Fig. 7d), replaced by a single homogomph falciger with long incurved blades and a terminal tendon, serrated in  $\frac{1}{2}$  the length of blade, present only in the posteriormost chaetigers (Fig. 7b), usually in the last 5–10 chaetigers. Neurochaetal supracicular fascicle with homogomph spinigers and heterogomph falcigers, both present throughout the whole body; spinigers with  $\frac{3}{4}$  length of the blade lightly serrated, evenly spaced (Fig. 7c), more numerous than falcigers in the same fascicle; falcigers with short incurved blades and a terminal tendon, serrated in  $\frac{2}{3}$  the length of blade (Fig. 7d). Neurochaetal subacicular fascicle with heterogomph spinigers (Fig. 7e) and heterogomph falcigers, both present throughout the whole body; spinigers similar to supracicular ones, less numerous than falcigers; falcigers similar to supracicular ones.

### Pygidium

With pair of slender anal cirri, as long as last 10–12 parapodia.

### Remarks

The type material supposedly deposited in the National Museum of Natural History (MNHN, France) seems to be non-existent or not yet catalogued in the Museum's official records. However, a vial identified as *Nereis dumerilii* by Audouin & Milne Edwards from La Rochelle, France (the type locality) was seen among other material in MNHN by Tulio F. Villalobos (pers. comm.). This misplaced vial could not be found again but we suspect this contains the originally described specimens. This information was provided to the museum's curator to locate the specimens that may be consulted in future studies.

All the specimens that were collected at the type locality, grouped in a single MOTU (Fig. 2, MOTU 4), appear to present morphological characteristics that fit the original description by Audouin and Milne Edwards (1833). These features relate to the apparently similar paragnath patterns, number of chaetigers, close ratios between the dorsal and ventral cirri to the respective ligules, tentacular cirri observations and presence of notopodial homogomph falcigers. Additionally, the reported reproductive trait with presence of a pelagic epitokous form (*heteronereis*) is also aligned with specimens from MOTU 4 (Wäge *et al.* 2017). Minor differences concern the pigmentation pattern and pharynx jaws compared to the original description. The holotype was reported as being yellowish with some brown spots at the basis of parapodia, although whether this refers to live or preserved organisms is uncertain. Audouin and Milne Edwards (1833) likely received the specimen from Cuvier using the d'Orbigny collection. The animal was not seen alive, so this possibly refers to preserved colouration (Tulio F. Villalobos, pers. comm.). The preserved specimens studied herein were yellowish-red with brown pigmentation covering most of the anterior region, with pigmentation dots also present adjacent to the parapodia and eyes. However, pigmentation may be absent in very small specimens or partially lost upon fixation in ethanol. The pharynx and jaws are incompletely described by Audouin and Milne Edwards (1833) but from the original illustrations (pl. XIII, fig. 12), jaws seem to have 10–11 teeth, surpassing the 7–9 observed in the topotypes examined herein, reflecting a similar variability previously reported by Claparède (1870). Furthermore, the original description presents morphological discrepancies compared to all other *Platynereis* species. The posterior parapodia are described as having an overgrown neuropodial postchaetal lobe and a clear separation between the notopodium and neuropodium (the latter also observed in the posterior parapodia from our specimens), suggesting that the specimens studied by those authors could be developing into a *heteronereis* stage. Another alternative may be related to the contraction of the neuropodial ligule, since no epitokal features (i.e. lamellae) were drawn, as the authors did, for example, for *Nereis lobulata* (Claparède 1870, pl. XV, fig. 7) and *Nereis podophylla* (pl. XV, fig. 13) on the same plate.

A detailed description from specimens collected in Croatia identified as *P. dumerilii* by Ehlers (1868) most likely represents the *massiliensis*-type. This clearly describes paragnaths absent from Areas I, II and V, and with a small group of rows in VII–VIII. Figures of chaetae are not sufficiently elaborate for further details. Ehlers' (1868) account corresponds to descriptions given here of *P. agilis* comb. nov. and *P. cf. massiliensis*. McIntosh (1910) presented a brief description of specimens from the UK, clearly indicating *dumerilii*-type specimens with paragnaths present in II and what appears to be similar in VI and VII–VIII as described here. Given ten genetic lineages of which five are described in our study, earlier works cannot be considered certain in

species identity according to current knowledge, although there are detailed descriptions (Ehlers 1868). Some of the older works are broad accounts summarising the status of knowledge from all published papers, also presenting brief descriptions of examined specimens (McIntosh 1910) that may include more than one molecular lineage.

Dorsal cirrus size can vary greatly among populations, e.g. in our specimen from Crete (Greece, DBUA0002440.01.v01, BIN: BOLD:AEH1225), cirri were 2.5 times longer than the dorsal ligule throughout the whole body, as opposed to the average 1.5 times reported for our topotypic specimens. The few Eastern Mediterranean specimens from this study also seem to present higher *COI* distances (~3.5% K2P) when compared to the West Mediterranean and Northeast Atlantic populations, and further sampling in the eastern part for the Mediterranean sea is desirable to further explore these deviations.

Özpolat *et al.* (2021) presents a review of the use of *Platynereis dumerilii* as a model system for genetics, regeneration, reproductive biology, development, evolution, chronobiology, neurobiology, ecology, ecotoxicology, and most recently also connectomics and single-cell genomics.

***Platynereis jourdei* Teixeira, Ravara, Langeneck & Bakken, sp. nov.**

(Fig. 8, 9)

ZooBank: urn:lsid:zoobank.org:act:9B29D31F-0DAF-49B0-9BF3-7DC4C07B6FA7

**Material examined**

*Type material.* Spain, Calpe, 1 spm, holotype and hologenophore, DBUA0002431.01.v02, 38°38'23.8"N, 0°03'30.0"E, low tide, among

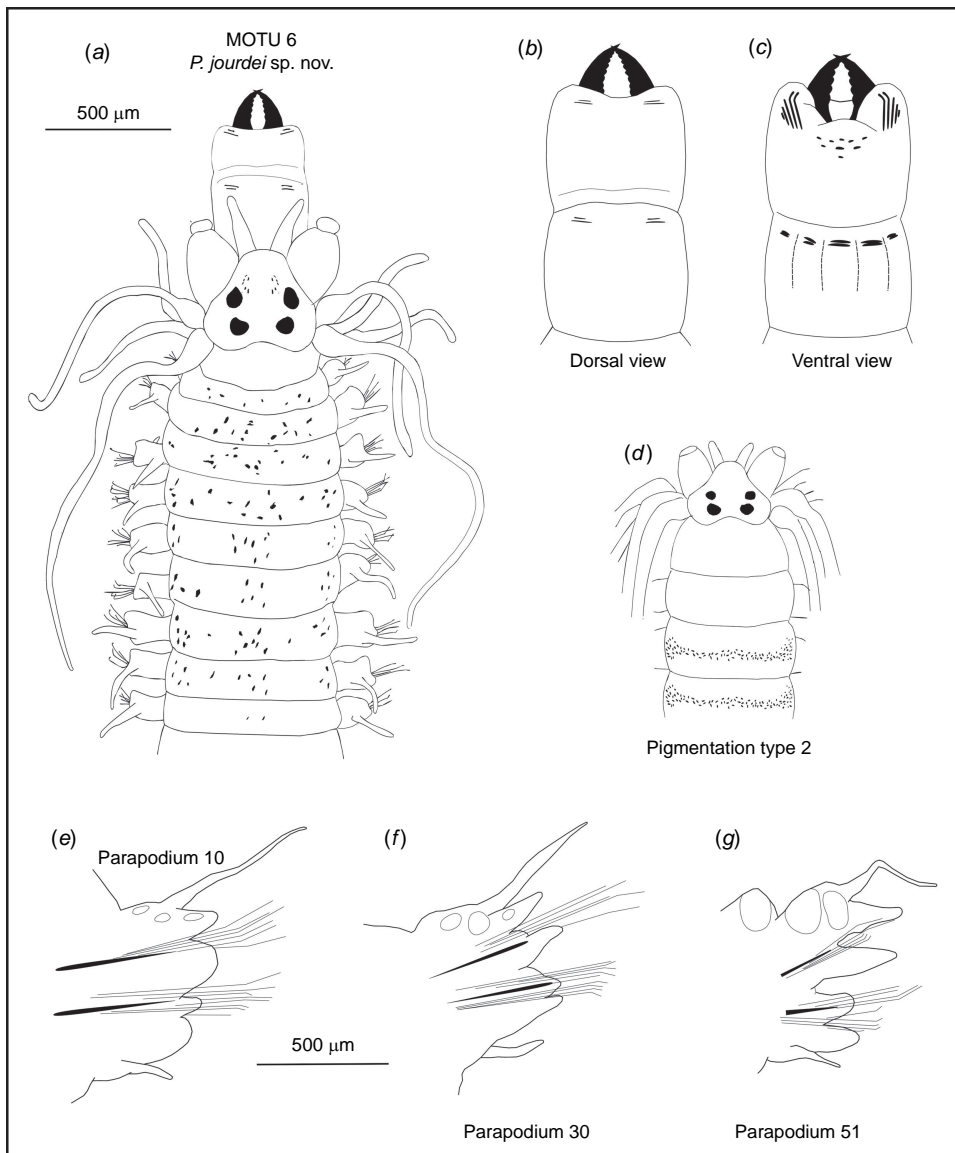


**Fig. 8.** *Platynereis jourdei* sp. nov. (MOTU 6). (a) Dorsal view of the anterior region with dot-like pigmentation; prostomium and pharynx based on the holotype (DBUA0002431.01.v02) and additional Italian samples (DBUA0002432.03.v01 and DBUA0002432.02.v05). (b) Dorsal view of the pharynx. (c) Ventral view of the pharynx. (d) Pigmentation with a well-defined ring-like dot pattern present after the first few chaetigers (DBUA0002432.02.v03). (e) 10th parapodium, posterior view. (f) 30th parapodium, posterior view. (g) 51st parapodium, posterior view.

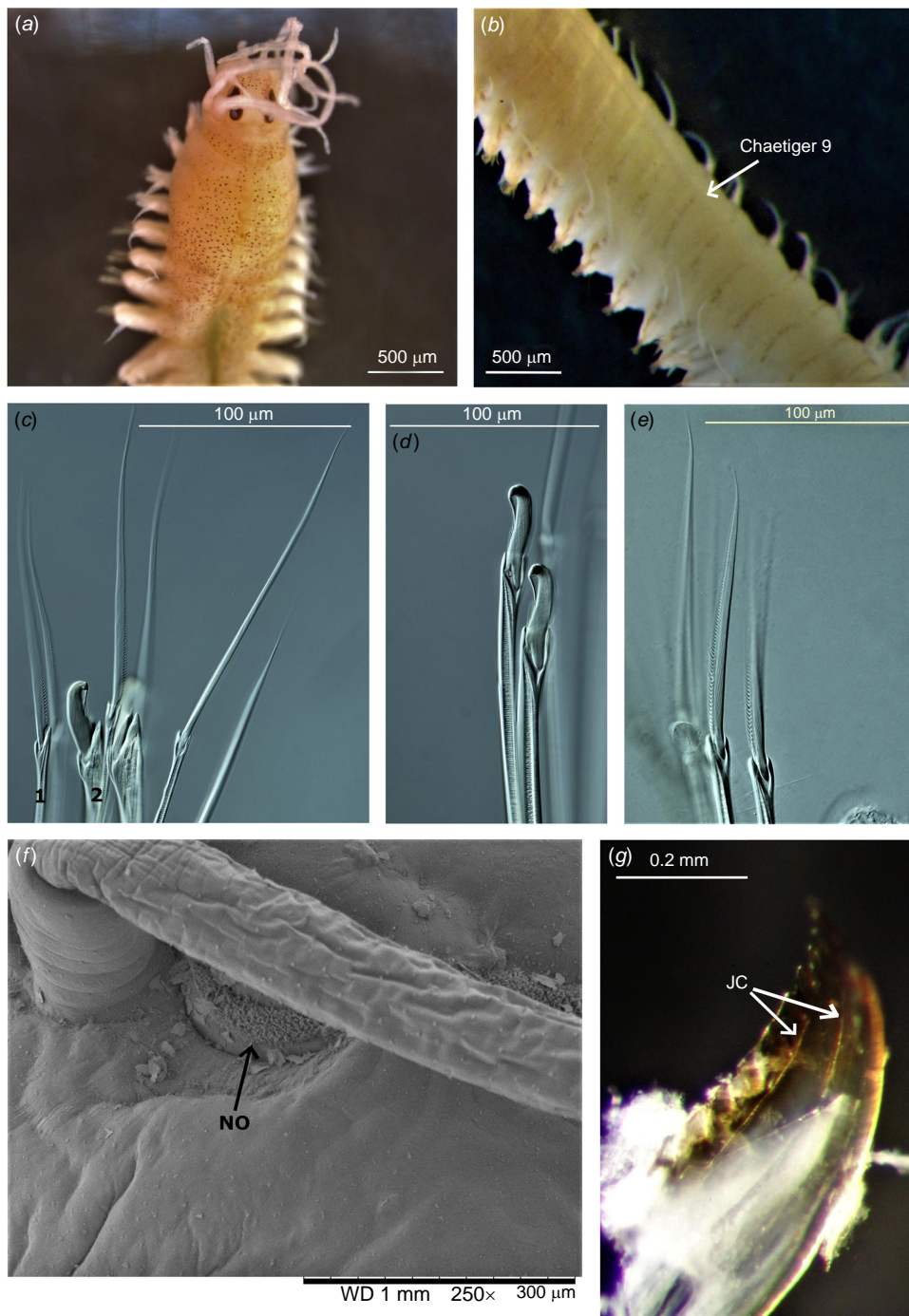


**Fig. 9.** *Platynereis jourdei* sp. nov. (MOTU 6). (a) Pigmentation as seen in a preserved specimen, with high dot density scattered around the anterior region (e.g. DBUA0002432.03.v01). (b) Pigmentation as seen in a preserved specimen, with a ring-like dot pattern in the anterior chaetigers (e.g. DBUA0002432.02.v03). (c) Neurochaetae, subacicular fascicle: heterogomph spinigers (1), heterogomph falcigers spinigers (2), chaetiger 35 (DBUA0002432.02.v08). (d) Notochaetae: homogomph falcigers, chaetiger 35 (DBUA0002432.02.v08). (e) Notochaetae: homogomph spinigers lightly serrated, chaetiger 35 (DBUA0002432.02.v08). (f) SEM scan (DBUA0002432.02.v03) of the nuchal organs (NO). (g) SEM scan (DBUA0002432.02.v03) of the jaw with two canals (JC) close to the inner edge (DBUA0002432.02.v08). WD, working distance between the sample and the lens.

algae, 05/08/2019. 8 spms, paratypes and paragenophores, DBUA0002431.01.v01, DBUA0002431.01.v03–v09, 38°38'23.8"N, 0°03'30.0"E, low tide, among algae, collected by Pedro E Vieira, 05/08/2019.

**Other material.** Italy (Tyrrhenian Sea), Pianosa Island: 5 spms, DBUA0002432.04.v01–v06, 42°34'59.8"N, 10°05'56.0"E, low tide, among algae, collected by Joachim Langeneck, 22/09/2020; Italy (Ligurian Sea), Calafuria: 1 spm, DBUA0002432.01.v01, 43°27'57.6"N, 10°20'24.0"E, low tide, among algae, collected by Joachim Langeneck, 11/01/2019. Italy (Ligurian Sea), Antignano: 1 spm, DBUA0002432.02.v02, 43°29'32.0"N, 10°19'01.2"E, 6-m depth, among *Posidonia*

*oceanica* rhizomes, collected by Joachim Langeneck, 20/09/2019; 4 spms, DBUA0002432.02.v03–v06, 43°29'32.0"N, 10°19'01.2"E, 3-m depth, among algae, collected by Joachim Langeneck, 10/09/2019; 3 spms, DBUA0002432.02.v07–v09, 43°29'32.0"N, 10°19'01.2"E, 3-m depth, among algae, collected by Joachim Langeneck, 27/06/2019; Italy (Tyrrhenian Sea), Montecristo Island: 6 spms, DBUA0002432.03.v01–v06, 42°20'05.9"N, 10°17'22.3"E, low tide, among algae, collected by Joachim Langeneck, 05/09/2020. France (Gulf of Lion), Banyuls: 1 spm, DBUA0002433.01.v01, 42°28'53.9"N, 3°08'00.3"E, low tide, among red algae, collected by Felicia Ulltin, 20/09/2020.

## Diagnosis

Specimens with well separated antennae; palpophores slightly longer than wider; nuchal organs deeply embedded, slightly convex, wider than posterior eyes; postero-dorsal tentacular cirri 1.6 times longer than antero-dorsal ones, reaching chaetigers 9–12. Pigmentation dots may be present throughout the dorsal body. Jaws with 2 canals, one of which is closer to the outer edge. Approximately 25–71 chaetigers. Maxillary ring: Area I, absent; Area II, with two slightly oblique and parallel rows in rectangular patch; Area III, three main transverse lines of short rows (distal, 5 rows; medial, 3 rows; proximal, 1 row) in triangular patch; Area IV, forming five rows varying in length (distal, long rows; medial, medium rows; proximal, short rows) in pyramidal arrangement. Oral ring: Area V, absent; Area VI, double parallel rows; Areas VII–VIII, two ridge rows, each composed of rod-like paragnaths grouped in 5 small rows (2 paragnath rows per ridge), in a single band, furrow regions without paragnaths. Dorsal ligule digitiform, uneven throughout body, becoming barely expanded and less globular from chaetigers 11–13; 1.8–2 times width of median ligule in posterior parapodia. Neuroacicular ligule short, round to triangular, longer but much narrower than a round ventral ligule in anterior chaetigers, equal in length to a digitiform ventral ligule from mid-body chaetigers. Dorsal cirrus cirriform, longer than dorsal ligule throughout body; much longer than ligule in anterior parapodia. Ventral cirri slightly shorter than ventral ligule. Homogomph spinigers with blades lightly serrated, evenly spaced; present in notopodia and neuropodial suprascicular fascicles. Heterogomph spinigers as homogomph ones; present in neuropodial subacicular fascicle. Heterogomph falcigers with short, incurved blades with a terminal tendon, present in both neuropodial fascicles. Two homogomph falcigers with long, incurved blades with a terminal tendon present in the notopodia of posteriormost chaetigers.

## Molecular data

*COI*, *16S* and *28SD2* sequences as in specimens DBUA 0002431.01.v01–v09, DBUA0002432.01.v01, DBUA0002432.02.v02–v09, DBUA0002432.03.v01–v06, DBUA0002432.04.v01–v05 and DBUA0002433.01.v01 (Supplementary Table S2). Phylogenetic relationship within the *Platynereis dumerilii* pseudo cryptic complex as in Fig. 2, belonging to MOTU 6, with high support values and low intraspecific (<3%) genetic divergence for both the mitochondrial and nuclear markers. Interspecific *COI* mean distances to the closest and distant neighbour are 18.5% (K2P, *P. dumerilii* s.s.) and 25.2% (K2P, MOTU 1) respectively. DOI for the species' holotype BIN: doi:10.5883/BOLD:ADW1653.

## Etymology

The species is named after Jérôme Jourde (CNRS/La Rochelle Université) for his sampling efforts and kindness in providing specimens of *Platynereis dumerilii* s.s. from

the type locality on behalf of the authors of this paper that proved fundamental in the establishment of the new species.

## Distribution and habitat

West Mediterranean Sea, in subtidal or low tide zones among algae and *Posidonia oceanica* rhizomes. Also present in CO<sub>2</sub> vents (Wäge et al. 2017).

## Reproduction

Gonochoric species, with a single reproductive event in life (semelparous) transforming into a pelagic epitokous form (*heteronereis*) and a larval stage with planktotrophic development (Wäge et al. 2017).

## Description

Specimens used: DBUA0002431.01.v02, DBUA0002432.02.v03, DBUA0002432.02.v07, DBUA0002432.02.v05, DBUA0002432.02.v08 and DBUA0002431.01.v06.

## Body measurements

Holotype, DBUA0002431.01.v02, atoke, posteriorly incomplete, total length = 26 mm, L15 = 7.40 mm, W15 = 1.66 mm and 71 chaetigers. Non-types, DBUA0002432.02.v03, DBUA0002432.02.v07, DBUA0002432.02.v05, DBUA0002432.02.v08 and paratype DBUA0002431.01.v06 smaller, posteriorly incomplete, TL = 6–15 mm, L15 = 3.3–4.55 mm, W15 = 0.5–0.98 mm, with 25–71 chaetigers.

## Pigmentation

Preserved specimens yellowish-brown, with faint scattered pigmentation dots covering most of the anterior region varying in density and in prostomium area adjacent to the eyes (Fig. 8a). The apodous anterior segment lacks a well-defined ring-like dot pattern (Fig. 8d, 9a) but this pattern may appear after the first few chaetigers (Fig. 9b), varying in pigment density. Pigmentation may be present in the middle and posterior part of the dorsal body adjacent to the parapodia.

## Head

Prostomium cordiform (Fig. 8a); approximately as long as wide. Palps with an oval, pronounced palpostyle (Fig. 8a); palpophore slightly longer than wider, two-thirds the entire length of prostomium. Antennae separated, gap subequal to antennal diameter (Fig. 8a); digitiform, slender, extending backward to equal the size of the palps. Eyes black, anterior and posterior pairs well separated (Fig. 8a, 9a). Anterior pair of eyes irregular to oval, wider than antennal diameter; posterior pair of eyes round to oval, slightly smaller than

anterior pair. Nuchal organs deeply embedded, slightly convex, wider than posterior eyes (Fig. 9f).

### Apodous anterior segment and tentacular cirri

Apodous anterior segment 2.5 times wider than long, slightly longer but narrower than chaetiger 1. Tentacular cirri pattern: postero-dorsal cirri 1.6 times longer than antero-dorsal ones; antero-ventral cirri slightly shorter than postero-ventral one. Antero-dorsal cirri reaching chaetigers 3–4; antero-ventral ones twice as long as palpophore. Postero-dorsal reaching chaetigers 9–12. Dorsal cirrophores wrinkled, cylindrical; postero-dorsal cirrophores longest, twice as long as postero-ventral wrinkled ones.

### Pharynx

Jaws dark brown to yellow-amber and finely toothed until a short distance as wide as 2 teeth from the tip, with 8–9 denticles; 2 longitudinal canals emerging from pulp cavity, one of which is closer to the outer edge (Fig. 9g). Pharynx consisting of maxillary and oral rings with rod-like paragnaths (Fig. 8b, c) arranged in tight rows: Areas I and V, absent; Area II, two slightly oblique and parallel rows in rectangular patch; Area III, three main transverse lines of short rows (distal, 5 rows; medial, 3 rows; proximal, 1 row) in triangular patch; Area IV, forming five rows varying in length (distal, long rows; medial, medium rows; proximal, short rows) in pyramidal arrangement; Area VI, forming double parallel rows; Areas VII–VIII, two ridge rows, each composed of rod-like paragnaths grouped in 5 small rows (2 paragnath rows per ridge) in a single band, furrow regions without paragnaths.

### Notopodia

Dorsal cirrus cirriform, longer than dorsal ligule throughout body; much longer than ligule until median parapodia (Fig. 8e, f), 1.9–2.1 times longer in anterior parapodia (Fig. 8e), 1.3–1.5 times longer in median (Fig. 8f), 1.1–1.3 times longer in posterior ones (Fig. 8g); cirrus longer than length of proximal part of dorsal ligule throughout body (Fig. 8e–g); cirri inserted on one-half in parapodia throughout the whole body (Fig. 8e–g). Dorsal ligule digitiform, uneven throughout body, becoming barely expanded and less globular from chaetigers 11–13 (Fig. 8e, f); 1.8–2 times width of median ligule in posterior parapodia (Fig. 8g). Distal part of dorsal ligule bluntly conical in anterior parapodia, conical from median parapodia; subequal to proximal one throughout (Fig. 8e–g). Dorsal ligule subequal in length to median ligule throughout the body (Fig. 8e–g). Presence of glandular patches in dorsal ligule (Fig. 8e–g). Dorsal and median ligules round from chaetigers 4–5 to 11–13. Median ligule triangular from median parapodia (Fig. 8f, g). Notopodial prechaetal lobe underdeveloped.

### Neuropodia

Neuracicular ligule round to triangular, short, twice as wide as ventral ligule in the anterior parapodia (Fig. 8e); subequal to ventral ligule from median parapodia (Fig. 8f, g). Ventral ligule subequal to the length of median ligule in anterior parapodia (Fig. 8e), 1.5 times smaller from median parapodia (Fig. 8f) and 1.3 times smaller in posterior ones (Fig. 8g). Ventral cirri cirriform, smaller than ventral ligule throughout body (Fig. 8e–g). Neuropodial postchaetal lobe absent.

### Chaetae

Notochaetae with homogomph spinigers and heterogomph falcigers; spinigers with almost full length of the blade lightly serrated (Fig. 9e), numerous and present throughout the whole body; falcigers similar to neuropodial ones, replaced by two homogomph falcigers with long incurved blades and with a terminal tendon, serrated in  $\frac{1}{2}$  the length of blade (Fig. 9d), in the posteriormost chaetigers, usually in the last 5–10 chaetigers. Neurochaetal supracticular fascicle with homogomph spinigers and heterogomph falcigers, both present throughout the whole body; spinigers similar to notopodial ones (Fig. 9e), more numerous than falcigers in same fascicle; falcigers similar to subacicular ones (Fig. 9c). Neurochaetal subacicular fascicle with heterogomph spinigers and heterogomph falcigers (Fig. 9c), both present throughout the whole body; spinigers similar to notopodial ones, less numerous than falcigers; falcigers with short incurved blades and with a terminal tendon, serrated in  $\frac{1}{3}$  the length of blade (Fig. 9c).

### Pygidium

Broken. Not observed.

### Remarks

*Platynereis jourdei* sp. nov. is morphologically similar and genetically close to *P. dumerilii* s.s., with both species grouping closely together within clade A2 of the phylogenetic tree (Fig. 2). However, the two species are distinguishable based on the palpophore size, number of notopodial homogomph falcigers and the disposition of the jaw canals. Palpophores are twice as long as wide in *P. dumerilii* s.s. as opposed to being much wider and smaller in *P. jourdei* sp. nov. Two notopodial homogomph falcigers are present in the parapodia of the new species, as opposed to the single one observed in *P. dumerilii* s.s. In *P. jourdei* sp. nov. the two jaw canals are further apart, one being closer to the outer edge of the jaw, whereas in *P. dumerilii* s.s., both canals are closer to the inner edge of the jaw. Furthermore, body pigmentation of preserved specimens usually presents lower pigmentation density in the new species and some specimens may have a ring-like pigment dot pattern in the anterior region (excluding the first few chaetigers, Fig. 8d). However, most specimens among these two species share similar irregularly scattered

dot patterns throughout the dorsal body. The molecular interspecific difference between the two species (18.5%, COI K2P) also justifies the erection of the new species. *Platynereis jourdei* sp. nov. and *P. dumerilii* s.s. are often sympatric in the West Mediterranean Sea, therefore requiring some caution in identification.

No apparent Western Mediterranean synonym seems to be related to *P. jourdei* sp. nov., since the two most relevant cases, *Nereis peritonealis* Claparède, 1868 and *Heteronereis malmgreni* Claparède, 1868, both described for the Gulf of Naples (Italy) seem to present features that deviate from the new species. *Nereis peritonealis* has a paragnath pattern (Claparède 1868) similar to that of the taxa in clade A3 (of *massiliensis*-type), contrasting with clade A2 (of *dumerilii*-type) where *P. jourdei* sp. nov. belongs. However, the reported small size of mature eggs for *N. peritonealis* would suggest that this is not a brooder but might have a planktonic larval stage (Sato and Masuda 1997). This is in line with clade A2 based on reproductive studies from Wäge et al. (2017) (more specifically to MOTU 4/*P. dumerilii* s.s. and MOTU 6/*P. jourdei* sp. nov.). Nevertheless, *N. peritonealis* might correspond to an entirely new lineage yet to be found and described. *Heteronereis malmgreni*, in turn and based on available morphological data, seems to have been described based on an epitoke form of *N. peritonealis*.

### *Platynereis nunezi* Teixeira, Ravara, Langeneck & Bakken, sp. nov.

(Fig. 10, 11)

ZooBank: urn:lsid:zoobank.org:act:BF21D349-6241-4AE4-B3EB-B702EED5C304

#### Material examined

*Type material.* Spain – Canary Islands, Tenerife: 1 spm, holotype and hologenophore DBUA0002429.01.v03, 28°25′53.3″N, 16°32′57.2″W, low tide, among red algae, collected by Marcos AL Teixeira, 10/04/2019; 2 spms, paratypes and paragenophores DBUA0002429.01.v01-v02, 28°25′53.3″N, 16°32′57.2″W, low tide, rocky beach among red algae, 10/04/2019.

*Other material.* Spain – Canary Islands, Tenerife: 3 spms, DBUA0002429.02.v01-v03, 28°34′17.1″N, 16°20′01.1″W, low tide, rocky beaches among algae, collected by Marcos AL Teixeira, 05/04/2019; Spain – Canary Islands, Lanzarote: 5 spms, DBUA0002429.03.v01-V05, low tide, rocky beaches among algae, 29°13′05.3″N, 13°26′30.4″W, collected by Marcos AL Teixeira, 04/04/2019. Spain – Canary Islands, Gran Canaria: 11 spms, DBUA0002429.04.v01-v11, low tide, rocky beaches among algae, collected by Marcos AL Teixeira, 27°59′06.5″N, 15°22′33.0″W, 06/04/2019. Spain – Canary Islands, La Palma: 5 spms, DBUA0002429.05.v01-v05, low tide, rocky beaches among algae, 28°48′19.8″N, 17°45′41.6″W, collected by Marcos AL Teixeira, 09/04/2019. Spain – Canary Islands, Fuerteventura: 5 spms, DBUA0002429.06.v01-v05, low tide, rocky beaches among algae, 28°03′59.7″N, 14°30′24.9″W, collected by Marcos AL Teixeira and Pedro E Vieira, 02/04/2019. Spain – Canary Islands, El Hierro: 1 spm, DBUA0002429.07.v01, low tide, rocky beaches among algae, 27°47′05.1″N, 18°00′41.7″W, collected by Pedro E Vieira, 2014;

Morocco, Mazagan: 2 spms, DBUA0002430.01.v01-v02, low tide, rocky beaches among algae, 33°15′50.5″N, 8°30′38.6″W, collected by Pedro E Vieira, 2014. Portugal, Madeira: 4 spms, DBUA0002428.03.v01-v04, 32°38′46.0″N, 16°49′27.0″W, low tide, rocky beaches among algae, collected by Pedro E Vieira, 2011. Portugal – Azores, Terceira Island: 3 spms, DBUA0002428.02.v01-v03, 38°40′60.0″N, 27°03′27.1″W, low tide, rocky beaches among algae, collected by Pedro E Vieira, 2015. Portugal – Azores, Santa Maria island: 3 spms, DBUA0002428.01.v01-v03, 36°56′59.7″N, 25°05′42.0″W, low tide, rocky beaches among algae, collected by Pedro E Vieira, 2014.

#### Diagnosis

Specimens with well separated antennae; palpophores almost as long as wide; nuchal organs deeply embedded, slightly oblique, subequal in width to posterior eyes, postero-dorsal tentacular cirri almost twice as long as antero-dorsal ones, reaching chaetigers 5–7. Pigmentation dots may be present throughout the dorsal body, with the presence of a well defined ring-like pigmentation pattern in the apodous segment. Jaws with 2 canals, one of which is closer to the outer edge. Approximately 35–49 chaetigers. Maxillary ring: Area I, absent; Area II, absent; Area III, three main transverse lines of short rows (distal, 4 rows; medial, 5 rows; proximal, 6 rows) in triangular patch; Area IV, forming five rows varying in length (distal, medium rows; medial, long rows; proximal, short rows) in pyramidal arrangement. Oral ring: Area V, absent; Area VI, forming a group of three short transverse rows (distal, 1 row; proximal, 2 rows); Areas VII–VIII, one ridge row composed of rod-like paragnaths grouped in 5 small rows (1 paragnath row per ridge), furrow regions without paragnaths. Dorsal ligule digitiform, uneven throughout body, becoming barely expanded and less globular from chaetigers 8–9; 2.6–2.8 times width of median ligule in posterior parapodia. Neuroacicular ligule triangular, longer than digitiform ventral ligule in anterior chaetiger, shorter than triangular ventral ligule from mid-body chaetigers, much shorter in posterior parapodia. Dorsal cirrus cirriform, longer than dorsal ligule throughout body. Ventral cirrus cirriform, shorter than ventral ligule throughout body. Homogomph spinigers with blades lightly serrated, evenly spaced; present in notopodia and neuropodial supracular fascicles. Heterogomph spinigers as homogomph ones; present in neuropodial subacicular fascicle. Heterogomph falcigers with short, incurved blades with a terminal tendon, present in both neuropodial fascicles. One Homogomph falciger with long, incurved blades with a terminal tendon present in the notopodia of posterior-most chaetigers.

#### Molecular data

COI, 16S and 28SD2 sequences as in specimens DBUA0002428.01.v01-v03, DBUA0002428.02.v01-v03, DBUA0002428.03.v01-v04, DBUA0002429.01.v01-v03, DBUA0002429.02.v01-v03, DBUA0002429.03.v01-V05, DBUA0002429.04.v01-v11, DBUA0002429.05.v01-v05, DBUA0002429.06.v01-v05, DBUA0002429.07.v01, DBUA0002430.01.v01-v02

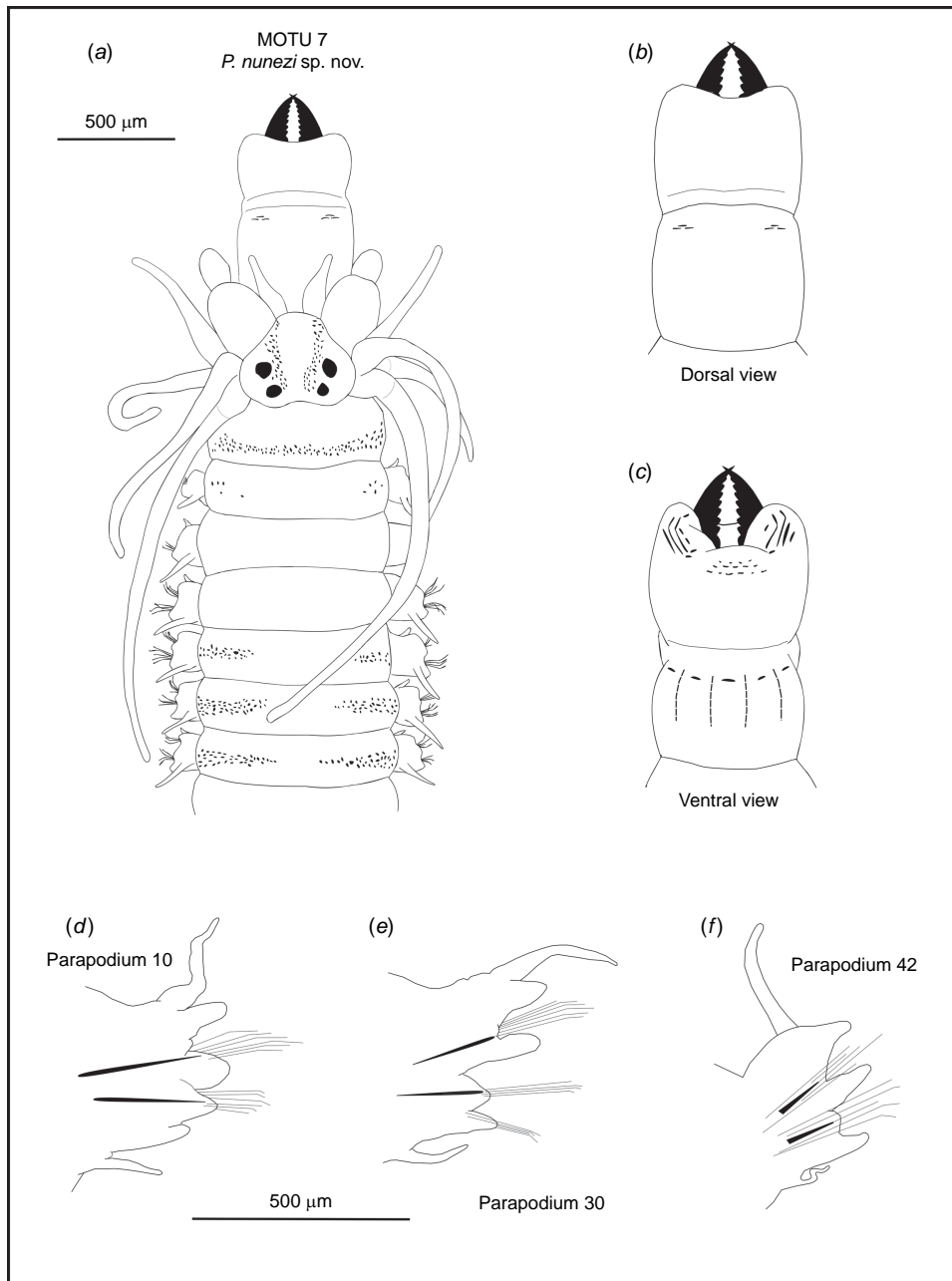


**Fig. 10.** *Platynereis nunezi* sp. nov. (MOTU 7). (a) Dorsal view of the anterior region with well-defined ring-like dot pigmentation in the apodous anterior segment; prostomium and pharynx based on the holotype (DBUA0002429.01.v03) and an additional sample from Tenerife (DBUA0002429.01.v02). (b) Dorsal view of the pharynx. (c) Ventral view of the pharynx. (d) 10th parapodium, posterior view (DBUA0002429.04.v03). (e) 30th parapodium, posterior view (DBUA0002429.04.v03). (f) 42nd parapodium, posterior view (DBUA0002429.04.v04).

(Supplementary Table S2). Phylogenetic relationship within the *Platynereis dumerilii* pseudo cryptic complex as in Fig. 2, belonging to MOTU 7, with high support values and low intraspecific (<3%) genetic divergence for both the mitochondrial and nuclear markers. Interspecific *COI* mean distances to the closest and most distant neighbour are 13.5% (K2P, MOTU 8) and 24% (K2P, *P. jourdei* sp. nov.)

respectively. DOI for the species' holotype BIN: doi:10.5883/BOLD:AEE1367.

### Etymology

The species is named after Jorge Núñez (Universidad de La Laguna, Tenerife), not only to honour his previous

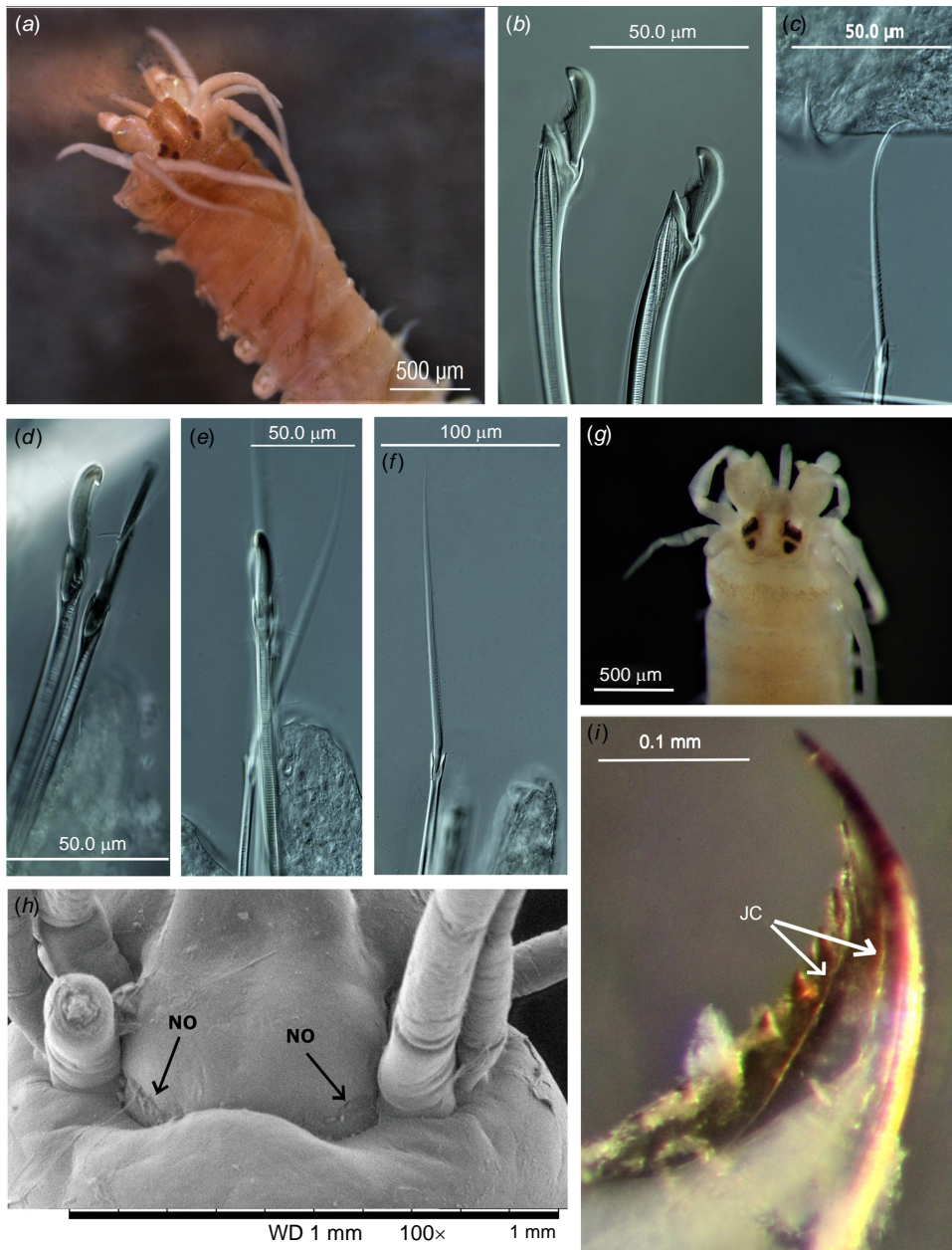


**Fig. 11.** *Platynereis nunezi* sp. nov. (MOTU 7). (a) Pigmentation as seen in a preserved specimen, with presence of well-defined ring-like dot pattern in the apodous segment and semi ring-like dot patterns in the anterior chaetigers from the dorsal body (e.g. DBUA0002429.01.v02). (b) Neurochaeta, subacicular fascicle: heterogomph falciger, chaetiger 30 (DBUA0002429.04.v04). (c) Neurochaeta, subacicular fascicle: heterogomph spiniger, chaetiger 39 (DBUA0002429.04.v03). (d) Notochaetae: homogomph falciger, chaetiger 23 (DBUA0002429.04.v07). (e) Notochaetae: homogomph falciger, chaetiger 39 (DBUA0002429.04.v03). (f) Notochaetae: homogomph spiniger, chaetiger 10 (DBUA0002429.04.v04). (g) Pigmentation as seen in a preserved specimen, with presence of well-defined ring-like dot pattern in the apodous segment (e.g. DBUA0002429.04.v03). (h) SEM scan (DBUA0002429.05.v01) of the nuchal organs (NO). (i) Jaw image with two canals (JC) close to the inner edge (DBUA0002429.04.v03). WD, working distance between the sample and the lens.

contributions in the study of Annelids, but also for all the assistance and knowledge provided to the first and third authors of this paper during the sampling campaign in the Canary Islands.

### Distribution and habitat

Azores and Webnesia islands (Madeira and Canary Islands); also occurring on the west coast of Morocco, on intertidal rocky beaches among green and red algae. Apparently not present on the island of Porto Santo (Madeira), being replaced by MOTU 8 (Fig. 2a, b), although a greater sampling effort in Porto Santo is needed to confirm this.

### Description

Specimens used: DBUA0002429.01.v03, DBUA0002429.05.v01, DBUA0002429.05.v03, DBUA0002429.04.v03, DBUA0002429.04.v04 and DBUA0002429.04.v07.

### Body measurements

Holotype, DBUA0002429.01.v03, atoke, posteriorly incomplete, total length = 15 mm, L15 = 4.63 mm, W15 = 0.925 mm, and 44 chaetigers. Non-types, DBUA0002429.05.v01, DBUA0002429.05.v03, DBUA0002429.04.v03, DBUA0002429.04.v04 and DBUA0002429.04.v07 smaller, posteriorly incomplete, TL = 7.4–14 mm, L15 = 3.79–4.4 mm, W15 = 0.55–0.89 mm, with 33–49 chaetigers.



## Pigmentation

Preserved specimens yellowish-red or yellowish-brown, with a well-defined ring-like pigmentation dot pattern on the apodous segment (Fig. 11g), either with a semi ring-like pattern (Fig. 10a, 11a) or randomly scattered in other anterior chaetigers. Pigmentation may not be visible in smaller preserved specimens and may also be present in the prostomium area adjacent to the eyes and in the middle and posterior part of the dorsal body adjacent to the parapodia.

## Head

Prostomium cordiform (Fig. 10a); approximately as long as wide. Palps with an oval, pronounced palpostyle (Fig. 10a); palpophore slightly longer than wide, shorter than the entire length of prostomium. Antennae separated, gap subequal of antennal diameter (Fig. 10a); digitiform, slender, extending backward but shorter than prostomium and slightly shorter than palps. Eyes black, anterior and posterior pairs well separated (Fig. 10a, 11a). Anterior pair of eyes irregular to oval, wider than antennal diameter; posterior pair of eyes round to oval, slightly smaller than anterior pair. Nuchal organs deeply embedded, slightly oblique, subequal in width to posterior eyes (Fig. 11h).

## Apodous anterior segment and tentacular cirri

Apodous anterior segment 3.5 times wider than long, slightly longer and wider than chaetiger 1. Tentacular cirri pattern: postero-dorsal cirri 1.8 times longer than antero-dorsal ones; antero-ventral cirri slightly shorter than postero-ventral one. Antero-dorsal cirri reaching chaetigers 2–3; antero-ventral two times longer than palpophore. Postero-dorsal reaching chaetigers 5–7. Dorsal cirrophores wrinkled, cylindrical; postero-dorsal cirrophores longest, 1.5 times the length of postero-ventral wrinkled ones.

## Pharynx

Jaws dark brown to yellow-amber and finely toothed until a short distance as wide as 2 teeth from the tip, with 8–9 denticles; 2 longitudinal canals emerging from pulp cavity, one of these closer to the outer edge (Fig. 11i). Pharynx consisting of maxillary and oral ring with rod-like paragnaths (Fig. 10b, c) arranged in tight rows: Areas I, II and V, absent; Area III, three main transverse lines of short rows (distal, 4 rows; medial, 5 rows; proximal, 6 rows) in triangular patch; Area IV, forming five rows varying in length (distal, medium rows; medial, long rows; proximal, short rows) in pyramidal arrangement; Area VI, forming a group of three short transverse rows (distal, 1 row; proximal, 2 rows); Areas VII–VIII, one ridge row composed of rod-like paragnaths grouped in five small rows (1 paragnath rows per ridge), furrow regions without paragnaths.

## Notopodia

Dorsal cirrus cirriform, longer than dorsal ligule throughout body; 1.2–1.4 times longer in anterior parapodia (Fig. 10d), 1.3–1.5 times longer in median (Fig. 10e), 1.2–1.4 times longer in posterior ones (Fig. 10f); cirrus longer than length of proximal part of dorsal ligule throughout body (Fig. 10d–f); cirri inserted one-third in anterior parapodia (Fig. 10d), two-thirds in median (Fig. 10e) and one-half in posterior ones (Fig. 10f). Dorsal ligule digitiform, uneven throughout body, becoming barely expanded and less globular from chaetigers 8–9 (Fig. 10d, e); 2.6–2.8 times width of median ligule in posterior parapodia (Fig. 10f). Distal part of dorsal ligule bluntly conical in anterior parapodia, conical from median parapodia; subequal to proximal one in posterior parapodia (Fig. 10f), longer than proximal in anterior ones (Fig. 10d) and shorter in median parapodia (Fig. 10e). Dorsal ligule 1.5 times longer than median ligule in posterior parapodia (Fig. 10f), 1.2 times longer in median ones (Fig. 10e), subequal in anterior parapodia (Fig. 10d). Dorsal and median ligules round from chaetigers 3–4 to 8–9. Median ligule round in anterior parapodia (Fig. 10d), digitiform in median parapodia (Fig. 10e) and triangular in posterior ones (Fig. 10f). Notopodial prechaetal lobe underdeveloped.

## Neuropodia

Neuracicular ligule triangular, shorter, wider than triangular ventral ligule from median (Fig. 10e) and posterior parapodia (Fig. 10f); much shorter than ventral ligule in posterior parapodia (Fig. 10f). Ventral cirri cirriform, smaller than ventral ligule throughout body (Fig. 10d–f). Neuropodial postchaetal lobe absent.

## Chaetae

Notochaetae with homogomph spinigers and heterogomph falcigers; spinigers with  $\frac{2}{3}$  length of the blade lightly serrated, evenly spaced (Fig. 11f), numerous and present throughout the whole body; falciger similar to neuropodial ones (Fig. 11b), replaced by single homogomph falciger with long incurved blades and with a distinct terminal tendon in the posteriormost chaetigers (Fig. 11d, e), usually in the last 5–10 chaetigers. Neurochaetal supracicular fascicle with homogomph spinigers and heterogomph falcigers both present throughout the whole body; spinigers similar to notopodial ones (Fig. 11f), more numerous than falcigers in same fascicle; falcigers similar to subacicular ones (Fig. 11b); neurochaetal subacicular fascicle with heterogomph spinigers (Fig. 11c) and heterogomph falcigers, both present throughout the whole body; spinigers similar to notopodial ones, less numerous than falcigers; falcigers with short incurved blades and with a distinct terminal tendon, serrated in  $\frac{2}{3}$  the length of blade (Fig. 11b).

## Pygidium

Broken. Not observed.

## Remarks

*Platynereis nunezi* sp. nov. can be easily distinguished from *P. dumerilii* s.s. by the lower number of chaetigers (usually slightly surpassing half the number of chaetigers for worms of similar size), the shorter tentacular cirri (reaching chaetiger 7, instead of 12), jaw disposition and the distinct paragnath arrangement and pigmentation pattern (see Table 6). *Platynereis nunezi* sp. nov. is closer to *P. cf. massiliensis*, since both share a shorter tentacular cirrus, a ring-like pigmentation pattern and a similar paragnath arrangement. However, these two species differ in the blades of the spinigerous chaetae, that are coarsely serrated in *P. cf. massiliensis*, whereas in *P. nunezi* sp. nov. the spinulation is lighter, and the homogomph falciger from the posterior-most chaetigers is located in the notopodium instead of the neuropodium as seen in *P. cf. massiliensis*. Genetic distances (mean 15.5% COI K2P) also distinguish these two species. Additionally, some pigmentation details in the anterior chaetigers are distinct from *P. cf. massiliensis*, with the presence of semi ring-like dot patterns in the new species. Unlike most other species from the complex that are widely

distributed along the Atlantic and Mediterranean coast of Europe, *P. nunezi* sp. nov. is widespread and unique to the Azores and Webbnesia islands, and sympatrically distributed with *P. cf. massiliensis* only on the west coast of Morocco. No reproductive studies were undertaken for this species but, given the genetic proximity to the nearest neighbour (MOTU 9 – *P. cf. massiliensis*), the species probably shares the same hermaphroditic features, egg brooding and lecithotrophic larval stages.

## *Platynereis cf. massiliensis*

(Fig. 12, 13)

### Material examined

Portugal, Canto Marinho: 14 spms, DBUA0002424.01.v01–v03, DBUA0002425.01.v01–v11, 41°44'13.2"N, 8°52'33.6"W, low tide, among algae, collected by Marcos AL Teixeira, 20/05/2019. Morocco, Mazagan: 1 spm, DBUA0002426.01.v01, low tide, rocky beaches among algae, 33°15'50.5"N, 8°30'38.6"W, collected by Pedro E Vieira,

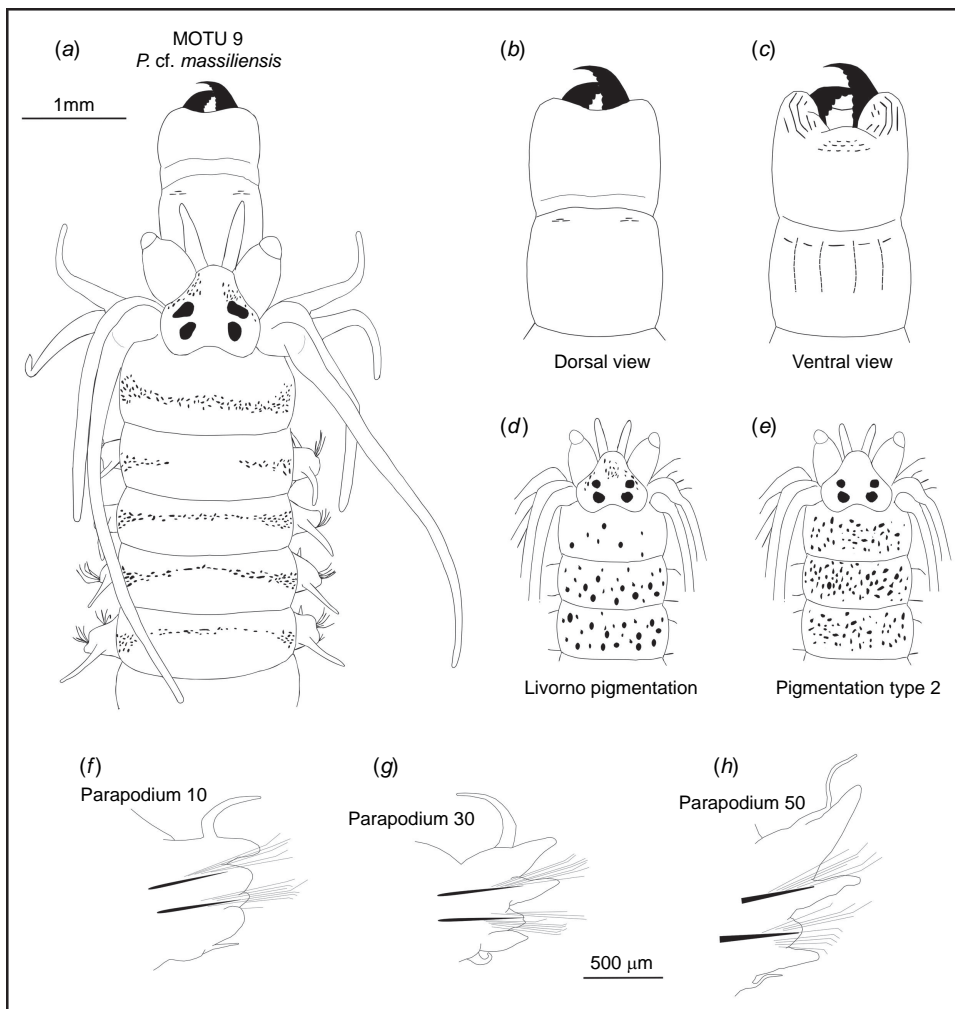


**Fig. 12.** *Platynereis* c.f. *massiliensis* (MOTU 9). (a) Dorsal view of the anterior region with ring-like dot pigmentation pattern in the apodous segment and in the remaining anterior chaetigers; prostomium and pharynx based on Portuguese samples (DBUA0002424.01.v03 and DBUA0002425.01.v10). (b) Dorsal view of the pharynx. (c) Ventral view of the pharynx. (d) Pigmentation with large circular-like dot patterns, typically found in populations from Porto di Livorno, Italy (e.g. DBUA0002427.01.v02). (e) Pigmentation with scattered dot patterns after the first few chaetigers (e.g. DBUA0002425.01.v09). (f) 10th parapodium, posterior view (DBUA0002425.01.v09). (g) 30th parapodium, posterior view (DBUA0002425.01.v09). (h) 50th parapodium, posterior view (DBUA0002425.01.v09).

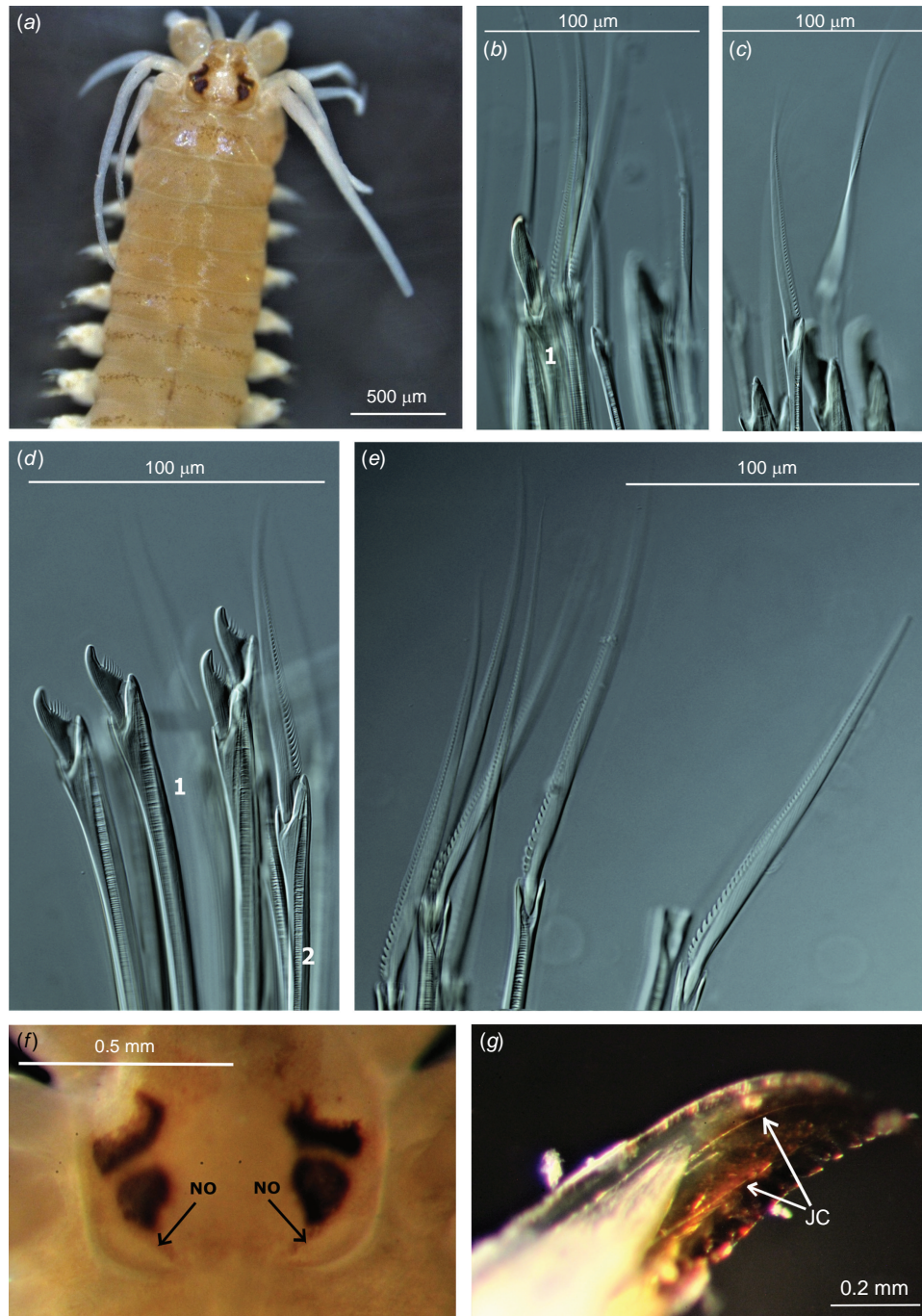


**Fig. 13.** *Platynereis* cf. *massiliensis* (MOTU 9). (a) Pigmentation as seen in a preserved specimen (e.g. DBUA0002425.01.v03), with ring-like dot pigmentation pattern present in the apodous segment and in the remaining anterior chaetigers. (b) Notochaetae: homogomph falciger, chaetiger 50 (DBUA0002425.01.v10). (c) Neurochaetae, subacicular fascicle: heterogomph falcigers, chaetiger 30 (DBUA0002425.01.v10). (d) Neurochaeta subacicular fascicle: heterogomph falcigers (1), heterogomph spinigers (2), chaetiger 10 (DBUA0002425.01.v10). (e) Notochaetae: homogomph spinigers with coarsely serrated blades, chaetiger 30 (DBUA0002425.01.v10). (f) Microscope image with the presence of nuchal organs (NO) in specimen DBUA0002424.01.v02. (g) Jaw image with two canals (JC), one of which is closer to the outer edge (DBUA0002424.01.v03).

2014. Italy (Ligurian Sea), Livorno: 3 spms, DBUA0002427.01.v01–v03, 43°32'45.6"N, 10°18'07.2"E, marina, pontoon scrapings among algae, collected by Joachim Langeneck, 23/10/2019.

## Diagnosis

Specimens with well separated antennae; palpophores almost as long as wide; nuchal organs deeply embedded, slightly oblique, subequal in width to posterior eyes, postero-dorsal tentacular cirri almost twice as long as antero-dorsal ones, reaching chaetigers 5–7. Pigmentation dots may be present throughout the dorsal body, with the presence of a well defined ring-like pigmentation pattern in the apodous segment. Jaws with 2 canals, one of which is closer to the outer edge. Approximately 23–55 chaetigers. Maxillary ring: Area I, absent; Area II, absent; Area III, three main transverse lines of short rows (distal, 4 rows; medial, 5 rows; proximal, 6 rows) in triangular patch; Area IV, forming five rows varying in length (distal, medium rows; medial, long rows; proximal, short rows) in pyramidal arrangement. Oral ring: Area V, absent; Area VI, forming a group of three short transverse rows (distal, 1 row; proximal, 2 rows); Areas VII–VIII, one ridge row composed of rod-like paragnaths grouped in five small rows (1 paragnath row per ridge), furrow regions without paragnaths. Dorsal ligule digitiform, uneven throughout body, becoming barely expanded and less globular from chaetigers 10–12; 1.9–2.1 times width of median ligule in posterior parapodia. Neuracicular ligule triangular, shorter, almost as wide as lanceolate ventral ligule from median and posterior parapodia; much narrower to globular ventral ligule in anterior parapodia. Dorsal cirrus cirriform, longer than dorsal ligule throughout the body. Ventral cirrus cirriform, much shorter than ventral ligule. Homogomph spinigers with blades coarsely serrated, evenly spaced; present in notopodia and neuropodial supracicular fascicles. Heterogomph spinigers as homogomph ones; present in neuropodial subacicular fascicle. Heterogomph falcigers with short, incurved blades with a terminal tendon, present in both neuropodial fascicles. One homogomph falciger with long, incurved blades with a terminal tendon present in neuropodial supracicular fascicles of posterior-most chaetigers.

## Molecular data

*COI*, *16S* and *28SD2* sequences as in specimens DBUA0002424.01.v01–v03, DBUA0002425.01.v01–v11, DBUA0002426.01.v01 and DBUA0002427.01.v01–v03 (Supplementary Table S2). Phylogenetic relationship within the *Platynereis dumerilii* pseudo cryptic complex as in Fig. 2, belonging to MOTU 9, with high support values and low intraspecific (< 3%) genetic divergence for both the mitochondrial and nuclear markers. Interspecific *COI* mean distances to the closest and distant neighbour are 5% (K2P, MOTU 10) and 24% (K2P, MOTU 5) respectively. DOI for the species' BIN

for the Mediterranean clade: doi:10.5883/BOLD:ACP6515; and Northeast Atlantic clade: doi:10.5883/BOLD:ABY1368.

## Distribution and habitat

Northeast Atlantic to the West Mediterranean Sea, from Portugal and Morocco to western Italy. Found on rocky beaches among algae in intertidal or subtidal habitats, including CO<sub>2</sub> vents (Wäge et al. 2017).

## Reproduction

Reproduction without epitokous transformation; a protandrous hermaphrodite, characterised by egg brooding and lecithotrophic larval stages with a semi-direct development (Schneider et al. 1992; Wäge et al. 2017). In the original description by Moquin-Tandon (1869), the species was described as a simultaneous hermaphrodite.

## Description

Specimens used: DBUA0002425.01.v09, DBUA0002425.01.v10, DBUA0002425.01.v03, DBUA0002427.01.v01, DBUA0002424.01.v03.

## Body measurements

Non-type, DBUA0002425.01.v09, atoke, complete, total length = 26.4 mm, L15 = 9.07 mm, W15 = 1.66 mm, and 51 chaetigers. Non-types, DBUA0002425.01.v10, DBUA0002425.01.v03, DBUA0002427.01.v01, DBUA0002424.01.v03 smaller, posteriorly incomplete, TL = 4.6–22 mm, L15 = 2.56–8.07 mm, W15 = 0.375–1.56 mm, with 23–55 chaetigers.

## Pigmentation

Preserved specimens yellowish-brown, with a ring-like pigmentation dot pattern in most of the anterior chaetigers (Fig. 12a, 13a), or a large number of dots scattered throughout the body, varying in dot size and density (Fig. 12e). Larger dot size only observed in the Livorno port (Italy) population (Fig. 12d, e.g.: specimen DBUA0002427.01.v02). Pigmentation may also be present in prostomium, adjacent to the eyes, and in the middle and posterior part of the dorsal body adjacent to the parapodia.

## Head

Prostomium cordiform (Fig. 12a); approximately as long as wide. Palps with an oval-shaped and pronounced palpostyle (Fig. 12a); palpophore slightly longer than wide, slightly shorter than the entire length of prostomium. Antennae separated, gap subequal to antennal diameter (Fig. 12a); digitiform, slender, extending backward but shorter than prostomium, equal to palp size. Eyes black, anterior and posterior pairs well separated (Fig. 12a, 13a). Anterior pair of eyes irregular to oval, wider than antennal diameter;

posterior pair of eyes oval, slightly smaller than anterior pair. Nuchal organs deeply embedded, slightly oblique, subequal in width to posterior eyes (Fig. 13f).

### Apodous anterior segment and tentacular cirri

Apodous anterior segment 3 times wider than long, slightly longer and wider than chaetiger 1. Tentacular cirrus pattern: postero-dorsal cirri 1.8 times longer than antero-dorsal ones; antero-ventral cirri slightly shorter than postero-ventral one. Antero-dorsal cirri reaching chaetigers 2–3; antero-ventral two times longer than palpophore. Postero-dorsal reaching chaetigers 5–7. Dorsal cirrophores wrinkled, cylindrical; postero-dorsal cirrophores longest, twice as long as the postero-ventral wrinkled ones.

### Pharynx

Jaws dark brown to yellow-amber and finely toothed until a short distance as wide as 2 teeth from the tip, with 8–9 denticles; 2 longitudinal canals emerging from pulp cavity, one of these closer to the outer edge (Fig. 13g). Pharynx consisting of maxillary and oral ring (Fig. 12b, c) with rod-like paragnaths arranged in tight rows: Areas I, II and V, absent; Area III, three main transverse lines of short rows (distal, 4 rows; medial, 5 rows; proximal, 6 rows) in triangular patch; Area IV, forming five rows varying in length (distal, medium rows; medial, long rows; proximal, short rows) in pyramidal arrangement; Area VI, forming a group of three short transverse rows (distal, 1 row; proximal, 2 rows); Areas VII–VIII, one ridge row composed of rod-like paragnaths grouped in five small rows (1 paragnath rows per ridge), furrow regions without paragnaths.

### Notopodia

Dorsal cirrus cirriform, 1.1–1.3 times longer than dorsal ligule throughout body (Fig. 12f–h); cirrus longer than length of proximal part of dorsal ligule throughout body (Fig. 12f–h); cirri inserted one-half in anterior (Fig. 12f) and median (Fig. 12g) parapodia, and one-third in posterior ones (Fig. 12h). Dorsal ligule digitiform, uneven throughout body, becoming barely expanded and less globular from chaetigers 10–12 (Fig. 12f, g); 1.9–2.1 times width of median ligule in posterior parapodia (Fig. 12h). Distal part of dorsal ligule bluntly conical in anterior parapodia, conical from median parapodia; subequal to proximal one in anterior and median parapodia (Fig. 12f, g), longer than proximal in posterior ones (Fig. 12h). Dorsal ligule 1.4 times longer than median ligule in anterior and median parapodia (Fig. 12f, g), 1.6 times longer in posterior ones (Fig. 12h). Dorsal and median ligules round from chaetigers 3–5 to 10–12. Median ligule triangular from median parapodia (Fig. 12g, h). Notopodial prechaetal lobe not observed.

### Neuropodia

Neuracicular ligule triangular, shorter, almost as wide as lanceolate ventral ligule from median (Fig. 12g) and posterior parapodia (Fig. 12h); much narrower to globular ventral ligule in anterior parapodia (Fig. 12f). Ventral ligule subequal the length of median ligule in anterior parapodia (Fig. 12f), and slightly shorter from median and in posterior ones (Fig. 12g, h). Ventral cirri cirriform, smaller than ventral ligule throughout body (Fig. 12f–h). Neuropodial postchaetal lobe absent.

### Chaetae

Notochaetae with homogomph spinigers; spinigers with almost full length of the blade coarsely serrated, evenly spaced (Fig. 13e), numerous and present throughout the whole body. Neurochaetal supracicular fascicle with homogomph spinigers and heterogomph falcigers both present throughout the whole body, except in the posterior region where the heterogomph falcigers are replaced by homogomph ones; spinigers similar to notopodial ones (Fig. 13e), more numerous than falcigers in same fascicle; heterogomph falcigers similar to subacicular ones (Fig. 13d); single homogomph falciger with long incurved blades and with a terminal tendon (Fig. 13b), present only in the posteriormost chaetigers, usually in the last 5–10 chaetigers. Neurochaetal subacicular fascicle with heterogomph spinigers and heterogomph falcigers (Fig. 13c), both present throughout the whole body; spinigers similar to notopodial ones, less numerous than falcigers; falcigers with short incurved blades and with a distinct terminal tendon, serrated in  $\frac{1}{2}$  the length of blade (Fig. 13d).

### Pygidium

With pair of slender anal cirri, as long as last 6–7 parapodia.

### Remarks

The original description of *P. massiliensis* by Moquin-Tandon (type locality: Marseille, France) is brief and lacks figures, with current identification of specimens as *P. massiliensis* being mostly tentative. Nevertheless, the original description reported the absence of paragnaths ('denticles') and parapodia similar to those of *Nereis bilineata* (i.e. '*Neanthes fucata*'), making these features considerably divergent from the original *P. dumerilii* and overall *Platynereis* species. The parapodia of *N. fucata* have characteristic broad leaf-like dorsal ligules, especially in the median region of the body, contrasting with the narrow ones of *P. dumerilii* (Núñez 2004) and all *Platynereis* specimens examined in our study. Regarding paragnaths, from our observations, partial paragnath loss can sometimes happen upon fixation in ethanol or due to sampling techniques. However, the complete absence of this feature relating to the previous reason is unusual and may suggest that the lack of paragnaths is indeed a feature

and not an artefact related to external factors. Phenotypic plasticity could justify these observations, since such paragnath variability was also reported for other species, e.g. in *Nereis zonata* (see Núñez 2004; Gravina et al. 2015). Despite these differences, Claparède (1870) appears to be the first regarding this species as the same as *P. dumerilii*, with further and more recent studies also treating *P. massiliensis* as morphologically very similar to *P. dumerilii*, when analysing the respective specimens (Hauenschild 1951; Schneider et al. 1992; Valvassori et al. 2015). Later, Wäge et al. (2017) used molecular data to detect two lineages sharing the same reproductive features as *P. massiliensis* (egg brooders). According to these authors, despite the lack of type material (also apparently not found in the National Museum of Natural History, MNHN, France), the congruence of the developmental observations with other studies (Hauenschild 1951; Schneider et al. 1992; Helm et al. 2014) suggests that the *Platynereis* population from Ischia represents *P. massiliensis* (MOTU 9 in our study, Fig. 2). The Vulcano population (egg brooder), grouped in our MOTU 1 (Fig. 2), that also has sequences from Banyuls (France). However, this MOTU 1 is closer to the original type locality reported for *P. massiliensis* (Marseille, France). Further sampling and reproductive studies in topotypic material is needed to confirm whether our lineage actually corresponds to specimens found in Marseille. For these reasons, we prefer to regard our specimens as *P. cf. massiliensis*.

In our study, the MOTU attributed to *P. cf. massiliensis* is sympatric to *P. dumerilii* s.s. and *P. jourdei* sp. nov. but differs from these species mainly in having much shorter dorsal tentacular cirri and a considerably low number of chaetigers for similar specimen sizes, a different paragnath arrangement with the absence of paragnaths on Area II and a triangular arrangement on Area III pointing distally (to maxillae), coarsely serrated chaetae and different pigmentation in some of the specimens. Additionally, high molecular distances (~22% COI K2P), and different reproductive strategies and life history distinguishes this species from *P. dumerilii* s.s. and *P. jourdei* sp. nov. (Wäge et al. 2017). Furthermore, from the five lineages described here, only *P. cf. massiliensis* is characterised by the unique presence of neuropodial homogomph falcigers in the posterior region, instead of these being located in the notopodium.

*Platynereis cf. massiliensis* possesses diverse pigmentation patterns, one of which is clearly distinct and apparently unique to the population from Porto di Livorno (Italy, e.g. DBUA0002427.01.v02). This pigmentation pattern has a large number of dots scattered throughout the body and is characterised by the larger dot size (almost circular-like) when compared to the Northeast Atlantic populations. An independent COI clade with 3.3% K2P mean distances distinguishes the Livorno variant from the Northeast Atlantic populations, however without enough divergence to be separated into an independent consensus MOTU (Fig. 2a). Additional specimens from this particular Italian population are desirable for further conclusions.

## Discussion

Some species within the family Nereididae have morphological features with very small variations that can often lead to misidentifications (Bakken and Wilson 2005; Glasby 2015). This is especially applicable when comparing small specimens of different species where one is significantly more abundant than the other. The difficulty in identifying the rare and lesser-known species might be attributed to the presence of juveniles, damage or loss of features, e.g. the size of the tentacular cirri due to the sampling techniques, a result from quick identifications undertaken in general ecological studies using several different groups of organisms and the pharynx might also not be everted, and this can be difficult and sometimes impossible to dissect in small specimens. All of these may lead to incorrect taxonomic conclusions. This was the case in our samples between clades A and B, where molecular data and a more careful morphological analysis found considerable differences between the two. However, finding *P. dumerilii* assigned to MOTU 11 (GenBank: KC591811.1) is still possible in the genetic databases, and our earlier first-pass assessment of some specimens from clade B also led to incorrect identifications (Teixeira et al. 2021). Maximum genetic distances between these two major clades were very high (see Table 3), especially in the 28SD2 locus where values rose to 36.9%, as opposed to the 3.9% found between MOTUs in clade A. Other annelid studies about cryptic complexes also reported similarly low 28S distances among neighbouring MOTUs (Teixeira et al. 2020, 2022; Sampieri et al. 2021). This nuclear locus is known for the poor utility in species-level discrimination in many groups of animals (Jörger et al. 2012) but is very efficient for reconstructing deeper phylogenies (Weitschek et al. 2014). These can improve bootstrap results when combined with other genetic markers and thereby provide higher confidence in the final tree topology. Based on these preliminary data, clearly either entirely new unreported species (MOTUs 12, 13) or new pseudo-cryptic lineages belonging to an existing group (MOTU 11) were found in clade B but a larger sampling effort and further morphological examination are needed to confirm this.

Regarding major clade A, the combined molecular data from three different loci provided compelling evidence for the existence of at least 10 deeply divergent and completely sorted lineages within the *P. dumerilii* complex in Europe. These deep genetic distances are a strong indication of long term isolation, therefore the lineages involved can qualify for recognition as separate species (Bickford et al. 2007; Churchill et al. 2014; Delić et al. 2017). Complementing the molecular data, some morphological variations within the most abundant MOTUs (4, 6, 7, 9, 10) were also found (Table 6). The genetic COI distances recorded in this clade (mean 19.8%, K2P) fit within the range reported for congeneric distances in comprehensive studies of COI variation targeting polychaetes. For example, mean COI distances

(K2P) of 16.5, 24.0 and 16.9% were found in the regional polychaete fauna of the Arctic (Carr *et al.* 2011), Northeast Atlantic (Lobo *et al.* 2016) and in South American *Laeonereis* (Nereididae) species (Sampieri *et al.* 2021). Additionally, Glasby *et al.* (2013) also compared COI genetic pairwise distances (K2P) in several Australian nereidid species displaying cryptic evidence (*Nereis denhamensis* Augener, 1913, *Perinereis suluana* (Horst, 1924), *Pseudonereis anomala* Gravier, 1899), where results showed two distance peaks (low, might indicate same lineages; high, different lineages) in the ‘within species’ distance data, with the higher and most common distance peaks averaging ~22–24, 28–30 and 20–22% respectively. The only exception to this are MOTUs 5 and 10 where the COI distances to the nearest neighbours (MOTUs 4 and 9) were much lower, namely 8.6 and 6.4% respectively, still a fair genetic distance but much higher than the usual intraspecific variation found in nereidids (<3.5%, Glasby 2005; Paiva *et al.* 2019).

### Untangling the *Platynereis* complex

The original description for *P. massiliensis* by Moquin-Tandon (1869) is brief and does not include figures (Moquin-Tandon 1869). Instead, the main reproductive features were highlighted since an errant polychaete is recorded as hermaphroditic for the first time. Further studies have been treating this species as morphologically similar to *P. dumerilii* when analysing the respective specimens (Hauenschild 1951; Schneider *et al.* 1992; Valvassori *et al.* 2015), despite some considerable differences in the parapodia morphology and absence of paragnaths described in the original description of *P. massiliensis*. Morphological variation in the number of jaw teeth and paragnath patterns was also reported for several specimens identified as *P. dumerilii* (Claparède 1870) and could be an indication of possible cryptic diversity. Based on Wäge *et al.* (2017), genetically pinpointing two lineages sharing the same reproductive features as *P. massiliensis* (egg brooders), mainly present in acidic waters and two other clades matching *P. dumerilii* (*heteronereis* stage), mostly living in non-acidic waters, was possible. These two *P. dumerilii* clades grouped in our clade A2, more specifically in MOTUs 4 and 6, with the first one occurring in the type locality. MOTU 4 (*P. dumerilii* s.s.) and MOTU 6 (*P. jourdei* sp. nov.) have a distinct paragnath distribution pattern from those in clade A3 (MOTUs 7, 9 and 10). Instead, the latter clade contains sequences of *P. massiliensis* from Wäge *et al.* (2017). As stated by Wäge *et al.* (2017), despite the lack of the type material, the congruence of the developmental observations with other studies (Hauenschild 1951; Schneider *et al.* 1992; Helm *et al.* 2014) suggests that the *Platynereis* population from Ischia represents *P. massiliensis* and group together with our sequences specifically from MOTU 9. The Vulcano population, also a brooder, grouped with our two sequences from Banyuls in MOTU 1 (clade A1) but observing the pharynx

and confirming whether similar paragnath patterns to those of MOTU 9 could also be identified was not possible.

Within the *massiliensis*-type clade A3, MOTU 7 (*P. nunezi* sp. nov.) and MOTU 8 are endemic to the Azores and Webbsnesia islands, MOTU GB1 has been reported from South Africa, and MOTUs GB2 and GB3 probably belong either to MOTU 9 or MOTU 10. Among the analysed material, only MOTU 10, also present in the Western Mediterranean, could qualify as a possible source for the originally described *P. massiliensis*. MOTU 10 is genetically close to MOTU 9 (maximum distances of 6.4% COI K2P) and these very likely share the same reproductive traits; however there are some visible morphological differences when compared to the latter. These differences seem to fit the description of *Nereis agilis* Keferstein, 1862, described for the north-eastern Atlantic (type locality: St Vaast, France) and hitherto considered as an unaccepted subjective synonym for *P. dumerilii*. In the original description, the analysed specimens seem to be simultaneous hermaphrodites without a *heteronereis* stage, tentacular cirri and dorsal cirri are longer than the ones usually reported for *P. dumerilii* and on parapodia four, ligules are noticeable, although the third (starting from the dorsal side) is very short but no mention is made of the pharynx (Keferstein 1862). Another unaccepted subjective synonym described for the Gulf of Naples (Italy), *Nereis peritonealis* Claparède, 1868, describes a similar paragnath pattern as the one presented here for clade A3. However, even though there are no detailed data on the reproductive mode, the reported small size of mature eggs (Claparède 1868) would suggest that this is not a species with direct development, i.e. not a brooder, but there may be a planktonic larval stage (Sato and Masuda 1997). This is in line with MOTUs 4 and 6 instead, even though paragnath patterns do not match. An interesting note regarding the description of *Nereis agilis* is that ovaries and testes are separated into two different sectors of the body (Keferstein 1862), whereas in *P. massiliensis* these should occur in the same segments (Moquin-Tandon 1869). The latter arrangement is very surprising from a biological perspective, as this would imply a high risk of self-fertilisation; nonetheless, such discrepancies might depend on different interpretations of the same structures by different scholars, and what is interpreted as a developing gonad might be a glandular structure in other sources. This calls for a new observation on the reproductive features and a description based on topotypic material to compare with our interpretation of *P. massiliensis*, and confirms whether the lineage identified in this and other studies matches the topotypic samples.

Other species with currently unaccepted names in European type localities are also available (Table 5) but these are incomplete and an unequivocal attribution to any of the MOTUs found in clade A seems impossible. Three additional European synonyms with *P. dumerilii*, i.e. *Heteronereis fucicola* Örsted, 1843, *Nereilepas variabilis* Örsted, 1843, and

*Heteronereis malmgreni* Claparède, 1868, were not included in this table because all refer to epitoke forms, that at the time were believed to be different species from the atoke forms. We cannot possibly reconstruct the morphological correspondence to the atoke specimens we studied but we can exclude that these are synonymous with *P. massiliensis*-like brooders. Taxa from Denmark described by Örsted represent different stages of the epitoke modification or different sexes, and based on distribution of MOTUs, might correspond either to *P. dumerilii* s.s. (MOTU 4) or MOTU 2. *Heteronereis malmgreni* was instead described for the Gulf of Naples and is probably a description of the epitoke form of *Nereis peritonealis* discussed before. *Heteronereis maculata* described for the Black Sea is also synonymised, however further details from this species were not included in Table 5 due the difficulty in translating the original Russian description, but together with *Nereis taurica* (also a description of an epitoke form, from the Black Sea), might be related to the unnamed MOTU 3 (Ionian Sea) based on type locality proximity.

### Reproduction strategies in *Platynereis*

The suggested reproduction modes based on genetic proximity indicated in this study, being fixed at the basis of the two major clades retrieved by Wäge *et al.* (2017) might not be correct. Instances of reproductive plasticity were reported in other Nereididae species, e.g. the suppression of epitoky as a probable answer to environmental pressures within the same lineage (Prevedelli and Cassai 2001; Daas *et al.* 2011). However, as no genetic data complemented these studies, this could also be a clue to unreported cryptic species. Several references, pointed out in Daas *et al.* (2011), that the presence of atokous and epitokous ‘races’ or ‘forms’ in *Perinereis cultrifera* (Grube, 1840) (e.g. Marcel 1962; Zghal and Ben Amor 1989; Scaps *et al.* 1992; Rouhi *et al.* 2008) might actually be linked to the evidence of cryptic species within this taxon, as reported in other studies. For example, upon further examination, *Perinereis* populations from the North of France and Algeria have distinct alloenzymes, number of paragnaths and number of teeth per half jaw (Scaps *et al.* 2000). Using similar methods to the previous example, distinct populations from the Elba Island (Western Italy) were also found, corresponding to two different habitat types between brackish waters and an adjacent marine site (Maltagliati *et al.* 2001). Nevertheless, this would still question whether sister lineages or other phylogenetically close species might or not have completely different reproduction modes. In the absence of studies on reproductive biology complemented with genetic data, we should not discard the possibility of different reproductive features within the *Platynereis* complex or even possible reproductive plasticity within the same MOTU. The morphology of sexually mature *Platynereis* worms may also prove useful in distinguishing between different lineages with the same reproductive epitoky feature, e.g. the differences

found in morphology of sperm papillae groups in males, and number of pre-natatory anterior segments in both sexes between different closely related *Perinereis* species reported by Read (2007).

The low dispersal rate in many marine brooding species with direct or semi-direct development without a planktonic larval stage is speculated to be able to promote genetic divergence and help to explain the genetic isolation of populations, whereas the free-swimming larvae easily migrate, resulting in higher probabilities of gene flow among populations (Palumbi and Baker 1994; Teske *et al.* 2011). Evidence that stressful conditions (e.g. hydrothermal vents, port and subtidal environments or brackish-water habitats) are better tolerated in the survival of *Platynereis* populations with a brooding strategy was noted in several studies (Lucey *et al.* 2015; Gambi *et al.* 2016; Wäge *et al.* 2017). Being volcanic in origin, the islands within the Lusitanian biogeographical province (Freitas *et al.* 2019) harbour a large number of CO<sub>2</sub> vents characterised by the low pH waters (Viveiros *et al.* 2020; González-Delgado *et al.* 2021) that might favour the proliferation of brooder worms instead of free spawners. Sampling in the CO<sub>2</sub> vents or even subtidal regions in general, could also provide additional *Platynereis* lineages yet to be explored, given the intertidal focus in this current study. Some lineages could even be unique to each island, given how important the Azores and Webbnesia archipelagos seem to be in the cryptic diversity of marine invertebrates, such as amphipods and isopods (Desiderato *et al.* 2019; Vieira *et al.* 2019).

### Final remarks

Among the 10 different *Platynereis* lineages from Europe uncovered with molecular data, seven of these had particular geographical distributions, either confined to the West (MOTUs 1 and 6) or East (MOTU 3) Mediterranean Sea, Northeast Atlantic (MOTU 2), Azores and Webbnesia islands (MOTU 7) and sometimes exclusive to a single island (MOTU 8) or limited to a few islands within a single archipelago (MOTU 5), also indicating a high level of endemism. MOTUs 4, 9 and 10 were sympatric with at least two other lineages from the group, with MOTUs 9 and 10 revealing geographically structured populations through the COI haplotypes. No considerable genetic structure was found in each sampled island within MOTU 7 despite the existence of two other lineages in this region of the Atlantic. These findings call for a better recognition of the role of both the Azores and Webbnesia archipelagos, and the Mediterranean Sea as promoters of extensive diversification of marine invertebrates and emphasise the importance of the conservation of the biodiversity of the intertidal rocky shore of these regions. Despite the two new species erected in this study (*P. nunezi* sp. nov. and *P. jourdei* sp. nov.) and further clarification regarding the status of *P. agilis*, *P. dumerilii*



and *P. massiliensis*, five other lineages remain unnamed and in need of further sampling effort and morphological examination. This particularly includes MOTU 2, an apparently rarer lineage from the Northeast Atlantic, that seems to be easy to find in Norway based on sampling campaigns under the Norwegian projects (BIN: BOLD:AAC5474, BOLD Systems). Moreover, sampling in subtidal regions could reveal additional hidden lineages to be added to the complex. Three other unaccepted synonyms are also reported for this area (e.g. Denmark), but descriptions are incomplete or refer only to epitoke forms. Topotypic specimens of *P. massiliensis* and further studies on the reproductive biology are also needed to determine whether this species corresponds to the lineage assumed in this, and previous studies (Calosi *et al.* 2013; Wäge *et al.* 2017; Kara *et al.* 2020).

Failure to recognise this hidden biodiversity may compromise the accuracy and interpretation of biomonitoring and ecological data for *Platynereis* and the use as a model species (Özpolat *et al.* 2021). Integrative taxonomy is therefore essential to solve these uncertainties and allow naming the undescribed species involved. Otherwise, most molecular data providing enough support for species hypotheses will continue to be unused, and large fractions of biodiversity will persist unnoticed.

## Supplementary material

Supplementary material is available [online](#).

## References

- Abbiati M, Castelli A (1992) *Platynereis nadiæ* sp. n. (Polychaeta: Nereididae) from Italian coasts. *Zoologica Scripta* **21**(2), 151–155. doi:10.1111/j.1463-6409.1992.tb00317.x
- Arvanitidis C (2000) Polychaete fauna of the Aegean Sea: inventory and new information. *Bulletin of Marine Science* **66**, 73–96.
- Astrin J, Zhou X, Misof B (2013) The importance of biobanking in molecular taxonomy, with proposed definitions for vouchers in a molecular context. *ZooKeys* **365**, 67–70. doi:10.3897/zookeys.365.5875
- Audouin JV, Milne Edwards H (1833) [Part 3.] Classification des Annélides et description de celles qui habitent les côtes de la France. *Annales des sciences naturelles, Paris (series 1)* **29**, 195–269.
- Bakken T, Wilson RS (2005) Phylogeny of nereidids (Polychaeta, Nereididae) with paragnaths. *Zoologica Scripta* **34**, 507–547. doi:10.1111/j.1463-6409.2005.00200.x
- Bakken T, Glasby CJ, Wilson RS (2009) A review of paragnath morphology in Nereididae (Polychaeta). *Zoosymposia* **2**, 305–316. doi:10.11646/zoosymposia.2.1.21
- Bakken T, Hårsaker K, Daverdin M (2021) Marine invertebrate collection NTNU University Museum. Version 1.976. Norwegian University of Science and Technology. Occurrence dataset. doi:10.15468/ddbs14
- Bellan G (1980) Relationship of pollution to rocky substratum polychaetes on the French Mediterranean coast. *Marine Pollution Bulletin* **11**, 318–321. doi:10.1016/0025-326X(80)90048-X
- Bickford D, Lohman DJ, Sodhi NS, Ng PKL, Meier R, Winker K, Ingram KK, Das I (2007) Cryptic species as a window on diversity and conservation. *Trends in Ecology & Evolution* **22**, 148–155. doi:10.1016/j.tree.2006.11.004
- Bouckaert R, Heled J, Kühnert D, Vaughan T, Wu C-H, Xie D, Suchard MA, Rambaut A, Drummond AJ (2014) BEAST 2: a software platform for Bayesian evolutionary analysis. *PLOS Computational Biology* **10**, e1003537. doi:10.1371/journal.pcbi.1003537
- Calosi P, Rastrick SPS, Lombardi C, de Guzman HJ, Davidson L, Jahnke M, Giangrande A, Hardege JD, Schulze A, Spicer JJ, Gambi M-C (2013) Adaptation and acclimatization to ocean acidification in marine ectotherms: an *in situ* transplant experiment with polychaetes at a shallow CO<sub>2</sub> vent system. *Philosophical Transactions of the Royal Society of London – B. Biological Sciences* **368**, 20120444. doi:10.1098/rstb.2012.0444
- Carr CM, Hardy SM, Brown TM, Macdonald TA, Hebert PDN (2011) A tri-oceanic perspective: DNA barcoding reveals geographic structure and cryptic diversity in Canadian polychaetes. *PLoS One* **6**, e22232. doi:10.1371/journal.pone.0022232
- Cerca J, Meyer C, Purschke G, Struck TH (2020) Delimitation of cryptic species drastically reduces the geographical ranges of marine interstitial ghost-worms (*Stygocapitella*; Annelida, Sedentaria). *Molecular Phylogenetics and Evolution* **143**, 106663. doi:10.1016/j.ympev.2019.106663
- Churchill CKC, Valdés Á, Foighil DÓ (2014) Molecular and morphological systematics of neustonic nudibranchs (Mollusca: Gastropoda: Glaucidae: *Glaucus*), with descriptions of three new cryptic species. *Invertebrate Systematics* **28**, 174–195. doi:10.1071/IS13038
- Claparède E (1868) Les annélides chétopodes du Golfe de Naples. *Mémoires de la Société de Physique et d'Histoire Naturelle de Genève* **19**, 313–584. Available at <https://www.biodiversitylibrary.org/page/14309905>
- Claparède E (1870) Les Annélides Chétopodes du Golfe de Naples. Supplément. *Mémoires de la Société de Physique et d'histoire Naturelle de Genève* **20**, 365–542.
- Clement M, Snell Q, Walke P, Posada D, Crandall K (2002) TCS: estimating gene genealogies. In 'Proceedings 16th International Parallel and Distributed Processing Symposium', 15–19 April 2001, Fort Lauderdale, FL, USA. (IEEE) doi:10.1109/IPDPS.2002.1016585
- Coll M, Piroddi C, Steenbeek J, Kaschner K, Lasram FBR, Aguzzi J, Ballesteros E, Bianchi CN, Corbera J, Dailianis T, Danovaro R, Estrada M, Froglià C, Galil BS, Gasol JM, Gertwagen R, Gil J, Guilhaumon F, Kesner-Reyes K, Kitsos MS, Koukouras A, Lampadariou N, Laxamana E, López-Fé de la Cuadra CM, Lotze HK, Martin D, Mouillot D, Oro D, Raicevich S, Rius-Barile J, Saiz-Salinas JJ, San Vicente C, Somot S, Templado J, Turon X, Vafidis D, Villanueva R, Voultsiadou E (2010) The biodiversity of the Mediterranean Sea: estimates, patterns, and threats. *PLoS One* **5**, e11842. doi:10.1371/journal.pone.0011842
- Conde-Vela VM (2018) New species of *Pseudonereis* Kinberg, 1865 (Polychaeta: Nereididae) from the Atlantic Ocean, and a review of paragnath morphology and methodology. *Zootaxa* **4471**, 245–278. doi:10.11646/zootaxa.4471.2.2
- Conde-Vela VM, Salazar-Vallejo SI (2015) Redescriptions of *Nereis oligohalina* (Rioja, 1946) and *N. garwoodi* González-Escalante & Salazar-Vallejo, 2003 and description of *N. confusa* sp. n. (Annelida, Nereididae). *ZooKeys* **518**, 15–49.
- Daas T, Younsi M, Daas-Maamcha O, Gillet P, Scaps P (2011) Reproduction, population dynamics and production of *Nereis falsa* (Nereididae: Polychaeta) on the rocky coast of El Kala National Park, Algeria. *Helgoland Marine Research* **65**, 165–173. doi:10.1007/s10152-010-0212-5
- Darriba D, Taboada GL, Doallo R, Posada D (2012) jModelTest 2: more models, new heuristics and parallel computing. *Nature Methods* **9**, 772–772. doi:10.1038/nmeth.2109
- Day JH (1967) 'A Monograph on the Polychaeta of Southern Africa. Vol. 2. Sedentaria.' (Trustees of the British Museum (Natural History): London, UK)
- Delić T, Trontelj P, Rendoš M, Fišer C (2017) The importance of naming cryptic species and the conservation of endemic subterranean amphipods. *Scientific Reports* **7**, 3391. doi:10.1038/s41598-017-02938-z
- Desiderato A, Costa FO, Serejo CS, Abbiati M, Queiroga H, Vieira PE (2019) Macaronesian islands as promoters of diversification in amphipods: the remarkable case of the family Hyalidae (Crustacea, Amphipoda). *Zoologica Scripta* **48**, 359–375. doi:10.1111/zsc.12339
- Ehlers E (1868) 'Die Borstenwürmer (Annelida Chætopoda) nach systematischen und anatomischen Untersuchungen dargestellt'. (Wilhelm Engelmann)
- Faulwetter S, Simbora N, Katsiaras N, Chatzigeorgiou G, Arvanitidis C (2017) Polychaetes of Greece: an updated and annotated checklist. *Biodiversity Data Journal* **5**, e20997. doi:10.3897/BDJ.5.e20997

- Fischer A, Dorresteijn A (2004) The polychaete *Platynereis dumerilii* (Annelida): a laboratory animal with spiralian cleavage, lifelong segment proliferation and a mixed benthic/pelagic life cycle. *Bioessays* **26**, 314–325. doi:10.1002/bies.10409
- Freitas R, Romeiras M, Silva L, Cordeiro R, Madeira P, González JA, Wirtz P, Falcón JM, Brito A, Floeter SR, Afonso P, Porteiro F, Viera-Rodríguez MA, Neto AI, Haroun R, Farminhão JNM, Rebelo AC, Baptista L, Melo CS, Martínez A, Núñez J, Berning B, Johnson ME, Ávila SP (2019) Restructuring of the ‘Macaronesia’ biogeographic unit: a marine multi-taxon biogeographical approach. *Scientific Reports* **9**, e15792. doi:10.1038/s41598-019-51786-6
- Fujisawa T, Barraclough TG (2013) Delimiting species using single-locus data and the generalized mixed Yule coalescent approach: a revised method and evaluation on simulated data sets. *Systematic Biology* **62**, 707–724. doi:10.1093/sysbio/syt033
- Gambi MC, Zupo V, Buia MC, Mazzella L (2000) Feeding ecology of *Platynereis dumerilii* (Audouin & Milne-Edwards) in the seagrass *Posidonia oceanica* system: the role of the epiphytic flora (Polychaeta, nereididae). *Ophelia* **53**, 189–202. doi:10.1080/00785326.2000.10409449
- Gambi MC, Musco L, Giangrande A, Badalamenti F, Micheli F, Kroeker KJ (2016) Distribution and functional traits of polychaetes in a CO<sub>2</sub> vent system: winners and losers among closely related species. *Marine Ecology Progress Series* **550**, 121–134. doi:10.3354/meps11727
- Giangrande A (1988) Polychaete zonation and its relation to algal distribution down a vertical cliff in the western Mediterranean (Italy): a structural analysis. *Journal of Experimental Marine Biology and Ecology* **120**, 263–276. doi:10.1016/0022-0981(88)90006-8
- Glasby CJ (2005) Polychaete distribution patterns revisited: an historical explanation. *Marine Ecology* **26**, 235–245. doi:10.1111/j.1439-0485.2005.00059.x
- Glasby CJ (2015) Nereididae (Annelida: Phyllococida) of Lizard Island, Great Barrier Reef, Australia. *Zootaxa* **4019**, 207–239. doi:10.11646/zootaxa.4019.1.11
- Glasby CJ, Wei N-WV, Gibb KS (2013) Cryptic species of Nereididae (Annelida: Polychaeta) on Australian coral reefs. *Invertebrate Systematics* **27**, 245–264. doi:10.1071/IS12031
- González-Delgado S, González-Santana D, Santana-Casiano M, González-Dávila M, Hernández CA, Sangil C, Hernández JC (2021) Chemical characterization of the Punta de Fuencaliente CO<sub>2</sub>-enriched system (La Palma, NE Atlantic Ocean): a new natural laboratory for ocean acidification studies. *Biogeosciences* **18**, 1673–1687. doi:10.5194/bg-18-1673-2021
- Gravina MF, Lezzi M, Bonifazi A, Giangrande A (2015) The genus *Nereis* Linnaeus, 1758 (Polychaeta, Nereididae): state of the art for identification of Mediterranean species. *Atti della Società Toscana di Scienze Naturali, Memorie Serie B* **122**, 147–164.
- Guindon S, Gascuel O (2003) A simple, fast, and accurate algorithm to estimate large phylogenies by maximum likelihood. *Systematic Biology* **52**, 696–704. doi:10.1080/106351503902335520
- Hartman O (1951) The littoral marine annelids of the Gulf of Mexico. *Publications of the Institute of Marine Science, Port Aransas, Texas* **2**, 7–124.
- Hartmann-Schroeder G (1996) Annelida, Borstenwuermer, Polychaeta. In ‘Tierwelt Deutschlands. Vol. 58’, 2nd edn. (Eds M Dahl, F Peus) (Gustav Fischer: Jena, Germany)
- Hauenschild C (1951) Nachweis der sogenannten atoken Geschlechtsform des Polychaeten *Platynereis dumerilii* Aud. et M.-Edw. als eigene Art aufgrund von Zuchtversuchen. *Zoologische Jahrbücher. Abteilung für Allgemeine Zoologie und Physiologie der Tiere* **63**, 107–128.
- Helm C, Adamo H, Hourdez S, Bleidorn C (2014) An immunocytochemical window into the development of *Platynereis massiliensis* (Annelida, Nereididae). *The International Journal of Developmental Biology* **58**, 613–622. doi:10.1387/ijdb.140081cb
- Hupało K, Teixeira MAL, Rewicz T, Sezgin M, Iannilli V, Karaman GS, Grabowski M, Costa FO (2019) Persistence of phylogeographic footprints helps to understand cryptic diversity detected in two marine amphipods widespread in the Mediterranean basin. *Molecular Phylogenetics and Evolution* **132**, 53–66. doi:10.1016/j.ympev.2018.11.013
- Hutchings P, Kupriyanova E (2018) Cosmopolitan polychaetes – fact or fiction? Personal and historical perspectives. *Invertebrate Systematics* **32**, 1–9. doi:10.1071/IS17035
- Ibarzábal DR (2006) Poliquetos del Archipiélago de Sabana-Camagüey, ecoregión norcentral de Cuba. *Cocuyo* **16**, 11–14.
- Jörger KM, Norenburg JL, Wilson NG, Schrödl M (2012) Barcoding against a paradox? Combined molecular species delineations reveal multiple cryptic lineages in elusive meiofaunal sea slugs. *BMC Evolutionary Biology* **12**, 245. doi:10.1186/1471-2148-12-245
- Kara J, Santos CSG, Macdonald AHH, Simon CA (2020) Resolving the taxonomic identities and genetic structure of two cryptic *Platynereis* Kinberg species from South Africa. *Invertebrate Systematics* **34**, 618–636. doi:10.1071/IS19072
- Keferstein W (1862) Untersuchungen über niedere Seethiere. *Zeitschrift für wissenschaftliche Zoologie* **12**, 1–147, plates 1–11. Available at <https://www.biodiversitylibrary.org/page/44977773>
- Kinberg JGH (1865) Annulata nova [Continuatio]. Öfversigt af Koninglich. Vetenskapsakademiens förhandlingar. *Stockholm* **22**, 167–179. Available at <https://biodiversitylibrary.org/page/32339443>
- King RA, Fagan-Jeffries EP, Bradford TM, Stringer DN, Finston TL, Halse SA, Eberhard SM, Humphreys G, Humphreys BF, Austin AD, Cooper SJB (2022) Cryptic diversity down under: defining species in the subterranean amphipod genus *Nedisia* Barnard & Williams, 1995 (Hadzioidea: Eriopisidae) from the Pilbara, Western Australia. *Invertebrate Systematics* **36**, 113–159. doi:10.1071/IS21041
- Kumar S, Stecher G, Li M, Knyaz C, Tamura K (2018) MEGA X: molecular evolutionary genetics analysis across computing platforms. *Molecular Biology and Evolution* **35**, 1547–1549. doi:10.1093/molbev/msy096
- Langeneck J, Scarpa F, Maltagliati F, Sanna D, Barbieri M, Cossu P, Mikac B, Galletti MC, Castelli A, Casu M (2020) A complex species complex: the controversial role of ecology and biogeography in the evolutionary history of *Syllis gracilis* Grube, 1840 (Annelida, Syllidae). *Journal of Zoological Systematics and Evolutionary Research* **58**, 66–78. doi:10.1111/jzs.12336
- Leigh JW, Bryant D (2015) popart: full-feature software for haplotype network construction. *Methods in Ecology and Evolution* **6**, 1110–1116. doi:10.1111/2041-210X.12410
- Librado P, Rozas J (2009) DnaSP v5: a software for comprehensive analysis of DNA polymorphism data. *Bioinformatics* **25**, 1451–1452. doi:10.1093/bioinformatics/btp187
- Lobo J, Teixeira MAL, Borges LMS, Ferreira MSG, Hollatz C, Gomes PT, Sousa R, Ravara A, Costa MH, Costa FO (2016) Starting a DNA barcode reference library for shallow water polychaetes from the southern European Atlantic coast. *Molecular Ecology Resources* **16**, 298–313. doi:10.1111/1755-0998.12441
- Lucey NM, Lombardi C, DeMarchi L, Schulze A, Gambi MC, Calosi P (2015) To brood or not to brood: are marine invertebrates that protect their offspring more resilient to ocean acidification? *Scientific Reports* **5**, 12009. doi:10.1038/srep12009
- McIntosh WC (1910) A monograph of the British annelids. Polychaeta. Syllidae to Ariciidae. *Ray Society of London* **2**, 233–524.
- Malmgren AJ (1867) ‘Annulata Polychaeta Spetsbergiae, Groenlandiae, Islandiae et Scandinaviae. Hactenus Cognita’. (Ex Officina Frenckelliana: Helsingforslä)
- Maltagliati F, Camilli L, Lardicci C, Castelli A (2001) Evidence for morphological and genetic divergence in *Perinereis cultrifera* (Polychaeta: Nereididae) from two habitat types at Elba Island. *Journal of the Marine Biological Association of the United Kingdom* **81**, 411–414. doi:10.1017/S0025315401004027
- Marcel R (1962) Cycle annuel de *Perinereis cultrifera* Grube (Annélide Polychète) à Alger. *Mémoires de la Société des Sciences Naturelles de Cherbourg* **19**, 39–54.
- Martin D, Gil J, Zanol J, Meca MA, Portela RP (2020) Correction: Digging the diversity of Iberian bait worms *Marphysa* (Annelida, Eunicidae). *PLoS One* **15**, e0226749. doi:10.1371/journal.pone.0233825
- Miralles L, Ardura A, Arias A, Borrell YJ, Clusa L, Dopico E, de Rojas AH, Lopez B, Muñoz-Colmenero M, Roca A, Valiente AG, Zaiko A, Garcia-Vazquez E (2016) Barcodes of marine invertebrates from north Iberian ports: native diversity and resistance to biological invasions. *Marine Pollution Bulletin* **112**(1–2), 183–188. doi:10.1016/j.marpolbul.2016.08.022
- Mikac B (2015) A sea of worms: polychaete checklist of the Adriatic Sea. *Zootaxa* **3943**, 1–172. doi:10.11646/zootaxa.3943.1.1
- Moquin-Tandon G (1869) Note sur une nouvelle annelide chetopode hermaphrodite (*Nereis massiliensis*). *Annales des sciences naturelles*,

- Paris (series 5) 11, 134. Available at <https://www.biodiversitylibrary.org/page/33087914>
- Norlinder E, Nygren A, Wiklund H, Pleijel F (2012) Phylogeny of scale-worms (Aphroditiformia, Annelida), assessed from 18S rRNA, 28S rRNA, 16S rRNA, mitochondrial cytochrome c oxidase subunit I (COI), and morphology. *Molecular Phylogenetics and Evolution* 65(2), 490–500. doi:10.1016/j.ympev.2012.07.002
- Núñez J (2004) Familia Nereididae Savigny, 1822. In: Viéitez JM, Alós C, Parapar J, Besteiro C, Moreira J, Núñez J, Laborda J, San Martín G. Annelida Polychaeta I. *Fauna Iberica* 25, 293–390.
- Nygren A (2014) Cryptic polychaete diversity: a review. *Zoologica Scripta* 43, 172–183. doi:10.1111/zsc.12044
- Nygren A, Parapar J, Pons J, Meißner K, Bakken T, Kongsrud JA, Oug E, Gaeva D, Sikorski A, Johansen R, Hutchings PA, Lavesque N, Capa M (2018) A mega-cryptic species complex hidden among one of the most common annelids in the North East Atlantic. *PLoS One* 13, e0198356. doi:10.1371/journal.pone.0198356
- Örsted AS (1843) Annulatorum danicorum conspectus. Auctore A.S. Örsted. Fasc. I. Maricolæ. (Quæstio ab universitate Hafniensi ad solvendum proposita et proemio ornata) Available at <http://www.biodiversitylibrary.org/bibliography/11849>
- Özpolat BD, Randel N, Williams EA, Bezares-Calderón LA, Andreatta G, Balavoine G, Bertucci PY, Ferrier DEK, Gambi MC, Gazave E, Handberg-Thorsager M, Hardege J, Hird C, Hsieh Y-W, Hui J, Mutemi KN, Schneider SQ, Simakov O, Vergara HM, Vervoort M, Jékely G, Tessmar-Raible K, Raible F, Arendt D (2021) The Nereid on the rise: *Platynereis* as a model system. *EvoDevo* 12, 10. doi:10.1186/s13227-021-00180-3
- Paiva PC, Mutaquilha BF, Coutinho MCL, Santos CSG (2019) Comparative phylogeography of two coastal species of *Perinereis* Kinberg, 1865 (Annelida, Polychaeta) in the South Atlantic. *Marine Biodiversity* 49, 1537–1551. doi:10.1007/s12526-018-0927-0
- Palumbi SR, Baker CS (1994) Contrasting population structure from nuclear intron sequences and mtDNA of humpback whales. *Molecular Biology and Evolution* 11, 426–435. doi:10.1093/oxfordjournals.molbev.a040115
- Pleijel F, Jondelius U, Norlinder E, Nygren A, Oxelman B, Schander C, Sundberg P, Thollesson M (2008) Phylogenies without roots? A plea for the use of vouchers in molecular phylogenetic studies. *Molecular Phylogenetics and Evolution* 48, 369–371. doi:10.1016/j.ympev.2008.03.024
- Popa LO, Popa OP, Krapal A-M, Iorgu EI, Surugiu V (2014) Fine-scale population genetics analysis of *Platynereis dumerilii* (Polychaeta, Nereididae) in the Black Sea: how do local marine currents drive geographical differentiation? *Journal of Experimental Zoology – A. Ecological Genetics and Physiology* 321, 41–47. doi:10.1002/jez.1835
- Prevedelli D, Cassai C (2001) Reproduction and larval development of *Perinereis rullieri* Pilato in the Mediterranean Sea (Polychaeta: Nereididae). *Ophelia* 54, 133–142. doi:10.1080/00785236.2001.10490461
- Puillandre N, Lambert A, Brouillet S, Achaz G (2012) ABGD, Automatic Barcode Gap Discovery for primary species delimitation. *Molecular Ecology* 21, 1864–1877. doi:10.1111/j.1365-294X.2011.05239.x
- Quatrefages A (1866) 'Histoire naturelle des Annelés marins et d'eau douce. Annelides et Géphyriens. Vol. 1'. (Librarie Encyclopédique de Roret: Paris, France) Available at <http://books.google.com/books?id=FV9IAAAAYAAJ>
- Rambaut A, Drummond AJ, Xie D, Baele G, Suchard MA (2018) Posterior summarization in Bayesian phylogenetics using Tracer 1.7. *Systematic Biology* 67, 901–904. doi:10.1093/sysbio/syy032
- Ratnasingham S, Hebert PDN (2013) A DNA-based registry for all animal species: the Barcode Index Number (BIN) system. *PLoS One* 8, e66213. doi:10.1371/journal.pone.0066213
- Read GB (2007) Taxonomy of sympatric New Zealand species of *Platynereis*, with description of three new species additional to *P. australis* (Schmarda) (Annelida: Polychaeta: Nereididae). *Zootaxa* 1558, 1–28. doi:10.11646/zootaxa.1558.1.1
- Read G, Fauchald K (Eds) (2021) *Nereis heterocirrata* Treadwell, 1931. In 'World Polychaeta Database'. Available at <https://www.marinespecies.org/polychaeta/aphia.php?p=taxdetails&id=329658> [Verified 12 May 2021]
- Read G, Fauchald K (Eds) (2022) *Platynereis dumerilii* (Audouin & Milne Edwards, 1833). In 'World Polychaeta Database'. Available at <https://www.marinespecies.org/aphia.php?p=taxdetails&id=130417> [Verified 13 June 2022]
- Ricevuto E, Benedetti M, Regoli F, Spicer JI, Gambi MC (2015) Antioxidant capacity of polychaetes occurring at a natural CO<sub>2</sub> vent system: results of an *in situ* reciprocal transplant experiment. *Marine Environmental Research* 112, 44–51. doi:10.1016/j.marenvres.2015.09.005
- Ronquist F, Huelsenbeck JP (2003) MrBayes 3: Bayesian phylogenetic inference under mixed models. *Bioinformatics* 19, 1572–1574. doi:10.1093/bioinformatics/btg180
- Rouhi A, Gillet P, Deutsch B (2008) Reproduction and population dynamics of *Perinereis cultrifera* (Polychaeta: Nereididae) of the Atlantic coast, El Jadida, Morocco. *Cahiers De Biologie Marine* 49, 151–160.
- Sampieri BR, Vieira PE, Teixeira MAL, Seixas VC, Pagliosa PR, Amaral ACZ, Costa FO (2021) Molecular diversity within the genus *Laeonereis* (Annelida, Nereididae) along the west Atlantic coast: paving the way for integrative taxonomy. *PeerJ* 9, e11364. doi:10.7717/peerj.11364
- Sato M, Masuda Y (1997) Genetic differentiation in two sibling species of the brackish-water polychaete *Hediste japonica* complex (Nereididae). *Marine Biology* 130, 163–170. doi:10.1007/s002270050235
- Scaps P, Retière C, Desrosiers G, Miron G (1992) Dynamique d'une population de *Perinereis cultrifera* (Grube) de la côte nord de Bretagne. *Cahiers De Biologie Marine* 33, 477–494.
- Scaps P, Rouabah A, Leprêtre A (2000) Morphological and biochemical evidence that *Perinereis cultrifera* (Polychaeta: Nereididae) is a complex of species. *Journal of the Marine Biological Association of the United Kingdom* 80, 735–736. doi:10.1017/S0025315400002587
- Schneider S, Fischer A, Dorresteijn AWC (1992) A morphometric comparison of dissimilar early development in sibling species of *Platynereis* (Annelida, Polychaeta). *Roux's Archives of Developmental Biology* 201, 243–256. doi:10.1007/BF00188755
- Struck TH, Feder JL, Bendiksbj M, Birkeland S, Cerca J, Gusarov VI, Kistenich S, Larsson K-H, Liow LH, Nowak MD, Stedje B, Bachmann L, Dimitrov D (2018) Finding evolutionary processes hidden in cryptic species. *Trends in Ecology & Evolution* 33, 153–163. doi:10.1016/j.tree.2017.11.007
- Teixeira MAL, Vieira PE, Pleijel F, Sampieri BR, Ravara A, Costa FO, Nygren A (2020) Molecular and morphometric analyses identify new lineages within a large *Eumida* (Annelida) species complex. *Zoologica Scripta* 49, 222–235. doi:10.1111/zsc.12397
- Teixeira MAL, Nygren A, Ravara A, Vieira PE, Hernández JC, Costa FO (2021) The small polychaete *Platynereis dumerilii* revealed as a large species complex with fourteen MOTUs in European marine habitats. *ARPHA Conference Abstracts* 4, e64937. doi:10.3897/aca.4.e64937
- Teixeira MAL, Vieira PE, Ravara A, Costa FO, Nygren A (2022) From 13 to 22 in a second stroke: revisiting the European *Eumida sanguinea* (Phyllodoctidae: Annelida) species complex. *Zoological Journal of the Linnean Society* 196, 169–197. doi:10.1093/zoolinnean/zlab100
- Teske PR, von der Heyden S, McQuaid CD, Barker NP (2011) A review of marine phylogeography in southern Africa. *South African Journal of Science* 107, 43–53. doi:10.4102/sajs.v107i5/6.514
- Thompson JD, Higgins DG, Gibson TJ (1994) CLUSTAL W: improving the sensitivity of progressive multiple sequence alignment through sequence weighting, position-specific gap penalties and weight matrix choice. *Nucleic Acids Research* 22, 4673–4680. doi:10.1093/nar/22.22.4673
- Treadwell AL (1931) Three new species of polychaetous annelids in the collections of the United States National Museum. *Proceedings of the United States National Museum* 80, 1–5. doi:10.5479/si.00963801.80-2902.1
- Valvassori G, Massa-Gallucci A, Gambi MC (2015) Reappraisal of *Platynereis massiliensis* (Moquin-Tandon) (Annelida Nereididae) a neglected sibling species of *Platynereis dumerilii* (Audouin & Milne Edwards). *Biologia Marina Mediterranea* 22, 113–116.
- Vieira PE, Desiderato A, Holdich DM, Soares P, Creer S, Carvalho GR, Costa FO, Queiroga H (2019) Deep segregation in the open ocean: Macaronesia as an evolutionary hotspot for low dispersal marine invertebrates. *Molecular Ecology* 28, 1784–1800. doi:10.1111/mec.15052

- Villalobos-Guerrero TF (2019) Redescription of two overlooked species of the *Perinereis nuntia* complex and morphological delimitation of *P. nuntia* (Savigny in Lamarck, 1818) from the Red Sea (Annelida, Nereididae). *Zoosystema* **41**, 465–496. doi:10.5252/zoosystema.2019v41a24
- Villalobos-Guerrero TF, Bakken T (2018) Revision of the *Alitta virens* species complex (Annelida: Nereididae) from the North Pacific Ocean. *Zootaxa* **4483**, 201–257. doi:10.11646/zootaxa.4483.2.1
- Villalobos-Guerrero TF, Carrera-Parra LF (2015) Redescription of *Alitta succinea* (Leuckart, 1847) and reinstatement of *A. acutifolia* (Ehlers, 1901) n. comb. based upon morphological and molecular data (Polychaeta: Nereididae). *Zootaxa* **3919**, 157–178. doi:10.11646/zootaxa.3919.1.7
- Viveiros F, Chiodini G, Cardellini C, Caliro S, Zanon V, Silva C, Rizzo AL, Hipólito A, Moreno L (2020) Deep CO<sub>2</sub> emitted at Furnas do Enxofre geothermal area (Terceira Island, Azores archipelago). An approach for determining CO<sub>2</sub> sources and total emissions using carbon isotopic data. *Journal of Volcanology and Geothermal Research* **401**, 106968. doi:10.1016/j.jvolgeores.2020.106968
- Wäge J, Valvassori G, Hardege JD, Schulze A, Gambi MC (2017) The sibling polychaetes *Platynereis dumerilii* and *Platynereis massiliensis* in the Mediterranean Sea: are phylogeographic patterns related to exposure to ocean acidification? *Marine Biology* **164**, 199. doi:10.1007/s00227-017-3222-x
- Weitschek E, Fiscon G, Felici G (2014) Supervised DNA barcodes species classification: analysis, comparisons and results. *BioData Mining* **7**, 4. doi:10.1186/1756-0381-7-4
- Zantke J, Bannister S, Rajan VB, Raible F, Tessmar-Raible K (2014) Genetic and genomic tools for the marine annelid *Platynereis dumerilii*. *Genetics* **197**, 19–31. doi:10.1534/genetics.112.148254
- Zeeck E, Hardege J, Bartels-Hardege H, Wesselmann G (1988) Sex pheromone in a marine polychaete: determination of the chemical structure. *Journal of Experimental Zoology* **246**, 285–292. doi:10.1002/jez.1402460308
- Zeeck E, Harder T, Beckmann M (1998) Uric acid: the sperm-release pheromone of the marine polychaete *Platynereis dumerilii*. *Journal of Chemical Ecology* **24**, 13–22. doi:10.1023/A:1022328610423
- Zghal F, Ben Amor Z (1989) Sur la présence en Méditerranée de la race épitoque de *Perinereis cultrifera* (Polychète). *Archives de l'Institut Pasteur de Tunis* **66**, 293–301.
- Zhang J, Kapli P, Pavlidis P, Stamatakis A (2013) A general species delimitation method with applications to phylogenetic placements. *Bioinformatics* **29**, 2869–2876. doi:10.1093/bioinformatics/btt499
- Zhou H, Zhang Z, Chen H, Sun R, Wang H, Guo L, Pan H (2010) Integrating a DNA barcoding project with an ecological survey: a case study on temperate intertidal polychaete communities in Qingdao, China. *Chinese Journal of Oceanology and Limnology* **28**, 899–910. doi:10.1007/s00343-010-9131-1

**Data availability.** New sequence data and specimen metadata were uploaded in the project '*Platynereis species complex*' (DS-MTPD) within BOLD (<http://v4.boldsystems.org/>) and in the following link: doi:10.5883/DS-MTPD. The alignments (FASTA and NEXUS formats) for each marker (*COI*, *16S* and *28SD2*) and the concatenated one (*COI* + *16S* + *28SD2*) are all publicly available online at Figshare (doi:10.6084/m9.figshare.21429000). The new biological material is deposited at the Biological Research Collection (Marine Invertebrates) of the Department of Biology of the University of Aveiro (CoBI at DBUA), Portugal, and specimens from Norway are deposited at the Norwegian University of Science and Technology, NTNU University Museum. Specimens from the Arrabida Natural Park (Lisbon, Portugal) were provided by the National Museum of Science and Natural History (MUHNAC, Portugal). All specimens are available upon request, with the exception of the ones exhausted in the DNA analysis mentioned in the Methods.

**Conflicts of interest.** The authors declare that they have no conflicts of interest.

**Declaration of funding.** This study was supported by the project ATLANTIDA – Platform for the monitoring of the North Atlantic Ocean and tools for the sustainable exploitation of the marine resources, with the reference NORTE-01-0145-FEDER-000040, co-financed by the European Regional Development Fund (ERDF), through Programa Operacional Regional do Norte (NORTE 2020). Thanks are due, for the financial support of Centro de Estudos do Ambiente e do Mar (CESAM) (UIDB/50017/2020 + UIDP/50017/2020), to the Portuguese Foundation for Science and Technology (FCT), and Ministry of Education and Science (MEC) through national funds, and the co-funding by the Fundo Europeu de Desenvolvimento Region (FEDER), within the PT2020 Partnership Agreement and Compete 2020. The research leading to these results also received partial funding from the European Union's Horizon 2020 research and innovation programme under grant agreement number 730984, ASSEMBLE Plus project (application number 8229, 4th CALL, 'Crypticism in the marine realm: DNA barcode-based outlook into selected invertebrate taxa of the Eastern Mediterranean'). Marcos A. L. Teixeira was supported by a PhD grant from the FCT, co-financed by European Social Fund (ESF) (SFRH/BD/131527/2017) and from the DNAqua-Net STSM grant 'Rich and hidden biodiversity not yet barcoded in the Canary archipelago (Spain) as an opportunity to enrich the DNA barcode reference library for European polychaetes', under the EU Cost action CA15219, 'Developing new genetic tools for bioassessment of aquatic ecosystems in Europe'. Pedro Vieira's work was supported by national funds through the FCT (Public Institute, I.P.) in the scope of the project "Early detection and monitoring of non-indigenous species in coastal ecosystems based on high-throughput sequencing tools" (PTDC/BIA-BMA/29754/2017). Ascensão Ravara was funded by national funds, through FCT, I.P., in the scope of the framework contract foreseen in the numbers 4, 5 and 6 of the article 23, of the Decree-Law 57/2016, of August 29, changed by Law 57/2017, of 19 July. Financial support was provided for Arne Nygren from the Norwegian Taxonomy Initiative (<http://www.biodiversity.no/Pages/135523>) (Cryptic polychaete species in Norwegian waters, kontraktnummer 49–13, prosjektnummer 70184228), the Swedish Taxonomy Initiative (<https://www.artdatabanken.se/en/the-swedish-taxonomy-initiative/>) (Polychaete species complexes in Swedish waters, diarienummer 140/07 1.4 and 166/08 1.4), and Kungliga Fysiografiska sällskapet Nilsson-Ehle donationerna (<https://www.fysiografen.se/sv/>). Financial support was provided for Torkild Bakken from the Norwegian Taxonomy Initiative project Polychaetes in Norwegian Ports project number 70184238. SEM work was performed at the European Multidisciplinary Seafloor and Water Column – Portugal (EMSO-PT) Laboratory of Biodiversity and Connectivity & CoBI, Universidade de Aveiro. EMSO-PT is funded by Portugal 2020, in the framework of COMPETE2020 (Programa Operacional Competitividade e Internacionalização, POCI), and FEDER (ref. 01/SAICT/2016) and by national funds, through Portuguese FCT and Ministry of Science, Technology and Higher Education (MCTES) (ref. PINFRA/22157/2016 EMSO-PT).

**Acknowledgements.** We thank Antonio Calado and Salomé Almeida (Univ. Aveiro) for the availability of the Zeiss Axioplan 2 imaging light microscope. Special thanks to Giorgos Chatzigeorgiou for scuba diving and providing nereidids from the island of Crete (Greece); Katerina Vasileidou for the northern Greek *Platynereis* specimens; Matilde Boschetti, Michela Del Pasqua, Chiara Ravaglioli, Jonathan Tempesti and Marco Zuffi for assistance in obtaining macrobenthic samples from several Italian localities; Celine Houbin and Nicolas Lavesque for the northern French *Platynereis* specimens; Jérôme Jourde for the type locality samples of *P. dumerilii* s.s., Jorge Núñez Fraga for all the assistance and knowledge provided during the Canary islands sampling campaign and to Andrea Desiderato for assistance in the morphological analysis of the *Nereis* spp. found in this study. Lastly, to the reviewers, including Tulio F. Villalobos, for time and dedication to this work, providing a remarkable and comprehensive review that considerably improved upon the original submission.

#### Author affiliations

<sup>A</sup>Department of Biology, Centre of Molecular and Environmental Biology (CBMA), University of Minho, Campus de Gualtar, PT-4710-057 Braga, Portugal.

<sup>B</sup>Institute of Science and Innovation for Bio-Sustainability (IB-S), University of Minho, Campus de Gualtar, PT-4710-057 Braga, Portugal.

<sup>C</sup>Dipartimento di Biologia, Università di Pisa, via Derna 1, I-56126 Pisa, Italy.

<sup>D</sup>Biología Animal, Edafología y Geología, Universidad de La Laguna, Tenerife, Spain.

<sup>E</sup>Museu de Zoologia, Instituto de Biologia, Universidade Estadual de Campinas (IB/UNICAMP), Rua Charles Darwin, Bloco N, Cidade Universitária, Campinas, SP, Brazil.

<sup>F</sup>Hellenic Centre for Marine Research, Institute of Marine Biology, Biotechnology and Aquaculture, Anávyssos, Greece.

<sup>G</sup>Katedra Zoologii Bezkręgowców i Hydrobiologii, Uniwersytet Łódzki, ulica Banacha 12/16, P-90-237 Łódź, Poland.

<sup>H</sup>Norwegian University of Science and Technology, NTNU University Museum, NO-7491 Trondheim, Norway.

<sup>I</sup>Department of Biology, Centre for Environmental and Marine Studies (CESAM), University of Aveiro, Campus Universitário de Santiago, PT-3810-193 Aveiro, Portugal.

<sup>J</sup>Institutionen for marina vetenskaper, Göteborgs Universitet, Tjörnö, Strömstad, Sweden.